Human Lung Cell Responses Caused by Roadside Particle Types

by

Xuan Jia

M.Sc., Fudan University, 2012

Thesis Submitted in Partial Fulfillment of the
Requirements for the Degree of
Doctor of Philosophy

in the
Department of Chemistry
Faculty of Science

SIMON FRASER UNIVERSITY
Spring 2019

Approval

Name: **Xuan Jia**

Degree: **Doctor of Philosophy (Chemistry)**

Title: ***Human Lung Cell Responses Caused by Roadside Particle Types***

Chair: Charles Walsby
Associate Professor

Examining Committee:

George R. Agnes
Senior Supervisor
Professor

Byron D. Gates
Supervisor
Associate Professor

Hua-Zhong Yu
Supervisor
Professor

Frank Lee
Internal Examiner
Associate Professor
Faculty of Health Sciences

Chung-Wai Chow
External Examiner
Associate Professor
Dalla Lana School of Public Health
University of Toronto

Date Defended/Approved: January 22, 2019

Abstract

Particulate matter (PM), especially traffic-derived particles, is associated with adverse effects on human health. An *in vitro* dose-response methodology using human lung cells A549 was adopted to investigate lung cell culture responses [cytokine expression Interleukin (IL) –6, IL-8, and cell death] following incubation with traffic-derived particles. The basis of this study was to investigate interactions between the known components on ambient particles proximal to roadways. In using ambient particle type ERM-CZ120, and laboratory mimics of PM, cellular responses clearly indicate the importance of insoluble particle types that are internalized via endocytosis. Particle size appears to not be a principal factor, but particle-air interface chemistries, while not investigated in this work, are likely important. The soluble species used herein did not effect a response when introduced alone, but when combined with insoluble particle types, the cellular response in excess of the insoluble particle alone was measured. A probable mechanism is that the insoluble particles function as carriers, via endocytosis, and that process provides an access route for internalization of soluble species. As evidenced by one set of experiments, prediction of overall cellular response to a given dose of a specific particle type is not trivial. Ferrous iron, when introduced with silica particles, effected significant down-regulation of expressed cytokines, whereas lead ions effected significant up-regulation, but when ferrous iron and lead ions were co-administered with silica particles, cytokine expression was down-regulated. These results indicate the necessity to measure specific cellular responses as an outcome following a dose with a specific particle composition of insoluble and soluble components for which detailed physical and chemical composition information is known, and not to extrapolate to other particle types.

Keywords: Particulate matter; traffic-derived particles; health effect; human lung cell response; chemical composition; compositional interaction

For My Parents

Acknowledgements

I must acknowledge my senior supervisor Dr. George R. Agnes for providing me the opportunity to work on this project, and giving me guidance and support throughout the entire research. His positive attitude, humor and willingness to encourage me to keep exploring and balance my life and work at the same time created an enjoyable environment that allowed me to conduct research with so much freedom. I consider myself extremely fortunate to have been a student under his supervision.

My appreciation also goes to my supervisory committee members, Dr. Byron Gates and Dr. Hua-Zhong (Hogan) Yu, and examining committee members, Dr. Charles Walsby, Dr. Frank Lee and Dr. Chung-Wai Chow for their advice and suggestions.

I would like to thank all my fellow Agnes group lab mates for making our lab as a second home. I am particularly grateful to Dr. Neil Draper for helping me to get familiar with the new environment quickly, Dr. Sean Fenwick for training me in cell culturing and characterization techniques, and always proving insightful suggestions, Femi Akintola for keeping my mind open in the later years.

I am also very glad to have built friendships with colleagues in the department of chemistry, especially with Lalangi Asha Chandrasena and Ameya Ranade. Their support and accompany provides me lots of courage to keep going as a scientist and as a person. And a special thank you goes to Dr. Jamie Scott Laboratory for letting me continue using their plate reader.

Finally, I am extremely thankful to my family and friends for respecting my decision and always being there. The journey to complete my studies is long and arduous, and I can never make it happen without their unconditional love and support.

Table of Contents

List of Tables

List of Figures

List of Acronyms

#	Number
%	Percent
~	Approximately
<	Less than
>	Greater than
≤	Less than or equal to
≥	Greater or equal to
±	Plus-minus
°	Degrees
°C	Degrees Celsius
σ or SD	Standard deviation
µg	Microgram
µl	Microlitre
µm	Micrometre or micron
µM	Micromolar
A549	Human lung carcinoma alveolar type II pneumocyte cell line
AI	Alveolar-interstitial
AIRS	Aerometric Information System
AQC	Air Quality Guideline
AQMS	Air Quality Management System
ATBS	2,2’-Azino-bis(3-ethylbenzothiazoline-6-sulfonic acid)
ATSDR	Agency for Toxic Substances and Disease Registry
Avg.	Average
BET	Brunauer–Emmett–Teller
BSA	Bovine serum albumin
CAA	Clean Air Act
CAAQS	Canada Ambient Air Quality Standards
CAT	Catalase
CB	Carbon black
CCME	Canadian Council of the Ministers of the Environment
cm	Centimeter

COPD	Chronic obstructive pulmonary disease
DALYs	Disability-adjusted life years
DCFH-DA	Dichlorodihydrofluorescein diacetate
dl	Decilitre
DNA	Deoxyribonucleic acid
e.g.	For example
EC	Elemental carbon
ED	Emergency department
EDTA	Ethylenediaminetetraacetic acid
EHC-93	Environmental Health Centre-93
ELF	Epithelium lining fluid
ELISA	Enzyme-linked immunosorbent assay
EPA	Environmental Protection Agency
ERM-CRM120	European reference material-certified reference material 120
ESR	Electron spin resonance
ET	Extrathoracic
etc.	And so on
FBS	Fetal bovine serum
GBD	Global burden of disease
GI	Gastrointestinal
GM-CSF	Granulocyte-macrophage colony-stimulating factor
GPx	Glutathione peroxidase
HBECs	Human bronchial epithelial cells
HEI	Health Effects Institute
HIF	Hypoxia-inducible factor
hrs	Hours
IARC	International Agency for Research on Cancer
i.e.	That is
IL	Interleukin
IPN	Inhalable Particulate Network
JRC-IRMM	Joint Research Centre – Institute for Reference Materials and Measurement
kDa	Kilodaltons
kg	Kilogram
km	Kilometer

L	Litre
LCT_{50}	Lethal concentration and time, 50%
LPS	Lipopolysaccharides
LRI	Lower respiratory infection
m	Meter
MCM	Menu of Control Measures
MFF	Metal fume fever
mg	Milligram
mins	Minutes
ml	Millilitre
mm	Millimeter
mM	Millimolar
mph	Miles per hour
MS	Mass spectrometry
MT	Metallothionein
MW	Molecule weight
N	Negative control
n	Number of samples
NAAQS	National Ambient Air Quality Standards
NAPS	National Air Pollution Surveillance
NEI	National Emissions Inventory
NF-κB	Nuclear factor kappa beta
ng	Nanogram
NHAPS	National human activity pattern survey
nm	Nanometer
NOM	Natural organic matter
NO_x	Nitrogen oxides
vol.	Volume
OC	Organic carbon
P	Positive control
PAHs	Polycyclic aromatic hydrocarbons
PAMPs	Pathogen-associated molecular patterns
PBS	Phosphate-buffered saline
pH	Numeric scale for acidity

PM	Particulate matter
$PM_{0.1}$ or UFPs	Ultrafine particles, with aerodynamic diameters smaller than 0.1 μm
$PM_{2.5}$	Fine fraction particles, with aerodynamic diameters smaller than 2.5 μm
$PM_{2.5-10}$	Coarse fraction particles, with aerodynamic diameters from 2.5-10 μm
PM_{10}	Thoracic fraction particles, with aerodynamic diameters smaller than 10 μm
ppm	Parts per million
PTFE	Polytetrafluoroethylene
RDE	Real-Driving Emissions
RNS	Reactive nitrogen species
ROFA	Residual oil fly ash
ROS	Reactive oxygen species
S	Sample
SEM	Scanning electron microscope
SMEs	Small and medium-sized enterprises
SOA	Secondary organic aerosol
SOD	Superoxide dismutase
SOF	Soluble organic fraction
t	Tons
TB	Tracheobronchial
TC	Total carbon
THP-1	Human peripheral blood acute monocytic leukemia monocyte cell line
TLR2	Toll-like receptor 2
TLR4	Toll-like receptor 4
TLRs	Toll-like receptors
TNF	Tumor necrosis factor
TPM	Total particulate matter
TSP	Total suspended particulate
UK	United Kingdom
USA or U.S.	United States of America
v/v	Volume over volume
WHO	World Health Organization

wt%	Weight percent
XPS	X-ray photoelectron spectroscopy

Chapter 1.

Introduction

1.1. Motivation

Ambient air pollution, especially ambient particulate matter (PM), is identified as a leading contributor to the global burden of disease (GBD), and this is particularly pronounced in low/middle-income countries.[1-2] According to a GBD study completed in 2016, which assessed the attributable deaths and disability-adjusted life years (DALYs) of 84 behavioural, environmental and occupational, and metabolic risk factors across 195 countries and territories from 1990 to 2016, the rank of ambient particles has increased from seventh in 1990 to sixth in 2016 in terms of DALYs. With respect to death data, the ambient particle was consistently among the top ten ranked risk factors in 2016. For instance, it was fourth and third place in developing counties such as China and India, respectively.[2] Another GBD study concluded that, in 2015, the fifth-ranking risk factor for mortality was exposure to $PM_{2.5}$ (PM with a median aerodynamic diameter smaller than 2.5 μm), based on data implicating approximately 4.2 million deaths and 103.1 million DALYs, which attribute 7.6% and 4.2% of the total global deaths and DALYs, respectively. A trend of increasing contribution of $PM_{2.5}$ to the GBD, was observed, based on 25 years data (from 1990 to 2015).[1] In Canada, ambient PM exposure was attributed to approximately 6958 deaths (2.56% of total deaths), and 109,373 DALYs (1.24% of total DALYs) in 2016, which ranked 12th and 14th, respectively.[3] Extensive data sets associate exposure to PM with several chronic diseases including lower respiratory infection (LRI), chronic obstructive pulmonary disease (COPD), cardiovascular disease, and lung cancer, all of which factor in DALYs.[1-2, 4-5]

In urban areas, traffic is a major source of PM. Higher PM concentrations are typically measured at sites near roadways versus sites further distant from roadways.[6-7] This suggests that individuals near the roadside or travelling in vehicles are likely to be exposed to higher levels of PM. According to the data from national human activity pattern survey (NHAPS), the time that individuals spend in vehicles and near vehicles based on the 95th percentile is 270 and 425 minutes per day in the United States (U.S.),

respectively.[8-9] Certain traffic-derived particle types and components, such as soots containing transition metals, are reported highly associated with adverse health effects.[10-11]

However, it remains to be clearly delineated through controlled experimentation the identity of the main contributors to the toxicity of the whole particle. In the limits, are specific particulate components significantly more toxic than others, versus, is it simply the overall cumulative effect of the component complexity of PM?

1.2. Overview of Particulate Matter

Particulate matter is defined as a heterogeneous mixture of fine solid and liquid particles suspended in the air.[12] Individual particles emitted directly to the atmosphere are known as primary particles. Particles formed through gas-to-particle conversion from gaseous precursors such as sulfur dioxide, ammonia, oxides of nitrogen, and volatile organics are termed secondary.[12-13]

Both types of particles can arise from natural and anthropogenic sources. The main natural sources include volcanic eruptions, wind erosion, dust storms, forest fires, ocean sprays, and some natural organic compounds such as soil humic materials, fungal spores, and living vegetation. Anthropogenic sources include fossil fuel combustion, transportation, industrial processes, construction activities, biomass burning, agricultural operations, and mining and quarrying. Of the anthropogenic sources, the traffic-related emission is one of the major sources of PM afflicting a large fraction of the planet's human population.[13-15] Generally, the characteristics of the particles can be highly variable due to different sources and changes in time and space. For instance, ambient particles can be further modified by homogeneous and heterogeneous tropospheric chemistry, or for re-suspended particles which may also carry with them back into the atmosphere compounds such as biologics, humic materials, and other dusts.[12, 14]

1.3. Characteristics of Particulate Matter

In this section, the discussion is restricted to particle characteristics that are associated with health outcomes.

1.3.1. Size

An ideal particle is defined as having a spherical shape and standard density of 1.0 g/cm^3.[16] However, in the atmosphere, each suspended particle is usually non-spherical and having an irregular shape and varied density. Thus, the size of ambient particles is described as an "equivalent" diameter (e.g., an ideal particle with that "equivalent" diameter would have the same physical behavior with the measured ambient particle).[16-17] Depending on the physical property being measured, several diameter types can be used to describe the size of particles. For instance, the optical diameter is determined by the optical properties of the particles, the thermodynamic diameter is determined by the diffusion coefficient of the particles in the air, and Stokes diameter and aerodynamic diameter are determined by the particle's aerodynamic behavior, or diffusion and gravitational settling, respectively.[17-18] Generally, the size of ambient particles can vary from nanometers to tens of micrometers.[12] Larger particles are suspended in exceptional circumstances, such as very high winds.

Aerodynamic diameter is the most commonly used size-characterization parameter. It is defined as the diameter of an ideal particle that settles at equal terminal gravitational velocity as the particle of interest.[16-17, 19] Particles' aerodynamic properties can determine the transportation and removal of the particles in the atmosphere, and their ability to deposit and retain in the human respiratory system. It is also associated with the sources and chemical compositions of particles.[5, 12, 14, 16] Based on their aerodynamic diameter, particles can be classified into different fractions (Figure 1.1). For instance, PM_{10} refers to PM with a median aerodynamic diameter less than 10 μm. PM_{10} is also known as thoracic particles due to their ability to penetrate beyond the larynx and deposit in the primary bronchi, while the larger particles with size up to 100 μm primarily deposit in the nasopharynx.[15, 19] Particles with aerodynamic diameters from 2.5 to 10 μm ($PM_{2.5-10}$) are defined as coarse fraction particles, and generally deposit in the extrathoracic and upper tracheobronchial regions. They are predominantly generated from natural sources through mechanical processes such as sea sprays and road dusts, but this size category can also include some secondary particles that have grown large under suitable environmental conditions.[15, 19] Important biological particle components such as endotoxin and pollen are mainly found in coarse fraction.[15] $PM_{2.5}$, the fine fraction particles, stand for PM with a median aerodynamic diameter < 2.5 μm. Particles with these sizes have the ability to reach the small airways and alveoli and are also

referred to as respirable particles. They are usually from anthropogenic sources, such as high-temperature combustion. Primary combustion particles usually grow through coagulation and condensation (become secondary particles) proximal to the emission source where particle-particle collisions are more probable.[14-15]

In recent years, a considerable amount of attention has been paid to ultrafine particles (UFPs) that are size-categorized as ≤ 0.1 μm in diameter ($PM_{0.1}$). UFPs are usually formed through combustion processes, and can grow into larger particles through coagulation and condensation quickly. However, there is increasing use of nanoparticles in industrial commodities, and not only are the emissions under scrutiny, but also the fate of nanoparticles in the commodities. The UFPs that deposit in the alveoli can translocate into the circulatory system. How UFPs, versus $PM_{2.5}$ and other size classifications of ambient particles, factor the pathogenesis of cardiovascular disease continues to receive considerable research attention, because a considerable body of epidemiological evidence correlates suspended particles with adverse effects on human health.[14-15, 20]

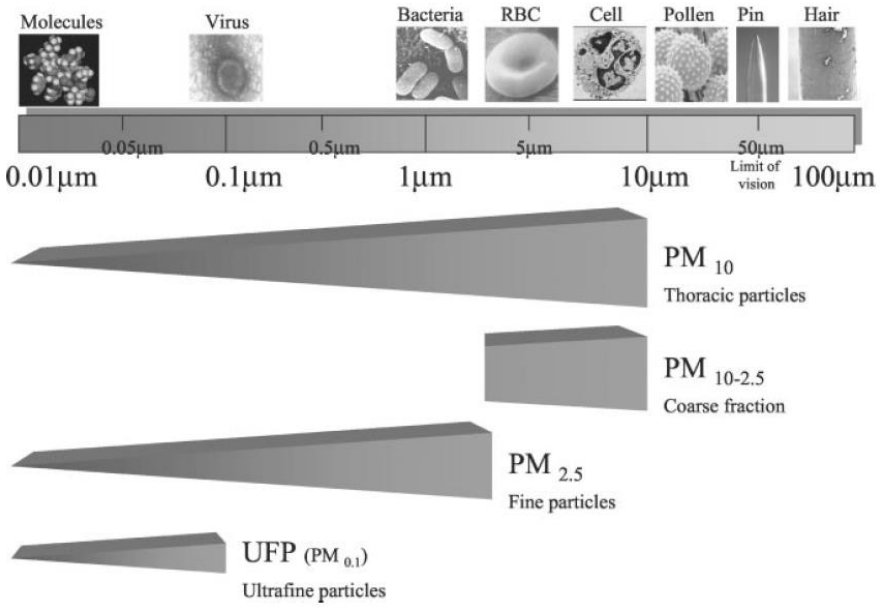

Figure 1.1 Classification of the particulate matter based on size, source: American Heart Association, Inc.[15]

Generally, it is believed that small particles could elicit greater toxicity than larger ones on a mass basis for the following reasons: small particles can penetrate into deep regions of the respiratory tract, bypass mucociliary clearance, and deposit in the alveolar

region of the lungs where they potentially come into contact with more cells than a comparable mass of larger particles. Smaller particles also have large surface areas which can absorb and retain toxic substances through heterogeneous surface chemistry while they are in the atmosphere.[5, 14-15]

However, definitive conclusions remain elusive. For instance, reports exist that conclude coarse PM leads to higher pulmonary responses than the fine and ultrafine PM on the comparative mass basis. In these studies, the size-specific chemistry of coarse PM, that includes chemical components such as endotoxin and crustal materials, appear prominently in the overall toxicity of particles.[21-23] A goal of the studies reported herein was to identify additional components that are toxic.

1.3.2. Chemical composition

The atmospheric particulate matter is a mixture of assorted chemical components that vary in time and space. In general, the main components that constitute fine particles include sulfates, ammonium, organic compounds such as polycyclic aromatic hydrocarbons (PAHs), elemental carbon, and transition metals, while sea salts, biogenic components (e.g. pollen and spores), and crustal elements including silicon, calcium, aluminium, magnesium, and iron are usually observed in coarse particles. Other common particle components include ammonium ions, nitrates, hydrogen ions, and particle-bound water.[12, 24-27] Among the trace elements that can be found in ambient particles, lead, iron, and copper have the highest concentrations.[12]

Certain particle components have been reported as playing an important role in the health effect of ambient particles. Metals, for instance in traffic-generated particles, are introduced in particles that were produced through the combustion of fuels, fuel additives, and in particles generated through wear and abrasion of brake and automobile tire wear. With these sources of metals in particles, there has also been research focus on redox-active transition metals, such as Fe, Cu, and Ni, due to their capability to generate reactive oxygen species (ROS) directly through redox-cycling in lung tissues, specifically mitochondria, which, can lead to subsequent oxidative stress, inflammation, and in turn factor in the pathogenesis of chronic respiratory diseases.[5, 10, 14-15, 26, 28-29] Non-redox-active metals, such as Zn, Al, and Pb influence the toxicity of the particles by either decreasing or increasing oxidative stress, as well as they have direct interaction

with functional groups on biological molecules, or displacement of normative metals ions from proteins.[5, 14, 29-32]

In addition to metals, organic compounds also are suggested as toxic. These compounds may originate from combustion, hydrocarbon emission, secondary formation, and biological sources. Over 200 organic compounds have been identified in ambient particulate matter, including alkanes, alkenes, oxygenated organic compounds, nitro-compounds, aromatics such as PAHs and their derivatives.[4, 12, 14, 26] Several compounds are quinones that can generate ROS through redox cycling in the presence of biological reductants. The PAHs that have no direct oxidative activity can undergo biotransformation by cytochrome P450 and dihydrodiol dehydrogenase intracellularly to form quinones.[5, 26] Other organic compounds, including PAHs, are known as high carcinogenic and mutagenic. They are associated with an increased risk of chronic diseases such as cardiovascular disease and lung cancer.[4, 26, 33]

Biological particle components can also contribute to the toxicity of the particles. An essential constituent of the outer cell wall of Gram-negative bacteria, endotoxin, is found absorbed to the surface of coarse particles.[25, 34] When endotoxin comes into contact with cells, the TLR4 (Toll-like receptors 4) pathway can be activated with the secretion of pro-inflammatory cytokines as the outcome. In turn, the cellular response increases oxidative stress and triggers a lung inflammatory response.[5, 15, 34] However, the role of each component in a mixture sorbed to an ambient particle in the overall toxicity remains to be clarified.

1.3.3. Surface properties

Increasing attention has been paid to the surface properties of the particles, especially the ultrafine particles and nanoparticles. The rationale is for the same mass of particles, a population of smaller particles will have a higher total particle number and larger surface area, assuming similar surface roughness. For instance, to reach an airborne mass concentration of 10 $\mu g/m^3$, the particle concentration would be 1200 per cm^3 of 250 µm diameter particles, having a total surface area of ~240 $\mu m^2/cm^3$, whereas for smaller particles having a diameter of 5 µm, the particle concentration would be $1.53x10^8$ particles per cm^3 having a total surface area of ~1200 $\mu m^2/cm^3$.[35] With the larger total surface area, the ultrafine/nanoparticles are capable of absorbing greater

quantities of toxic components, and undergo more reactions on their surface, hence are potentially more reactive and toxic than the equivalent larger particles at the same total mass.[36-37] It is suggested that the amount of surface molecules increases exponentially as the particle diameter decreases, and with that, several other studies have speculated that ultrafine/nanoparticles could cause greater toxicity than larger particles of identical chemical compositions and mass dosages.[36, 38-42] Due to its significant role, the particle surface area is suggested as a dose metric to assess the toxicity of low solubility particles, especially those that are alone of low-toxicity.[41-44]

The surface charge of particles, usually measured as the zeta-potential, is defined as the electric potential between the charged groups on the particle surface and the particle suspension medium.[42, 45] The zeta potential will change dynamically based on the absorption salts and proteins from a supporting solution. For example, nanoparticles adsorb macromolecules having opposite charge in biological fluids, such as proteins, to form the corona on the particle surfaces, and thereby reduce the surface charge. This process forms an electrical double layer at the solid particle/liquid interface (e.g. electrolyte solution, lung lining fluid etc.) as an outcome of the interaction between the ions/molecules in the solution and the atoms/molecular features presented at the particle surface. Counter-ions in the solution are attracted to the particle surface (Stern layer). The counter-ions screen the particle's surface charge, and in turn, another layer, termed the diffuse layer, forms. This is directly analogous to the double layer that forms at an electrode immersed in a conductive solution. In acting to neutralize the particle surface charge, the concentration of counter-ions in the Stern layer can be enriched by factors of ~ 10 or more relative to the bulk electrolyte concentration.[46-47] The pH of the suspension medium will also affect the particle's surface charge.[42, 45] The zeta-potential of most metal oxide nanoparticles is negative in neutral solution with pH of 7.4, and slightly negative in lung lining fluids, and positive in acidic medium (pH = 5.6).[42]

The surface charge on a particle influences cellular uptake. In general, with the cell membrane being negatively charged, positively charged particles tend to be taken up by the cells more favorably than neutral or negatively charged particles due to electrostatic attractions, and thus tend to be more toxic.[42, 45, 48-49]

Surface reactivity is a direct determinant of particles' toxicity, especially for the low-solubility particles such as crystalline silica, as it describes the capability of the particles to induce ROS through interaction with the immediate environment.[42, 50-51] Surface reactivity can be affected by several particle characteristics, including size, surface area, and active surface sites, and chemical components absorbed on the particle surface such as transition metals.[42, 51-52] Electron spin resonance (ESR) (cell-free environment), hemolytic potential assay (*in vitro*), and 2'-7' dichlorodihydrofluorescein diacetate (DCFH-DA) assay (cell-free environment or *in vitro*) can be used to assess the surface reactivity of the particles.[42, 45]

1.4. Traffic-derived particles

Traffic is a major source of PM, including both fine and coarse fraction, especially in urban areas.[10] Proximal to major roadways, particulate matter is ubiquitous and at elevated concentrations as compared to locations further from roadways.[8] Due to their special characteristics, traffic-derived particles are reported highly associated with adverse health effects.[10-11, 53]

1.4.1. Main particle types/components

Particles derived from traffic can be divided into two general types: I. vehicle exhaust particles, usually known as soot; II. non-exhaust emissions, including particles from brake, tire and road wear, and the re-suspended road dust due to the turbulence generated by the motion of an automobile.[8, 53-54]

Soot is defined as an unwanted by-product of incomplete combustion or pyrolysis of carbon-containing materials, such as fuel oil, diesel, gasoline, coal, and wood.[55-56] Its physical and chemical properties can be highly variable, depending on the starting materials and combustion conditions. For traffic-derived soot, factors include engine type, fuel (e.g. gasoline, diesel, biofuel, and natural gas), additives, operation condition, and emission control technologies.[8, 53, 57] Engine exhaust soot is mainly composed of elemental carbon (nominally < 60%), inorganic compounds including transition metals and ammonium sulfate and nitrate, and adsorbed organic material.[53, 55] There are hundreds of organic compounds that have been identified in soot. Most of them are PAHs and their derivatives which are known to have strong carcinogenic or mutagenic

potential. Example compounds are benzo(a)anthracene, benzo(a)-pyrene, benzo(k)fluoranthene, 1-nitropyrene, and 3-nitrofluoranthene.[10, 33, 53] Other organic components identified in soot include phenols, heterocyclic compounds, nitroarenes, and other nitrogen- and oxygen-containing derivatives. In addition, the transition metals, e.g. Fe, Cu, and Ni have also been reported to contribute to the toxicity of the particles through the generation of oxidative stress.[5, 10, 29]

Compare to gasoline fuel engine exhaust soot, the numbers of soot particles emitted from diesel fuel engine can be more than 100-fold larger due to the greater proportion of fine and ultrafine particles per unit mass of the total particulate matter.[53, 58] As mentioned before, small particles can penetrate deeper into the lung and have larger surface area, thus could absorb and retain more toxic substances than large particles. Therefore, diesel soot represents one of the main harmful traffic-derived particle types due to its large number concentration and adverse health effects. It is for this reason, as of ~2015, that most diesel fuel automobiles sold in North America have exhaust systems that filter and trap many of these particles.

As previously mentioned, non-exhaust vehicle emissions including particles from brake, tire and road surface wear, and the re-suspended road dust are predominately generated through mechanic processes. As such, the size range of these particle types spans several hundreds of nanometers to tens of micrometers, except brake wear generated particles that can be smaller in size.[8, 53-54, 59] It is reported that 27% of the PM_{10} mass of brake wear particles are coarse fractions ($PM_{2.5-10}$), 35% are fine fractions ($PM_{2.5-0.1}$), and the rest 38% are ultrafine particles ($PM_{0.1}$).[60] Metals including Fe, Cu, Pb, and Zn are reported as the most abundant and ubiquitous in brake wear particles.[54, 59] Other main element components include phosphorus, silicon, sulfur, and chlorine.[60] Organic compounds are also main components of brake wear particles as they've been used as binders and reinforcing fibres in brake lining manufacture. However, there is very limited information about what specific organic compounds are present.[53-54, 59-60]

Tire wear particles are generated through the friction between the road surface and tire tread. Their amount and properties are affected by tire characteristics, road surface condition, and vehicle operation.[8, 54] Generally, most tire wear emissions are coarse particles, with less than 10% being fine particles.[54] Tire wear particles primarily consist of organic components, including benzothiazole, styrene-butadiene-rubber,

natural rubber, n-alkanes, n-alkanoic acid PAHs.[8, 54] They also contain approximately 13% of inorganic components from accelerators, curing agents and other additives, such as Cd, Cu, Pb, and Zn. Among them, Zn has been considered as a marker for tire wear particles due to its wide usage in tire manufacture.[54]

Road dusts refer to particles from various sources, including all of the aforementioned (e.g., vehicle exhaust, tire and brake wear), plus mineral particles from both road wear and other crustal sources, particle types from proximal industrial related activities, as well as background particle types from distal emission sources. All of these particle types can deposit on the road surface, and are thus available for resuspension due to wind and turbulence generated by vehicles.[8, 10, 14, 53-54, 59] Among all the non-exhaust particles, road dust is the largest contributor to the total mass of particulate matter, especially in dry climates.[53, 59]

Despite their complex sources, roadway dusts are found to be mainly associated with crustal materials.[8, 54] An analysis of road dusts from both paved-road and unpaved-roads showed that approximately 10% of the total suspended particulate (TSP) is $PM_{2.5}$, while 50% of TSP is PM_{10}, and the rest of the mass consists of particles with diameters larger than 10 μm.[61] Han *et al.* found that the ratio of $PM_{2.5}$ to PM_{10} concentration in re-suspended road dusts ranged from 0.25 to 0.40.[62] The composition of road dusts varies greatly depending on the local condition. In general, road dusts consist of organic compounds (an important constituent of both soil and vehicle exhaust, e.g. PAHs), crustal elements such as Si, Ca, Al, and Fe, metals from the vehicles (e.g. Pb, Cu, Cd, and Zn), and some biogenic components such as endotoxin.[8, 54, 62]

1.4.2. Ambient level of traffic-derived particle

Traffic emission is one of the main contributors of particulate matter, especially in urban areas. It is reported that traffic-derived particles account for 14% to 48% of PM_{10} and 9% to 49% of $PM_{2.5}$ in urban areas, and 1% to 4% of PM_{10} and 5% to 7% of $PM_{2.5}$ in rural areas in Europe (data quoted was a 24-hr mass concentration).[53] The annual emissions of traffic-derived PM_{10} and $PM_{2.5}$ in the United States in 2017 were 4.5×10^5 and 2.9×10^5 t, respectively, and these values have decreased by approximately 27% and 45%, respectively, since 1997 (Figure 1.2). From 1997 to 2017, the contribution from traffic sources to the total emission of particles in the United States ranges from

2.2% to 3.5% for PM_{10} and from 5.4% to 11.5% for $PM_{2.5}$.[63] Compare to the U.S. and Europe, the contribution of traffic sources is lower in Canada (Table 1.1). The annual emissions of total particulate matter (TPM), PM_{10} and $PM_{2.5}$ from transportation are 7.4×10^5, $4.9\times10^5$and 3.6×10^5 t, respectively, in Canada in 2016. These values account for 0.32%, 0.68% and 2.3% of the total emissions of TPM, PM_{10} and $PM_{2.5}$, respectively.[64]

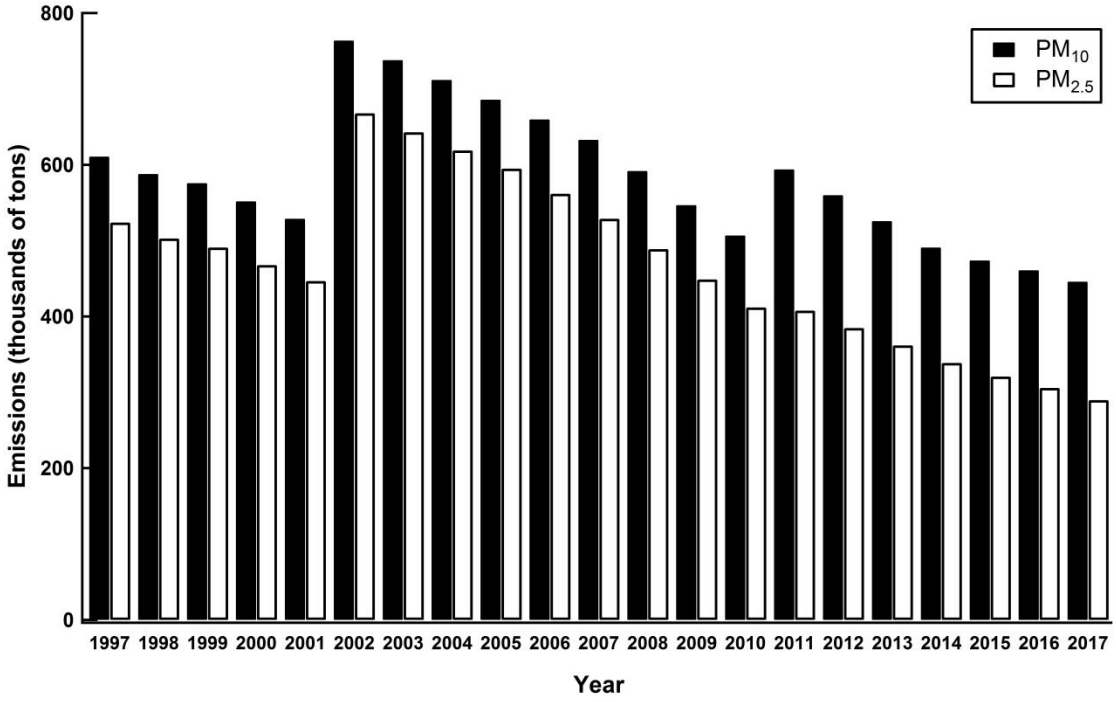

Figure 1.2 Annual emissions of traffic-derived PM_{10} and $PM_{2.5}$ in the United States from 1997 to 2017. Data source: U.S. Environmental Protection Agency, National Emissions Inventory (NEI) Air Pollutant Emissions Trends Data, retrieved from https://www.epa.gov/air-emissions-inventories/air-pollutant-emissions-trends-data[63]

Table 1.1 Summary of annual emissions of total and traffic-derived PM2.5 in Canada from 1990 to 2016[64]

Year	Total $PM_{2.5}$ Emission (t)	Traffic-derived $PM_{2.5}$ Emission (t)	The contribution of Traffic-derived $PM_{2.5}$ (%)
1990	2.0×10^6	9.6×10^5	4.8
2000	1.7×10^6	9.7×10^5	5.7
2005	1.5×10^6	8.0×10^5	5.3
2011	1.6×10^6	6.0×10^5	3.8
2012	1.7×10^6	5.5×10^5	3.2
2013	1.7×10^6	5.3×10^5	3.2
2014	1.6×10^6	5.1×10^5	3.2
2015	1.6×10^6	4.0×10^5	2.5
2016	1.6×10^6	3.6×10^5	2.3

The concentration of traffic-derived particles is affected significantly by the volume of automobiles per unit time.[8, 10, 53] Lin *et al.* reported that, at a roadside site with high traffic volume (72,000 vehicles per day, and 542 vehicles per km^2), the concentrations of PM_{10} and $PM_{2.5}$ ranged from 135 to 289 $\mu g/m^3$ with mean of 192 $\mu g/m^3$, and 88.9 to 210 $\mu g/m^3$ with an average of 141 $\mu g/m^3$, respectively. The particle concentrations adjacent to a high volume roadside site was ~3 times of those at a rural site.[6] Janssen *et al.* investigated the mass concentrations of particles in two traffic-volume roadside locations, of 8,900 and 15,000 vehicles per day, and both sites were deemed low volume by the investigators. The average concentrations of PM_{10} were 39.3 and 74.5 $\mu g/m^3$ at the two sites, with ranges from 16 to 56 $\mu g/m^3$ and 34 to 147 $\mu g/m^3$, respectively. Those concentrations were 1.3 times higher than the background.[7] Generally, the mean roadside PM_{10} concentrations are below 50 $\mu g/m^3$, and for $PM_{2.5}$, it usually ranges from 14.4 to 59.0 $\mu g/m^3$.[8]

Particle concentrations tend to exhibit a decay gradient based on distance from a roadway, especially for ultrafine particles.[8, 65-66] Meteorology also plays an important role. Cho *et al.* investigated the effect of size-fractionated PM collected at distances of 20 m and 275 m from an interstate highway, categorized as near and far roadway, respectively. The overall chemical compositions of near road PM and far road PM were similar, however, the near road PM had larger particle concentrations, and endotoxin and metal abundance as compared to the far road PM.[22] In general, the particle concentrations drop to background levels within ~200 m away from the roadway on the upwind side, whereas for the downwind side, this distance varies from 300 up to 500 m.[8]

1.4.3. Health effects of traffic-derived particle

Numerous epidemiological studies have demonstrated the association of traffic emissions with adverse health outcomes. Exposure to traffic emissions may increase the risk of mortality and morbidity of lung cancer, respiratory and cardiovascular diseases, including asthma, bronchitis, and arteriosclerosis, and exacerbate the symptoms of existed diseases.[8, 11, 67-69] Schwartz *et al.* found a linear relationship between concentrations of traffic-related $PM_{2.5}$ and daily mortality by analyzing the data of six U.S. cities using a hierarchical model. Across all observed exposure concentrations of particulate matter, an increase of 10 $\mu g/m^3$ traffic-related $PM_{2.5}$ is associated with an ~3.4% increase in daily death.[67] Highway proximity study, which focus on people living near major roadways and the commensurate exposure to a higher level of traffic emissions as compared to people living farther from roadways, indicates significantly greater risk of cardiovascular morbidity and all-cause mortality for people living proximal to major roadways, defined as 50 to 100 m, versus those living at distances > 200 m.[11, 70-72]

The generation of oxidative stress is one of the mechanisms involved in the health effects induced by traffic-derived particles. As ubiquitous components of both exhaust and non-exhaust traffic-derived particles, transition metals, especially the redox-active metals, such as Fe, Cu and Ni, can generate ROS directly through redox-cycling in lung tissues. The ROS can lead to subsequent oxidative stress and factors in inflammation and pathogenesis of chronic respiratory diseases.[8, 10, 14, 29] Non-redox-active metals, such as Pb, and biological components, e.g. endotoxin, that can be found on road dust, can also influence the toxicity of the particles by interacting with functional groups on biological molecules and increasing oxidative stress indirectly.[5, 10, 14, 31]

PAHs are organic compounds that are mainly found in soots from vehicle exhaustion. The number of different molecules of PAHs is large. Following internalization within cells, PAHs that are labile (e.g., not bound to a particle) undergo biotransformation to form quinones, which can generate ROS through redox cycling in the presence of biological reductants.[5, 26, 58] Several of the PAHs, and nitro-PAHs, are known to be highly mutagenic and genotoxic.[10] Therefore, soots, especially the ultrafine ones, are considered as having high toxicity potential due both their size and chemical compositions.[10-11, 34, 58]

1.5. Overview of the human immune response to the inhalation of particulate matter

1.5.1. Human respiratory system

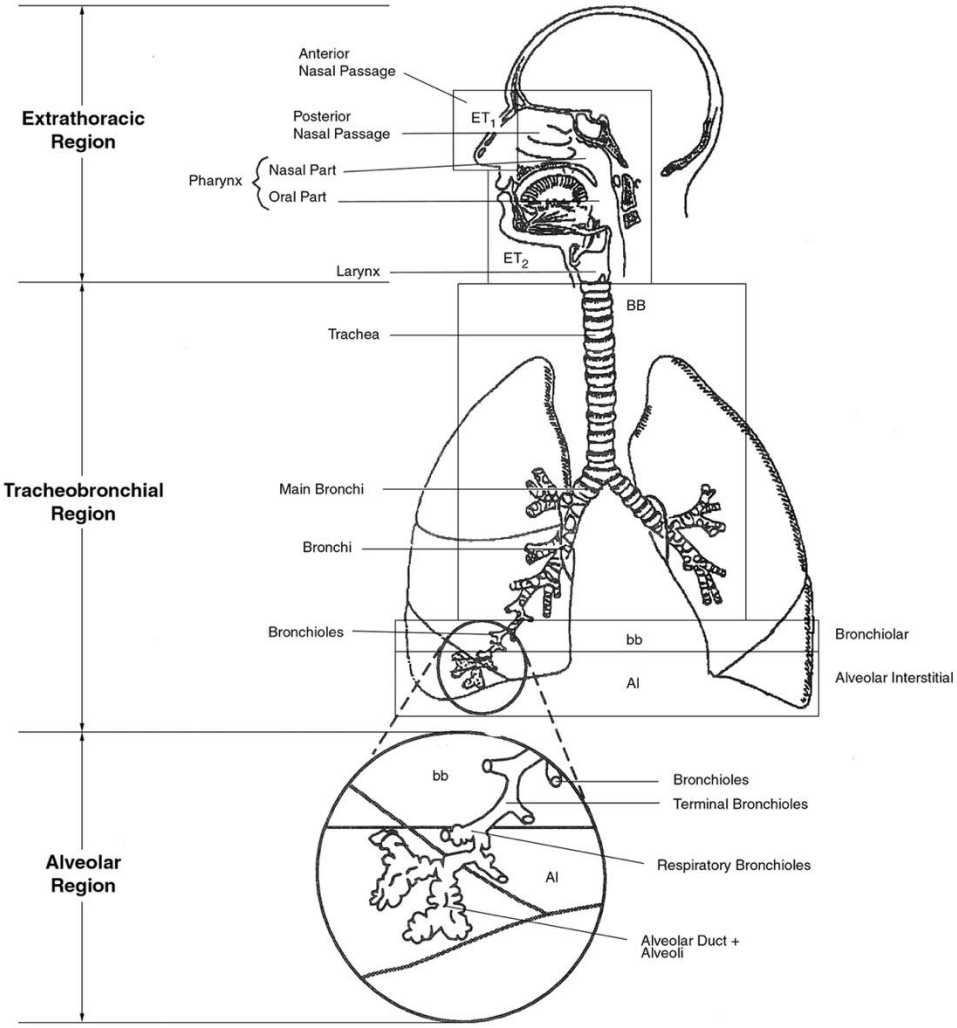

Figure 1.3 Schematics of the human respiratory system, source: Hofmann *et al.*[73] ET1: anterior nasal passages; ET2: posterior nasal passages, naso-oropharynx, and larynx; BB: bronchial region, including trachea and bronchi; bb: bronchiolar region consisting of bronchioles and terminal bronchioles; AI: alveolar-interstitial region

The respiratory system generally includes the extrathoracic (ET) region, tracheobronchial (TB) region and alveolar-interstitial (AI) region.[5, 74] A schematic of the human respiratory system is depicted in Figure 1.3. Based on a functional perspective, the respiratory tract can be divided into a conducting zone (ET region and TB region) which is a passageway for air to move into and out of the lung, and a respiratory zone

(AI region) where gas exchange occurs. In an analogous manner, an anatomical division of the human respiratory system includes the upper respiratory tract (e.g., ET region) and lower respiratory tract (e.g., the TB and the AI region).[74-76]

The extrathoracic region includes the nose, mouth, nasal and oral cavities, pharynx (throat), and larynx (voice box).[77] The tracheobronchial region starts from the trachea (windpipe) which is a single airway that bifurcates into the two bronchi, which connect to the left and right lung respectively. In continuing further into the lung, the bronchi branch into small airways and then further into smaller airways that are termed bronchioles, and the terminal bronchioles. The whole structure is known as the respiratory tree. The division point that an airway branch into smaller airways is called a generation. The human respiratory tree consists of 23 generations, on average.[74, 76] The alveolar-interstitial region begins with respiratory bronchioles, and continues with alveolar ducts and alveoli which are tiny sacs rich with capillaries. The exchange of gases, i.e. oxygen and carbon dioxide, between the respiratory system and the circulatory system takes place in this region. The lung tissue of a healthy adult consists of millions of densely packed alveoli. This design maximizes the lung surface area and provides optimal conditions for the gases exchange.[74, 76, 78]

The lower respiratory tract is covered by ciliated, pseudostratified columnar epithelium. It is mainly made up by three types of cells, ciliated cells, goblet (mucus) cells and basal cells.[78-79] The respiratory epithelium is lined with a layer of mucus, which is known as epithelium lining fluid (ELF). ELF is approximately 5 to 20 µm deep in a healthy human adult. It consists of two phases, a low-viscosity periciliary fluid produced by ciliated cells, and a thick viscous mucus layer above it that is secreted by goblet cells and tracheal glands.[78, 80-81] The ELF contains granulocytes, lymphocytes, surface macrophages and many biomolecular species such as mucins and glutathione.[78-79, 82] ELF plays an important role in capturing and interacting with the inhaled particles.[5, 83] Cilia extend from the respiratory epithelium to the mucus layer. Through oscillatory motion, cilia can transport the inhaled particles which were trapped by ELF upward to the pharynx and clear them from the respiratory system. This process is known as mucociliary clearance.[5, 74] Basal cells are firmly attached to the basal membrane. It has been suggested that a basal cell is a stem cell of the respiratory epithelium that can differentiate to other epithelium cell types.[84]

In the alveolar-interstitial region, the epithelial is not ciliated.[5] There are three main cell types, alveolar macrophages, and two human lung epithelial cell types, the membranous pneumocytes that are Type I cells and the granular pneumocytes that are Type II cells.[79, 85] 96% of the pulmonary epithelium surface area is covered by Type I cells, and the remainder is Type II cells.[86] Type I cells have very thin structures to facilitate gas exchange between alveoli and the blood capillaries. And they are unable to divide.[79] Together with pulmonary endothelium lining close to alveolar epithelium, Type I cells function as the blood-gas barrier.[87] In comparison to Type I cells, Type II cells are more numerous and have special functions (e.g., Type I cells are branched with multiple cytoplasmic plates and have large diameter relative to Type II cells).[85-86, 88-90] Type II cells have a cuboidal structure with microvilli. They are capable of synthesis and secretion of pulmonary surfactant that reduces alveolar surface tension, and they can divide and differentiate into Type I cells to replace injured cells.[5, 79, 86, 88] In response to inhaled particles, type II cells are able to endocytose particles, and secrete pro-inflammatory mediators to stimulate the recruitment of macrophages.[5, 91-92] Alveolar macrophages mediate defense against inhaled particles by internalization into cells via phagocytosis.[5, 79] In addition, the pulmonary endothelium has also been reported to interact with inhaled particles.[93-94] It is a thin layer of squamous pulmonary endothelial cells, lining the interior surface of pulmonary blood vessels. Pulmonary endothelium plays a critical role in regulating vascular homeostasis. The interaction between the pulmonary endothelial cells and inhaled particles can contribute to the local pulmonary injury as well as the systemic effect via releasing mediators to the circulation.[87, 95]

1.5.2. Agency guidelines and policy

The World Health Organization (WHO) Air Quality Guideline (AQG) for particulate matter suggests maximum concentrations of 20 $\mu g/m^3$ and 50 $\mu g/m^3$ for PM_{10} as annual mean and 24-hour mean, respectively. The $PM_{2.5}$ guideline values of 10 $\mu g/m^3$ and 25 $\mu g/m^3$ with respect to annual mean and 24-hour mean, respectively. They were calculated using $PM_{2.5} = PM_{10} \times 0.5$, which is based on a $PM_{2.5}/PM_{10}$ ratio typically measured in an urban area of developing countries. Those guideline values are selected based on relationships between exposure to particulate matter and their long-term (corresponding to annual mean guideline values) and short-term (corresponding to 24-hour mean guideline values) adverse health outcomes.[96] For instance, the long-term

guideline value of $PM_{2.5}$, 10 μg/m^3, represents the lower threshold that significant effects on mortality which was observed in the study of American Cancer Society.[96-97]

Different countries tend to have their own national guidelines to control the emissions of particulate matter. The United States Environmental Protection Agency (EPA) set the National Ambient Air Quality Standards (NAAQS) for six principal pollutants including particulate matter and lead (Table 1.3).[98] Based on the Clean Air Act (CAA), two types of standards are defined, primary standards, which provide health protection, e.g. health of sensitive populations, and secondary standards, which provide public welfare protection, e.g. damage to animals, vegetation and buildings caused by decreased visibility.[99] It is interesting that lead concentrations are specifically monitored in the atmosphere, because lead is toxic. It was an additive in gasoline post World War II. Since 1996, it has been phased out as an additive in the United States. [100]

Table 1.2 National Ambient Air Quality Standards of lead and particulate matter[98]

Pollutant	Primary/Secondary	Averaging Time	Level	Form
Lead (Pb)	Primary and secondary	Rolling 3 month average	0.15 μg/m^3	Not to be exceeded
$PM_{2.5}$	primary	1 year	12.0 μg/m^3	Annual mean, averaged over 3 years
	secondary	1 year	15.0 μg/m^3	Annual mean, averaged over 3 years
	Primary and secondary	24 hours	35 μg/m^3	98^{th} percentile[1], averaged over 3 years
PM_{10}	Primary and secondary	24 hours	150 μg/m^3	Not to be exceeded more than once per year on average over 3 years

[1] n^{th} percentile refers to the n^{th} highest 24-hour mean concentration

To assist the reduction of existing emissions, a Menu of Control Measures (MCM) has been released by the EPA to provide information of emission reduction control measures and their efficiency and cost-effectiveness for different PM sources. Traffic-related PM source categories include paved roads, unpaved roads, and on-road and non-road vehicles. Detailed control measures are provided based on specific conditions, for example, a maximum speed limit of 25 mph, road surface stabilization, and dust suppressant is suggested for unpaved roads, and continuous inspection and maintenance is required for vehicles.[101] Since the 1970s, the federal emission standards for on-road and nonroad engines and vehicles have been established by EPA under the

Clean Air Act to regulate exhaust emissions from vehicles and other forms of transportation.[99]

In Canada, the Canadian Council of the Ministers of the Environment (CCME) adopted a Canada-wide Air Quality Management System (AQMS) to manage air issues in 2012. Under AQMS, more stringent standards as defined by Canada Ambient Air Quality Standards (CAAQS) for fine particulate matter, sulfur dioxide, and ozone were adopted to replace the previous Canada-wide Standards, which had been developed in 2000.[102] According to CAAQS, the standards of $PM_{2.5}$ are 28 $\mu g/m^3$ and 27 $\mu g/m^3$ for 24-hour mean and 98th percentile, averaged over 3 years by 2015 and 2020, respectively, and 10 $\mu g/m^3$ and 8.8 $\mu g/m^3$ annual mean and averaged over 3 years by 2015 and 2020, respectively.[103] No national standard for PM_{10} has been developed so far in Canada. To regulate the transportation emissions, the AQMS mainly works on reducing emissions from mobile sources through adopting advanced transportation technologies, vehicle inspection, and maintenance, increased utilization of green fleets, and addressing in-use emissions from diesel-engine automobiles and generators.[102]

The European Commission adopted an air quality standard as 50 $\mu g/m^3$ (annual mean) and 8.8 $\mu g/m^3$ (24-hour mean) with respect to PM_{10}, and 25 $\mu g/m^3$ (annual mean) with an additional exposure concentration obligation of 20 $\mu g/m^3$ (annual mean, averaged over 3 years) by 2015, and a reduction of 0-20% by 2020 with respect to $PM_{2.5}$.[104] Emission regulations are adopted as a part of a common legal framework for approval of road vehicles after 2007. Also, Real-Driving Emissions test procedures (RDE) were developed in 2017 to provide better knowledge of actual on-road emissions.[105]

In summary, guidelines of particulate matter vary between nations, and as such, it is difficult to compare them directly due to the different conditions of nations, e.g. populations, geography, automobile roadways, and usages, etc. Though numerous regulations and measures have been adopted to control the traffic-derived particles, most of these are focused on vehicular high-temperature combustion exhaust emissions.

1.5.3. Particle deposition and clearance

In traversing the respiratory tract, inhaled particles have several physical mechanisms that act to remove them from the air stream, causing them to deposit on the surrounding airway walls. The principal ones are impaction due to inertial forces, sedimentation due to gravitational forces, and Brownian diffusion which depends on the thermal properties of air molecules. The magnitude of above deposition mechanisms and the particle deposition probability on different regions/ sites of the respiratory system depends on the dynamics of inhaled particles (size, density, and shape), geometry of the respiratory tract (e.g. radius, branching angle), and the breathing pattern which would determine the velocity of airflow and the residence time of the particles.[5, 73] For instance, impaction is effective in the ET region and upper bronchial airways due to the relatively high ratio of (air/particle) velocity, whereas in lower bronchial airways and AI region, diffusion and sedimentation processes dominate. Fast breathing leads to higher particle velocity, thus would benefit impaction, whereas slow breathing relies on diffusion and sedimentation due to longer residence time to remove particulates before the air mass enters the ET.[73, 106]

In general, large particles with aerodynamic diameters > 1.5 µm primarily deposit in the ET region and large airways due to impaction. The inhalation flow rate plays an important role in this process. Smaller particles with aerodynamic diameters > 0.5 µm can pass through the bifurcation zone and deposit in small airways and deep inside the lung (TB region and AI region) due to sedimentation. For very small particles with (thermodynamic) diameters < 0.5 µm, Brownian diffusion is the most effective mechanism for their deposition. Very small particles behave similarly to diffusing gas molecules and can thus penetrate deep into lung where they ultimately deposit in alveolar region. Ultrafine particles (< 100 nm) can even translocate across the air-epithelium barrier. Such particles are thus distributed throughout the organism. [5, 107] Figure 1.4 indicates the total and regional deposition of inhaled particles of different sizes in the human respiratory system under mouth breathing pattern. Total deposition refers to the mean probability of an inhaled particle depositing in the respiratory system.[106]

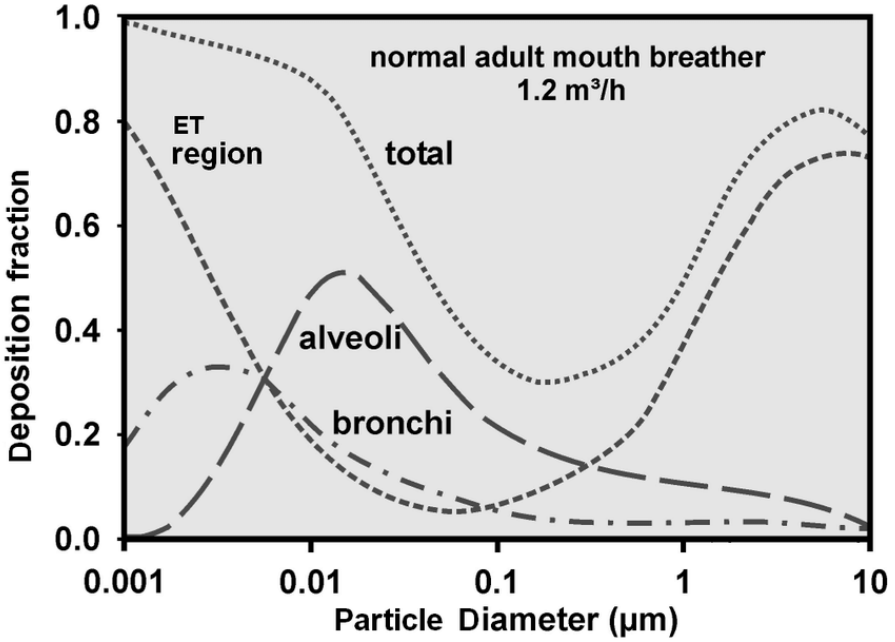

Figure 1.4 Total and regional particle deposition in the human respiratory system under mouth breathing pattern. Source: *Hussain et al.*[108]

After depositing in the respiratory system, inhaled particles can be cleared through several mechanisms, e.g. chemical clearance through the mucosal layer (dissolution, leaching, and protein-binding), mucociliary escalator transport, and phagocytosis. Three routes are generally followed: absorption to the circulatory system (in case of soluble particle components, and ultrafine particles), transport to the gastrointestinal (GI) tract, and transport to the lymphatic system.[5, 107, 109]

An ambient particle is usually a mixture of multiple chemical components. When a particle deposits on the respiratory tract or lung, it will interact with the ELF or pulmonary surfactant first, and its water-soluble and lipid-soluble fractions would be expected to dissolve in the liquid, and undergo any possible biochemical reactions with the ions and biomolecules in the ELF or pulmonary surfactant as well as the cell membrane receptors of the epithelium cells. Eventually, those soluble particulates will pass through the fluid layer, epithelial cells, the interstitium and endothelial cells, and ultimately be cleared by the bronchial and pulmonary circulations.[5, 107, 110] This process is usually rapid and can be observed immediately after inhalation. The physicochemical properties of the particle do play important roles in the aforementioned process.[107] For example, ultrafine particles either interacting directly with epithelial cells by endocytosis

or pass through the junctions between adjacent cells, enter into circulation and translocate to secondary organs, such as the liver, brain, spleen, kidney, and heart.[5, 111]

Two main mechanisms are responsible for the clearance of the insoluble particles: mucociliary clearance, and the alveolar macrophage-mediated phagocytosis. The insoluble particles that deposited in TB region can be trapped by the ELF, and transported by cilia towards the pharynx, from where they can be swallowed into the GI tract, or blown from the nose. This mucociliary clearance process is also known as rapid clearance, as the particles usually can be cleared within 24 hours.[5, 107] Small particles have a probability to penetrate the fluid and be engulfed by airway macrophages, or they can enter epithelium cells resulting in a slower clearance.[5] In the AI region, where there is no mucociliary action, the particles are phagocytized by the alveolar macrophages, and go through lysosomal digestion within the cells. Macrophages loaded with particles move towards the most distal ciliated airways and there they are removed by mucociliary clearance. Also, macrophages penetrate into the interstitium and migrate to the lymphatics and lymph nodes, where the retention time in the organism is long.[107] Macrophage-mediated clearance can take ~100 days, thus it is also known as a chronic clearance process.[110, 112] Several studies show that excessive alveolar dust burdens of insoluble particles do impair the alveolar macrophage-mediated clearance processes, and even inhibit particle clearance completely as evidenced by 'black' lung tissues observed in the human autopsy. This nonspecific, particle-induced phenomenon is “particle-overload” in the lung.[5, 107, 113-114]

1.5.4. Cellular internalization of particles

After deposition in the human respiratory system, the ambient particles can be taken up by the cells. The process that mammalian cells internalize extracellular substances via various mechanisms is termed as endocytosis. Depending on different mechanisms, there are several types of endocytosis, including phagocytosis, pinocytosis, clathrin-dependent receptor-mediated endocytosis and clathrin-independent endocytosis.[115] Fine particles with micro-size, can be taken up via phagocytosis and macropinocytosis.[116]

Phagocytosis, also known as “cell eating”, refers to the uptake of large particulate ligands with the size larger than 1 μm.[117] It is conducted primarily by specialized cells,

such as macrophages, neutrophils and monocytes, as a critical process for innate immunity to clear pathogens. The phagocytosis is initiated by the interaction between the phagocytic receptors on the cell membranes and the ligands on the particle surfaces.[116-117] It can lead to the rearrangements of the actin cytoskeleton, and the internalization of the particle by forming a phagocytic vacuole, i.e. phagosome, surrounding the particle.[116, 118-119] After internalization, most phagosome fuse with lysosomes which contains degradative enzymes to degrade the vacuolar content.[119] The surface chemistry of the particles plays an important role in phagocytosis. [119] Macropinocytosis ("cell drinking") is a form of endocytosis that take up small antigens, nutrients and solute non-selectively.[120] Similar to phagocytosis, macropinocytosis is also an actin-driven process that the surface membrane of cells forms large endocytic vacuoles, i.e. macropinosomes, to internalize a large amount of solute non-selectively.[116, 120] And macropinosomes can fuse with lysosome after internalization as well.[121] Macropinocytosis is normally triggered by growth factor signalling pathways, and can be highly active in macrophages for antigen capture.[120-121]

Nanoparticles were reported to enter cells via both endocytic pathways and non-endocytic pathways, of which the mechanisms are not clear yet. Some possible mechanisms include diffusion through the cell membrane, adhesive interactions (related to Van der Waals or steric interactions, and electrostatic forces)[116, 122] It is reported that nanoparticles can active or disrupt cell functions through interacting with expressed membrane proteins, cytoskeletal and intercellular junctional proteins.[123-124] Thus, it is possible that nanoparticles may not have to be internalized to induce cellular response.[116]

1.5.5. Particle-induced oxidative stress and inflammation

Reactive oxygen species refers to oxygen-atom-containing radicals including hydroxyl ($OH^{\cdot}$), oxyl ($RO^{\cdot}$), peroxyl ($RO_2^{\cdot}$), hydroperoxyl ($HO_2^{\cdot}$) radicals, and superoxide anion ($O_2^{\cdot -}$), plus non-radical oxidizing agents that can convert to free radicals easily, such as hydrogen peroxide (H_2O_2), hypochlorous acid (HOCl) and ozone (O_3).[125] They can be produced intracellularly during metabolism via cytosolic enzymatic reactions, activation of nuclear transcription factors, proliferative regulation pathways, and mitochondrial electron transport, as well as be triggered by exogenous sources such as inhaled particles. ROS are involved as host defence with phagocytic cells.[125-126] They

can function as signalling molecules to trigger specific pathways under both physiological and pathophysiological conditions. At the same time, ROS can interact with various cell components, including cell membranes, lipids, proteins, and DNA, and cause damage due to their high reactivity. The extent of damage depends on the availability of the antioxidant defense system which consists of several enzymatic and non-enzymatic antioxidants, e.g. catalase (CAT), superoxide dismutase (SOD), and glutathione peroxidase (GPx) that, ideally stoichiometrically exceed ROS, and thus react with ROS and maintain the physiological homeostasis.[126]

In situations where the quantity of ROS is elevated relative to the physiological homeostasis level, adverse biological effects including oxidation of cell components and inflammation are defined as oxidative stress. The degree of oxidative stress is determined by the relative quantity of ROS and the antioxidant defences.[4-5, 126] Studies have demonstrated that ambient particles are capable of inducing ROS production and thus oxidative stress through several pathways.[4-5, 26] For instance, quinones can generate ROS through redox cycling in the presence of biological reductants directly.[5, 26] Redox-active transition metals, such as Fe, can generate ROS directly through Fenton reaction.[127-128] Particle types like freshly fractured quartz may have $Si^{\cdot}$ and $Si\text{-}O^{\cdot}$ radicals on their surfaces. Through interaction with lung lining fluid, those particle-surface radicals can give rise to ROS such as $OH^{\cdot}$, and H_2O_2.[129-131] The increase of ROS and oxidative stress can trigger inflammation through activation of redox-sensitive signalling pathways, while the inflammation itself can further stimulate the generation of ROS due to the recruitment and activation of phagocytes, and thus lead to a cycle of oxidative impairment.[4-5]

Inflammation is an important form of innate immunity. It usually involves a multifactorial network that includes chemical signalling by cytokines/chemokines, activation and migration of leukocytes, and host response to clear exogenous antigens and heal the injured tissue.[132-133] In the case of exposure to inhaled particles, the particles may deposit in the upper airways, interact with ELF and the bronchial epithelial cells, and be cleared through mucociliary clearance as mentioned in the particle clearance section. [5, 107] In contrast, particles depositing in AI regions which are not ciliated can lead to inflammation. The particles interact with alveolar epithelial cells (type I and type II cells) first and lead to the secretion of pro-inflammation cytokines/chemokines [e.g. human tumor necrosis factor-α (TNF-α), interleukin-6 (IL-6),

and interleukin-8 (IL-8)] by type II cell to recruit phagocytic cells. The physiological functions of these cytokines are summarized in Chapter 2. Alveolar macrophages then migrate to the location of the particles to phagocytose particles in response to the stimulation of the cytokines/chemokines. Those engulfed particles are expected to be cleared from the lung subsequently through the migration of macrophages either to lymph nodes or to the mucociliary escalator.[5, 109]

This acute inflammation process requires a complex network of multiple signalling pathways which can be activated by inhaled particles through several mechanisms, such as the generation of ROS and oxidative stress, and the macrophage toll-like receptors (TLRs) pathways.[4-5, 109] TLRs are a family of antigen-specific receptors that can recognize molecular motifs of pathogens [pathogen-associated molecular patterns (PAMPs)] directly. As the first step of the innate immune response, TLRs can initiate dendritic cells and phagocytes, and lead to the production of inflammatory mediators. Both lung epithelial cells and macrophages express TLRs.[5, 109] Among them, TLR4 (Toll-like receptor 4) and TLR2 (Toll-like receptor 2) are the main receptors that bind particulates and initiate inflammatory signalling pathways in response to certain particulate bio-components that are usually associated with coarse particles. Examples are endotoxin of which lipopolysaccharides (LPS) the main bioactive component, and β-glucans. Endotoxin is found in the outer cell wall of gram-negative bacteria, and β-glucans is the peptidoglycan of gram-positive bacteria.[34, 109, 134]

1.5.6. From Inflammation to Disease

The acute inflammation process mentioned above can be modulated by environmental factors such as the pathogenic particles and their toxicity. For instance, the ROS generated by inhaled particles interact with cell membranes and cause damage to macrophage receptors expressed on the cell surfaces.[109] Nanoparticles may have a long residence time in the AI region due to their size. The prolonged exposure of lung epithelial cells to nanoparticles could cause hypersecretion of pro-inflammatory mediators, disruption of the chemotactic gradient, and decreased migration of particle-laden macrophages from the lung. Instead of being cleared by the mucociliary escalator, those macrophages remain within the respiratory region.[5] In general, decreased particle clearance is associated with chronic inflammation and pathogenesis of various diseases.

Chronic inflammation is defined as a prolonged pathological condition with persistent active inflammation response that can cause tissue damage and contribute to fibrosis and carcinogenesis.[5, 135] The ROS induced by inflammation interact with cell components, e.g. cell membrane, protein and DNA, potentially lead to mutation.[4-5, 135] One of the products of the inflammatory process is mitogenic stimuli which can simulate the proliferation of epithelial cells. As the cell proliferation increases, the risk that damaged DNA cannot be repaired successfully before cell division and a mutation could be passed to the daughter cells increases.[5] As a consequence, it may lead to fibrosis and structural change of airways which would result in respiratory diseases such as asthma, interstitial pulmonary fibrosis, and COPD.[5, 136-137] The pro-inflammatory mediators secreted by lung cells can also enter circulation to recruit leukocytes and monocytes, thus resulting in systemic inflammation, and potentially cause adverse effects on the cardiovascular system. For instance, the formation of atheroma and arterial damage can lead to cardiovascular diseases such as atherosclerosis and heart disease.[4-5] It is suggested that chronic inflammation could be a significant cause of cancer and some chronic diseases, and the ROS and oxidative stress induced by inflammation plays an important role.[4-5, 132, 135]

1.6. Summary and Study Objectives

Exposure to ambient particulate matter is correlated positively with adverse health effects. Within the lung, interactions between type II epithelial cells and deposited particles in the lower respiratory tract can lead to inflammation, secretion of pro-inflammatory mediators, and lung injury.[5, 138] Known effects span pulmonary inflammation to chronic diseases such as asthma, COPD, lung cancer and cardiovascular diseases, and even death.[2, 4-5, 139] Traffic-derived particles are suggested to have a high correlation with adverse health effects, either as an outcome of their chemistry and/or the fact that their concentrations are elevated adjacent to roadways.[8, 10-11, 53] Identifying prominent toxic particle components/types will help to improve the understanding of how ambient particles cause adverse health effects, and ideally motivate change in existing regulations to reduce the burden of this environmental exposure risk.

In vitro dose-response methodology has been widely used to investigate acute effects of ambient particles, and evaluate toxic particle types and components by

introducing single component, or single material (e.g., commercially available particles) to measure a specific cellular response to a specific dose.[79, 140-141] Most previous studies focus on the cellular response of either whole particles or single particle component.[14, 79, 141-142] However, the cytotoxicity of how individual components factor, specifically in the context of cytotoxicity of the whole particle, is not well defined.

Based on the hypothesis that the cellular response caused by the ambient particle, which is a mixture of assorted chemical components and particle types, does not simply equal to the sum of the response caused by each individual particle components/types, rather it could be modified by the interactions between different particle components/types, we adopted an *in vitro* methodology (details described in Chapter 2) to enable investigation of two general questions: i. Do interactions between insoluble particle types affect toxicity? We chose this question to address experimentally because others have shown the physical and chemical properties of insoluble particles, such as size, surface area, and chemistry are important. ii. Do interactions between insoluble particle types and soluble components, and between soluble components affect toxicity?

Certified reference material ERM-CZ120 (European reference material-certified reference material 120), an ambient particle type collected in a high-volume automobile tunnel, was used to illustrate the relative roles of the insoluble and soluble fractions of ambient particulate matter (Chapter 3). Specific insoluble particle types, including commercially available carbon black nanoparticles, crystalline silica particles, and nickel nanoparticles were chosen as laboratory mimics of the insoluble fraction of diesel soots, a re-suspended roadside dust type, and an insoluble metal particle type, respectively. Investigation of the cellular response of different insoluble particle types alone, as well as their effects when combined, has been conducted and described in Chapter 4. Chapter 5 mainly focuses on how specific soluble components affect cytotoxicity when they were dosed either alone, or in varied combinations together with an insoluble particle type. Inorganic water-soluble components including nitrate or chloride salts of Zn, Fe and Pb and ammonium nitrate were chosen for the study.

Chapter 2.

Methodology

2.1. Tools and Methods for *in vitro* dose Response Studies

Different approaches to study the health effects of ambient particulate matter have been described, spanning epidemiology to the human clinical/animal to tissue cultures.[4, 14, 140-141] Each experimental platform is able to address specific questions that often provide unique information.

Epidemiological studies provide the most relevant population-based information regarding acute and chronic toxic effects of inhaling ambient particles. Examples of acute exposures are industrial accidents, natural forest fires, or volcanic eruptions. Chronic exposures also include occupation exposures, as well as lifestyle exposures such as residential living adjacent to a major roadway. This method delineates impact factors that provide a robust correlation between exposure to ambient particles and the adverse health effect, but this method does have difficulty addressing detailed methodological questions.[140, 143]

In vivo studies provide important, complementary information with respect to epidemiological studies. This approach has been shown to establish biological plausibility and provide more detailed information about underlying mechanisms. Ethical consideration around its use is real and significant, and experimentation is rigorously reviewed. *In vivo* studies involving non-human subjects are limited to the extent that extrapolation to human health and risk is tenuous at best, to not realistic.[79, 140-141, 144]

In vivo studies, and epidemiology studies, are both complex, time-consuming, and expensive.[79, 140] By comparison, *in vitro* methodology is less complex, easier to control experimental factors, faster, and cost-efficient. Several lung cell *in vitro* models have been developed to investigate the cytotoxicity of the ambient particles as well as the related cellular pathway and biochemical processes at the molecular level.[79, 140-141, 144-145] A significant caveat with *in vitro* experimental methods is that extrapolation to system responses, especially inflammation, is not possible, but could be possible in the

future with advanced multi-cell type tissue culture methods. However, the triggers to initiate many cellular regulation pathways are activated similarly for both *in vitro* and *in vivo* methods. In addition, *in vitro* methods can be tailored specifically to investigate details of evidence gleaned/suggested from *in vivo* and epidemiology studies.[140-141] *In vitro* methodology is not well suited to the effect of chronic exposure to ambient particles.

In vitro methodology continues to be used extensively to investigate acute effects of ambient particles, and by comparison rapid screening of toxic particle types and components.[79, 140-141] Many strategies involve exposing cell cultures to ambient particles or the extracted particulate fraction or a single component found in ambient particles, by introducing an aliquot of a solution or suspension into the culture media.[14, 79, 141-142] Doses using the whole particle or a particle fraction provide information about the cellular response induced by these components. In intending this approach, investigators can introduce single compounds, or single materials (e.g., commercially available particles) to measure a specific cellular response to a specific dose. Despite the long-term use of this methodology, how the cytotoxicity of individual components factor, specifically in the cytotoxicity of the whole particle, is not well defined in *in vitro* studies, and to a considerably lesser extent, in *in vivo* and epidemiology studies.

In this work, we adopted an *in vitro* methodology to enable investigation of the cellular responses of different particle types and components alone, as well as their effects when combined. Certified reference material ERM-CZ120, an ambient particle type, was used, albeit not in chronological order, to illustrate the relative roles of the insoluble and soluble fractions of ambient particulate matter. The ERM-CZ120 results emphasize the critical need to evaluate ambient particle - human health implications under conditions that approximate as closely as possible, the nature of ambient particle exposure. As delineated in Chapter 1, we built our experimental methodology to generate data regarding components of ambient particle types commonly measured in locations at or near major automobile roadways. For the particles, commercially available carbon black nanoparticles, crystalline silica particles, and nickel nanoparticles were chosen as laboratory mimics of the insoluble fraction of diesel soots, a re-suspended roadside dust type, and an insoluble metal particle type, respectively. Regarding water-soluble components, with biologics like endotoxin having proven toxicity, and organic compound groups such as polycyclic aromatic hydrocarbons also having proven deleterious effect on human health, this study focused on soluble

transition metal ions, nitrate or chloride salts of Zn, Fe, and Pb. In addition, ammonium nitrate was also studied as a reference soluble particle component because it is near-ubiquitous in ambient particle samples. The aim of this work was to study the effect of these different particle components on lung cell cultures, and especially interactions between them, to increase the understanding of how specific soluble compounds affect cytotoxicity when they were dosed in varied combinations together with a particle type.

2.2. Particles and compounds

2.2.1. Certified reference material ERM-CZ120

Certified Reference Material ERM-CZ120 was purchased from Sigma–Aldrich (Oakville, Ontario, Canada). It is an ambient particle type that had been collected in a high-volume automobile tunnel, named the “Wislostrada”, in Warsaw, Poland. The particles were sieved and ground with a jet mill to obtain a PM_{10}-like fine dust with 50 vol.% of the particles’ aerodynamic diameter below 7.59 µm. The morphology of the particles is varying from each other, including sphere, cubes, fibres, and irregular shapes.

ERM-CZ120 has been certified by the Joint Research Centre – Institute for Reference Materials and Measurement, European Commission (JRC-IRMM). The concentrations by mass of all of the elements have been certified (Table 3.1). Note the original material was separated, and one fraction only was certified regarding organic components such as PAHs, named as ERM-CZ100, thus in the ERM-CZ120 we used, there are likely organic components present (Table 2.1). In addition, in the samples of ERM-CZ120 used in our laboratory, contamination with bacteria was observed when the cells were exposed without antibiotics presenting in the growth medium, but no confirmation of any bio-components in ERM-CZ120 was provided by JRC-IRMM.

Table 2.1 Mass fraction of certified PAHs in ERM-CZ100

PAH	Mass Fraction (mg/kg)
Benzo[*a*]anthracene	0.91
Benzo[*a*]pyrene	0.72
Benzo[*b*]fluoranthene	1.42
Benzo[*j*]fluoranthene	0.75
Benzo[*k*]fluoranthene	0.67
Dibenzo[*a,h*]anthracene	0.18
Indeno[1,2,3-c,*d*]pyrene	1.07
Sum of benzo[*b*] fluoranthene, Benzo[*k*]fluoranthene and Benzo[*j*]fluoranthene	2.84

The ERM-CZ120 material was stored in a 5 ml amber glass vial with a rubber stopper [coated with polytetrafluoroethylene (PTFE)] and an aluminium cap at 18 ± 5 °C in the dark. As recommended by JRC-IRMM, this material was set in an air-conditioned environment with a temperature of 20 ± 1 °C and a relative humidity of 50 ± 5 % to reach equilibrium for a period of 48 hours. Then after being shaken for the purpose of re-homogenisation, a small fraction of the material was taken from the vial immediately for cell exposure.

The water-soluble fraction and the insoluble fraction of ERM-CZ120 were prepared by suspending 0.1000 ± 0.0005 g whole particles in 10 ml sterilized deionized water at a concentration of 10 mg/ml. The suspension was sonicated in an ultrasonic water bath for 1 hour and shaken overnight before being centrifuged at 209 × g for 5 mins. The supernatant of this suspension was collected, filtered with a syringe filter (diameter 25 mm, polypropylene membrane, pore size 0.2 µm, Lot #12472914, Pall Corporation, New York, USA) and then subsequently used as the soluble fraction. The particles that were recovered from the suspension as a pellet were washed 3 times with 10 ml sterilized deionized water each time, freeze dried and used as the insoluble fraction of ERM-CZ120. Approximately 54% of the total particle mass was recovered from the suspension as insoluble fraction. Both the defined soluble and insoluble fractions of ERM-CZ120, prepared as described above, were reconstituted in serum-free medium freshly and vortexed prior to use.

2.2.2. Crystalline silica Min-U-Sil® 5

Commercially available crystalline silica (model: Min-U-Sil® 5) was provided by the U.S. Silica Company (Berkley Springs, WV, USA). This material is declared as high purity, inert, white crystalline silica from a natural source. Based on the information provided by U.S. Silica Company, at least 98-99% of the particles are SiO_2 with a median diameter around 1.7 µm. The diameters of 92% of the particles are less than or equal to 5 µm.

Min-U-Sil® 5 is well-characterized and widely used as a model for investigating the toxicity caused by inhalation of crystalline silica.[146-148] The purity of Min-U-Sil ® 5 is 99%，and the impurities may vary due to different geological sources. According to the manufacturer, the main impurities of our sample include aluminium oxide (< 1%), iron oxide (< 0.1%) and titanium oxide (< 0.1%) which may also contribute to the toxicity of the quartz particles. There is evidence to suggest that the surface properties of particles, including silica, influence significantly the toxicity of the insoluble particles which is discussed in Chapter 4.[30, 131, 149-152]

2.2.3. Nanoparticles

The sample of carbon black (CB) nanoparticles (Lot #1211NH, 100 nm) was purchased from Nanostructured & Amorphous Materials Inc. (Houston, USA). The purity of CB nanoparticles is 88.1%, and impurities include ash (5.8%) and water (1.06%).

The sample of nickel nanopowder (Lot #577995, < 100 nm) was purchased from Sigma-Aldrich (Oakville, Ontario, Canada). The purity of nickel nanopowder is ≥ 99% based on the trace metals analysis.

2.2.4. Chemical compounds

Reagent grade soluble salts [NH_4NO_3, $FeCl_2$, $FeCl_3$, $Zn(NO_3)_2$, and $PbCl_2$] with purity ≥ 99% were purchased from Sigma–Aldrich (Oakville, Ontario, Canada).

2.3. Cell culture

There are two main human lung epithelial cell types, the membranous pneumocytes that are Type I cells and the granular pneumocytes that are Type II cells.[85] 96% of the pulmonary epithelium surface area is covered by Type I cells, and the remainder are Type II cells.[86] Although Type II cells cover much less surface area than Type I cells, they are more numerous and have special functions, especially in response to lung injury.[85-86, 88-89]

Type II cells are capable of synthesis and secretion of pulmonary surfactant, and can differentiate into Type I cells to replace injured cells.[79, 86, 88] When type II cells interact with cytotoxic compounds, such as metal ions, these cells can generate storage proteins and superoxide dismutase, which together act to mitigate and eliminate the toxic species.[89] They are also able to endocytose particles, and secrete pro-inflammatory mediators to stimulate the recruitment of macrophages, and therefore have an important role in the process of inflammation induced by particles.[5, 91-92] The secretion of cytokines, and observation of irreparable damage to these cells when exposed to species that injure these cells is the experimental basis of using them in the experiment to evaluate the cytotoxicity of a toxin.

The human lung alveolar epithelium cell line A549 (CCL-185, American Type Culture Collection, Rockville, MD, USA) used in this work is a type II pulmonary epithelial cell model. The cells originated from lung carcinomatous tissue, removed from a 58-year-old male in 1972.[153-154] These cells have been immortalized, and are termed A549. The A549 cells retain similar features as the primary Type II cells as they were isolated directly from biopsy, remain biologically relevant, but as such they do not have a proliferation limitation, can be passaged continually, and have been used extensively in *in vitro* studies.[79, 85-86, 89, 141]

In this work, the A549 cells were cultured in 10 ml growth medium at 37 °C in a humidified atmosphere of 5% CO_2 in air using Petri dishes (100×20 mm, Lot #664161, Greiner Bio-one, Monroe, USA). Prior to dosing the cells in a culture, cells were first seeded into 6-well culture dishes (surface area/well 8.87 cm^2, Lot #83.1839.300, Sarstedt, Nümbrecht, Germany) with 2.5 ml of growth medium in each well and grown to confluence.

The glassware was bleached, rinsed with distilled deionized water 3 times and autoclaved before being used to store cell culture solutions. And all the sterilized plasticware used for cell culturing was disposable.

2.4. Tissue culture reagents

The culture medium, Nutrition Mixture F12 HAM Kaighn's modification (model: F-12K, Lot #N3520), penicillin-streptomycin (10,000 units/ml, Lot #15140122), human tumor necrosis factor-α (Lot #H8916), sodium bicarbonate (bioreagent, Lot #S5761, 99.5%-100.5%) and trypan blue solution (Lot #T8154) were purchased from Sigma–Aldrich (Oakville, Ontario, Canada). Phosphate-buffered saline (PBS, Lot #OXBR0014G), fetal bovine serum (FBS, Lot #12483) and trypsin-EDTA solution (0.05%, phenol red, Lot #25300-054) were obtained from Fisher Scientific/Life Technologies (Pittsburgh, PA, USA).

2.4.1. Growth medium

The growth medium was used for cell proliferation. It was prepared with F-12K medium supplemented with 10% (v/v) fetal bovine serum. 1% of penicillin-streptomycin (10,000 units/ml) was added to the growth medium for cells exposed to ERM-CZ120. Sodium bicarbonate was used to maintain physiological pH of the medium based on the instruction from the manufacturer. The growth medium was sterilized through filtration (Rapid-Flow filter units, diameter 75 mm, SFCA membrane, pore size 0.2 µm, Lot #0974028C, Fisher Scientific, Pittsburgh, PA, USA).

2.4.2. Serum-free medium

The serum-free medium was used during the period that A549 cells were exposed to a dose of particles and/or soluble particle components. No cell proliferation was expected during this period, and it was not observed. This medium was prepared with the F-12K medium, and only for cells exposed to ERM-CZ120, it also contained 1% penicillin-streptomycin (10,000 units/ml). Sodium bicarbonate was used to maintain physiological pH of the medium based on the instruction from the manufacturer. The growth medium was sterilized through filtration.

2.4.3. PBS solution

The PBS solution was used as a wash solution, and prepared from PBS salt tablets. 10 tablets per 1 L distilled deionized water was adopted as per the manufacturer's instructions. The solution was autoclaved for 20 mins at 121 °C prior to use.

2.4.4. Tumor necrosis factor - α

TNF-α is a potent pro-inflammatory cytokine produced by many cell types, including macrophages, T lymphocytes, and epithelial cells.[155-156] It plays a significant role in the recruitment of inflammatory cells in the lung, including induction of cytokine networking between alveolar macrophages and the pulmonary epithelium.[157] When exposure to inhaled allergens, airway macrophages may release TNF-α, which would then stimulate the expression of other cytokines such as interleukin (IL) -6 and IL-8.[155-157]

In this study, a stock solution of TNF-α (10 μg/ml) was prepared with sterilized deionized water. And then 10 μl aliquot of the stock solution was added to the cultures incubated with 2 ml serum-free medium to a final concentration of 50 ng/ml TNF-α. Those cultures incubated with 2 ml serum-free medium containing 50 ng/ml human TNF-α for 18 hours are served as the positive controls.

2.5. Exposure of Cell Cultures to Materials

Aliquots of stock solutions containing particle fractions, particles and/or different soluble salts were prepared, diluted to specific concentrations, and then introduced to A549 cell cultures in 6-well culture dishes with an 18-hour exposure period. Serial dilutions of stock solutions were performed using the serum-free medium. The volume of serum-free medium/solutions that bath a culture in each dish is 2 ml. A representative set of examples are presented in Figure 2.1 for A549 cultures that have been incubated with and without CB nanoparticles added to the serum-free medium.

(a) (b)

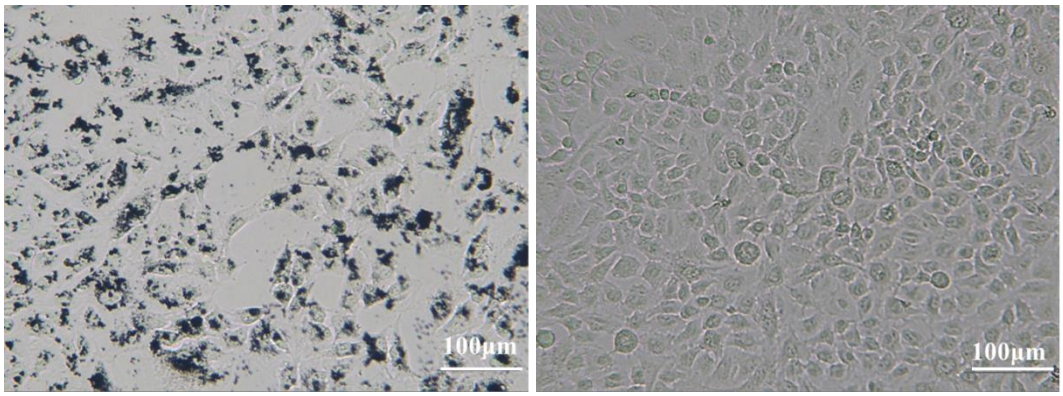

Figure 2.1 A549 cells as viewed after an 18 hour incubation period (a) with 125 μg/ml CB nanoparticles, and (b) without any particles/particle components (negative control). Images were obtained using a bright-field microscope, at 100X magnification.

For exposure to a single particle type or particle fraction, cell cultures were incubated with particles suspended in serum-free medium at dosages from 0 to 700 μg/ml for CB nanoparticles and crystalline silica, and from 0 to 100 μg/ml for Ni nanoparticles. Regarding ERM-CZ120, its whole particles and water-insoluble fractions, the 'concentrations' ranged from 0 to 1250 μg/ml. Regarding the water-soluble fraction, cell cultures were incubated with the supernatant of particle suspensions at equivalent dosages from 0 to 1250 μg/ml, where the original stock solution was obtained using ERM-CZ120 particles at 10 mg/ml. For doses involving a mixture of CB nanoparticles and crystalline silica particles, the mass ratios of CB nanoparticles to crystalline silica particles used were fixed at 0.7, 1.4 and 2.8, and the total mass dosages of the particles were varied from 0 to 700 μg/ml. Regarding dosages of crystalline silica particles plus Ni nanoparticles, silica was used from 62.5 to 125 μg/ml, and nickel nanoparticles from 10 to 40 μg/ml.

Metal salts at 100 μM for $FeCl_3$, and $Zn(NO_3)_2$, from 0 to 1000 μM for $FeCl_2$, and from 0 to 500 μM for $PbCl_2$ in serum-free medium were used for cells exposed to the water-soluble particle components. And the dosages of the particles mixed with the salts are from 0 to 175 μg/ml (details in Chapter 5). For NH_4NO_3, two concentrations, 0.23 and 0.94 μM in serum-free medium, were used to dose cultures.

Table 2.2 Materials and mass range of the materials used to dose cell cultures.

	ERM-CZ120 (mass ratio %)	Laboratory mimics (mass ratio %)	Laboratory mimics (dosage)
Elemental carbon (CB nanoparticle)	4.54	25.93 - 84.85[A]	0 - 700 μg/ml
Silicon (Crystalline silica particle)	22.90	15.15 - 74.07[A] (CB/SiO_2 mixture) 60.98 – 92.59[A] (Ni/SiO_2 mixture)	0 - 700 μg/ml
Ni (Ni nanoparticle)	0.0058	7.41 – 39.02[A]	10 - 40 μg/ml
NH_4NO_3	-	13.04 – 37.50[B]	18.75 – 75.00 μg/ml 0.23 - 0.94 μM
Zn	0.12	3.60 - 9.47[C]	6.54 μg/ml (100 μM)
Fe(II)	3.81 (total iron)	0.032 - 30.88[C]	0.056 - 55.85μg/ml (1-1000 μM)
Fe(III)	3.81 (total iron)	3.09 - 8.94[C]	5.58 μg/ml (100 μM)
Pb	0.011	0.12 - 62.37[C]	0.21 - 103.60 μg/ml (1-500 μM)

Note: for ERM-CZ120, data represent the mass ratio of respective elements in the particles [for Fe(II) and Fe(III), only the data of total iron was given]. [A] The mass ratio of particles in the mixture of insoluble particle types. [B] The mass ratio of NH_4NO_3 salt in the mixture. [C] The mass ratio of Zn, Fe(II), Fe(III) and Pb in the mixture added to the serum-free medium.

Cultures incubated with particle-free serum-free medium, and serum-free medium containing human TNF-α at 50 ng/ml served as the negative and positive controls, respectively. All samples/controls were run in duplicate per experiment. Three or more independent experiments with the same dose were performed throughout. Delineation of the dosages and the mass ratios of the above chemical components are summarized in Table 2.2. All the sterilized plasticware used for solution preparing, cell exposure, and cell response assays was disposable.

2.6. Measurement of IL-6 and IL-8 concentrations in supernatants

2.6.1. Brief Background Rationale for Selection of IL-6 and IL-8 for Measurement

IL-6 is a pro-inflammatory cytokine that has an important role in both human innate and adaptive immunity.[158] It is involved in acute-phase immune response through several pathways, including the activation and growth of T cells, and the differentiation of both T and B cells. For example, it is speculated to exert an anti-inflammatory effect via inhibiting the expression of pro-inflammatory cytokines and chemokines.[155, 158-159] Known activators of IL-6 expression are IL-1β and TNF. Regarding the production of IL-6, it is widely produced in organs in any organism as almost all stromal cells, which form connective tissues, produce it.[158]

IL-8 is a chemotactic cytokine that can be released by monocytes and epithelial cells upon stimulation of pro-inflammatory cytokines such as IL-1 and TNF-α.[155] Its characterized function is as a neutrophil chemoattractant and activator, and it thus plays a causative role in acute inflammation.[155, 160]

Both IL-6 and IL-8 have been reported to be produced by A549 cells that have been stimulated.[161-162] In this study, the concentrations of these two cytokines in the supernatant of A549 cells following exposure to particles and/or particle components were used to assess the extent of stimulation of the cells as a function of the dose.

2.6.2. Quantitation of IL-6 and IL-8 using enzyme-linked immunosorbent assay

Enzyme-linked immunosorbent assay (ELISA) is a widely used technique to detect and quantify biological molecules presented at physiological concentrations, which for cytokines are typically ng/ml.[163] Following the dose to the particles, the incubation period was 18 hours in duration, after which the supernatants of A549 cells were collected and stored at –80°C until analysis. The longest period of supernatant storage prior to analysis was < 1 month. The concentrations of IL-6 and IL-8 in the supernatants were quantified using ELISA kits (IL-6, model #900-M16, IL-8, model #900-

M18, Cedarlane, Burlington, Ontario, Canada) as per the manufacturer's instructions/protocols.

A sandwich ELISA was adopted in this study. In general, the surfaces of 96-well microtiter plates were covered with a known quantity of capture antibody of IL-6 or IL-8 (goat anti-human IL-6 + d-mannitol or rabbit anti-human IL-8 + d-mannitol) and incubated overnight. Bovine serum albumin (BSA, Lot #A7030, Sigma-Aldrich, Oakville, Ontario, Canada) was then introduced to the plates for the purpose of interacting with specific and nonspecific binding sites. Following that, the samples (cell supernatants) or standard solutions (recombinant human IL-6 + BSA + d-mannitol or recombinant human IL-8 + BSA + d-mannitol) containing antigen, IL-6 and/or IL-8, were applied to the plates. These antigens displace the albumin at binding sites specific to these antigens. A known amount of specific primary antibodies (detection antibody, biotinylated goat anti-human IL-6 + d-mannitol or biotinylated rabbit anti-human IL-8 + d-mannitol) that "sandwiched" the antigen was then added to the plates. Enzyme-linked secondary antibodies (avidin-horseradish peroxidase conjugates for both IL-6 and IL-8) were then added to bind to the primary antibodies. Chromogenic 2,2'-Azino-bis(3-ethylbenzothiazoline-6-sulfonic acid) liquid substrate system (ABTS liquid substrate, Lot #A3129, Sigma-Aldrich, Oakville, Ontario, Canada), were introduced. In the presence of active enzyme, peroxidase, which was linked to the secondary antibodies, the ABTS subtract could become a soluble green product via redox reactions. This visible colour change was associated with the concentrations of antigen in the samples/standards, and was then quantified through the plate reader (Infinite M200Pro, Tecan) at the wavelengths 405 nm and 650 nm (as a reference). A minimum of 3 washes was adopted between each step to wash off the extra/unbound samples/reagents/antibodies. All the ELISA assays were performed in triplicate.

The mean and standard deviation (SD) of the concentrations of IL-6 and IL-8 were determined using the method of external standards and least squares regression analysis (Figure 2.2). The values obtained were then normalized against the positive and negative control, using the equation $s_{final}=\frac{S-N}{P-N}$ (S: samples, N: negative control, P: positive control).

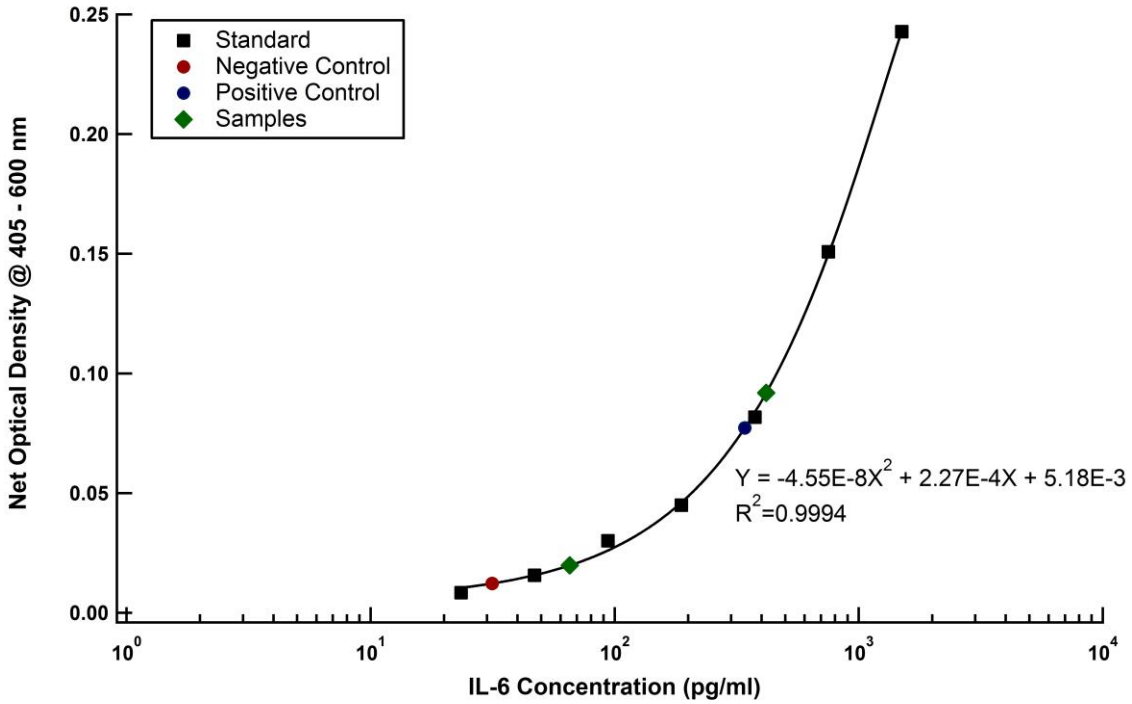

Figure 2.2 **Sample calculation of the concentrations of IL-6 of the positive/negative control and samples using the method of external standards and least squares regression analysis. The IL-6 concentrations of the positive/negative control and 2 samples were calculated as 341.18, 31.43, 417.46 and 0.09 pg/ml, respectively.**

2.7. Trypan blue assay

A dye exclusion test with trypan blue was used to measure the viability of the A549 cells after 18-hour exposure period. Trypan blue is a dye that is added to a cell suspension to visualize non-viable cells. Live cells, having intact cell membranes exclude trypan blue, thus have clear transparent cytoplasm, whereas dead cells have compromised membrane integrity, and will therefore have blue cytoplasm via taking up the dye.[164]

After collection of supernatant, the culture in each well of a 6-well plate was washed three times with 2 ml PBS, and a trypan blue viability assay was immediately performed. Cells were incubated with 2 ml of 5% (v/v) trypan blue in PBS solution at 37 °C for up to 5 minutes, washed three times with 2 ml of PBS solution, and then kept moist with 2 ml PBS. The numbers of viable and non-viable cells were counted using a hemacytometer (0.1 mm, Bright-Line™) and a bright-field microscope (TMS-F, Nikon)

following the procedure of trypan blue exclusion test.[164] The hemacytometer and its coverslip were cleaned with 70% ethanol, and then followed by distilled water.

The viabilities of cells for samples were normalized against negative controls as viability (%) = $\frac{\text{total number of viable cells per ml of sample aliquot}}{\text{total number of cells per ml of negative control aliquot}} \times 100\%$.

2.8. Statistical analysis

The data acquired on cell viability, and the expression of IL-6 and IL-8 are reported as mean values ± standard deviation (1σ). The student t-test was used to compare the cell viability and cytokine expression between samples, and controls and samples. The threshold for statistical significance was set as $p < 0.05$, and when $p < 0.01$ was obtained it is reported.

2.9. Summary

An *in vitro* method using human lung alveolar epithelium cell line A549 cell was developed and used to measure the response of cell cultures to doses of water-insoluble and soluble components of ambient particles. Certified reference ambient particle ERM-CZ120, including its insoluble and soluble fractions, was used. Commercially available carbon black nanoparticles, crystalline silica and nickel nanoparticles which were chosen as laboratory mimics of insoluble diesel soots, re-suspended roadside dusts and an insoluble metal particle type, respectively. Metal nitrate or chloride salts of Zn, Fe, and Pb, and ammonium nitrate were investigated. Cell viability and the expression of IL-6 and IL-8 were adopted to evaluate the cellular response to different particle types/components or the combination of them.

Chapter 3.

Human lung cell responses induced through dosage with whole, or fractions of, an ambient particle type sampled adjacent to a highway

3.1. Abstract

Ambient particle standard ERM-CZ120, a certified particle type, was characterized with respect to effecting lung cell responses *in vitro*. Cultures of lung epithelial cell type, A549, were exposed to the whole particle, the insoluble fraction, and the soluble fraction, at mass concentrations in the supernatant spanning 0 to 1250 µg/ml. Using an incubation period of 18 hours, the induced expression of pro-inflammatory cytokines IL-6, and IL-8, and the extent of cell death as a function of mass dose were measured. At the same mass dosages, the whole particle induced similar cell viability but higher IL-6 expression than the insoluble particle fraction. No differential expression of cytokines and cell viability relative to the negative control was effected by the water-soluble fraction. However, the whole particle effected a dose-dependent expression of IL-6 that was consistently greater than the insoluble fraction, indicating that the soluble fraction does, in fact, contribute to the overall particle toxicity. Thus, the insoluble fraction of particle type ERM-CZ120 is the primary, mass dependent, factor in determining the overall cytotoxicity. The soluble fraction of this particle type is a cytotoxic non-factor when dosed alone, but via endocytosis when dosed together with the insoluble fraction, is then another important factor that is also dose-dependent.

3.2. Introduction

Particulate matter is defined as a heterogeneous mixture of fine solid and liquid material suspended in the atmosphere.[12] Epidemiology studies have concluded that long durations of time proximal to major roadways, either because of occupational or residential or both reasons, is a factor in adverse effects on human health. Consequently, the ambient particulate matter near roadways has been the subject of many studies. Suspended particulate matter proximal to roadways is ubiquitous and at elevated concentrations, as compared to locations further away from roadways.[8] Particle types identified in roadway air samples include soots from incomplete combustion of fossil fuels, vehicular wear materials (e.g., metals, brakes, and tires), re-suspended crustal dusts and road salts, particle types from proximal industrial activities, as well as background particle types from distal emission sources.[10, 14] Each of these particle types, classified chemically based on their emission sources, can be further modified, by homogeneous and heterogeneous tropospheric chemistry.[165] In addition, re-suspended particles can carry on them via sorption, biologics, humic materials, and other dusts. Elucidating what ambient particle component effects what biological response is an open research question.

The effects of different chemical fractions of ambient particles (e.g. water-soluble and insoluble fractions) continue to be investigated. The scientific basis for these studies is, after inhalation, the water-soluble fraction of the particles can separate from the particle and re-distribute in the pulmonary fluid layer. Previous studies suggest it is possible that the insoluble fraction can act independent of, as well as together with the soluble fraction, in interactions with lung tissues and cells that effect downstream responses.[142, 166-168] Several studies have shown the water-soluble particle fraction alone is capable of causing oxidative stress, induction of cytokine production, and commensurate lung injury.[166, 169-170] Specific soluble fraction components such as metal cations, that have the potential to generate reactive oxygen species through a Fenton reaction, were proposed as primary factors in the particles' toxicity.[166, 169, 171-172] Prieditis *et al.* concluded that the toxicity of an atmospheric dust, Environmental Health Center (EHC) -93, was mainly attributed to the soluble particle fraction. Interestingly, Prieditis *et al.* attributed a majority of the toxicity to soluble zinc. Zn, Cu, V, Ni, Fe, Pb, and other metal ions were found in this particulate matter, but Zn and Cu were suggested as the

main contributors to the lung injury and inflammation.[173] A study by Kodavanti *et al.* on the pulmonary responses to residual oil fly ash (ROFA) particles indicated that the water-leachable metal content of the particle is highly associated with the toxic effect of the particles.[171] They suggested that the ions of V and Ni were important. Palleschi *et al.* investigated the soluble fraction of fine airborne particulate matter using a bio-compatible solution as the solvent used for isolation and recovery of the soluble fraction. Their results illustrated that bioactive components induce significant cellular oxidative stress and stimulate cell migration of lung epithelial cells in as short a period of time as a few minutes after contact with the biocompatible solution. They suggested that cations of Cu and Ni, and PAHs from $PM_{2.5}$ were the most probable species responsible for the measured cellular responses. Further, they noted that low molecule weight (MW) soluble components (< 3 kDa) were principal contributors to the oxidative stress,[168, 174] whereas high MW soluble and/or insoluble compounds mainly contributed to oxidation of extracellular thiols and an increase of homocysteine concentration.[168]

The insoluble fraction of ambient particulate matter exerts its toxicity primarily through cell-particle interactions.[142, 166, 175] Adamson *et al.* investigated the toxic effect of different particulate fractions as well as the whole particle of atmospheric dust particle type EHC-93 on rats (e.g., *in vivo*). All samples induced inflammation, however, measurably different responses from different doses were observed. The insoluble fraction was observed to readily recruit macrophages that subsequently lead to the secretion of pro-inflammatory cytokines, whereas the soluble components mainly interacted with lung epithelium.[166] Zou *et al.* found that through cell-particle interactions, the insoluble fraction of $PM_{2.5}$ induced cell membrane damage, which was speculated to allow increased access of water-soluble faction components to the interior of cells.[142] However, there remains no clear definitive experimental result to indicate what species are most important with respect to effecting lung cell responses. For example, other studies have concluded that, in comparison to water-soluble fractions, the insoluble fractions mediate a higher toxic response, via an outcome of endocytosis, whereby toxic water/lipid-soluble compounds, such as endotoxin and metals, are co-internalized.[167, 175-178] In addition, Imrich *et al.* have reported that endotoxin primes alveolar macrophages, and ultimately generate greater, adverse, cellular response.[175] This is of interest as large complex molecules, including and especially endotoxin, readily adsorb onto particles.

Based on this broad base of knowledge, a prevailing school of thought is that both water-soluble and insoluble particulate fractions are capable of inducing toxic effects on lung tissues, though different mechanisms are involved.[142, 166, 177-178] In contrast, many others have no consensus as to whether the water-soluble or the insoluble fraction is the main contributor of the whole particle's toxicity. This is likely due to the heterogeneous nature of individual particles that collectively comprise an ambient particle sample, which in turn makes it difficult to elucidate specifics regarding the biological mechanisms of tissue injuries as to how individual components, and specifically soluble fraction components, contribute to the overall toxicity in these samples.[10, 15, 168-169, 179]

The basis of this thesis is to measure cellular responses following *in vitro* doses of water-soluble and insoluble components of an ambient particle type (this chapter), and then use the method in an effort to elucidate how mixtures of, and individual components of ambient particles effect cellular responses (subsequent chapters). In this chapter, an ambient particle type collected in a high-volume automobile tunnel, identified as ERM-CZ120 was investigated. It is a material that is certified for its elemental components that together constitute 100% of the mass of the material (Table 3.1). The whole particle ERM-CZ120 was subjected to a single step water-soluble fractionation. The two fractions obtained are termed as the water-soluble and the water-insoluble fractions. Both of these fractions, as well as the whole particles, were incubated with lung cells, *in vitro* (human lung epithelial cell line A549). Readouts used in these dose-response experiments were two pro-inflammatory cytokines, IL-6 and IL-8, and cell viability.

3.3. Methodology

3.3.1. Reagents used in culturing

The culture medium, Nutrition Mixture F12 HAM Kaighn's modification (model: F-12K, Lot #N3520), penicillin-streptomycin (10,000 units/ml, Lot #15140122), human tumor necrosis factor-α (Lot #H8916), sodium bicarbonate (bioreagent, Lot #S5761, 99.5%-100.5%) and trypan blue solution (Lot #T8154) were purchased from Sigma–Aldrich (Oakville, Ontario, Canada). Phosphate-buffered saline (PBS, Lot #OXBR0014G), fetal bovine serum (FBS, Lot #12483) and trypsin-EDTA solution

(0.05%, phenol red, Lot #25300-054) were obtained from Fisher Scientific/Life Technologies (Pittsburgh, PA, USA).

3.3.2. Particles and compounds

Certified Reference Material ERM-CZ120 was purchased from Sigma–Aldrich (Oakville, Ontario, Canada). It is an ambient particle type collected in a high-volume automobile tunnel, and certified by the Joint Research Centre – Institute for Reference Materials and Measurement, European Commission. ERM- dust, CZ120 is a PM_{10}-like fine and it is certified for all elements including elemental carbon, silicon, nickel, iron, lead, zinc, arsenic, and cadmium, such that the total mass composition of this material is known (Table 3.1). Note, oxygen is not quantitated, but oxides have been assumed to comprise the remaining mass difference calculated based on the values in Table 3.1. ERM-CZ120 may also contain organic components such as PAHs, and endotoxin (details in Chapter 2), each at low concentrations.

Table 3.1 Mass fraction of the certified elements in ERM-CZ120. Units for the mass fraction are mg/kg.

Element	Mass Fraction	Element	Mass Fraction	Element	Mass Fraction
Al	34100	Fe	38144	Si	229000
As	7.1	Ga	8.7	Sm	4.1
Au	0.02	Hf	8.4	Sr	251
Ba	562.2	K	10998	Ta	1.0
Br	10.2	La	25.0	Tb	0.6
Ca	63043	Mg	13200	Th	7.0
Ce	56.8	Mn	611	Ti	4372
Cd	0.90	Mo	33.2	TC[3]	111333
Cl	10033	Na	14211	U	2.6
Co	14.3	Nd	22.2	V	72.4
Cr	201	Ni	58	W	4.1
Cs	3.1	OC[2]	76633	Yb	1.7
Cu	462	Pb	113	Zn	1240
Dy	3.3	Rb	52.3	Zr	341
EC[1]	45433	Sb	64.7		
Eu	0.8	Sc	7.4		

[1] Element Carbon, [2] Organic Carbon, [3] Total Carbon

The water-soluble fraction and the insoluble fraction of ERM-CZ120 were obtained by suspending whole particles in sterilized deionized water at a concentration of 10 mg/ml. The suspension was sonicated in an ultrasonic water bath for 1 hour and shaken overnight, at normal laboratory temperature, before being centrifuged at 209×g

for 5 mins. The supernatant of the suspension was then filtered and collected as the soluble fraction. The particles that were recovered from the suspension as a pellet were washed 3 times, freeze dried, and then later used as the insoluble fraction of ERM-CZ120. Approximate 54% of the total particle mass was recovered from the suspension as insoluble fraction. Both the soluble and insoluble fraction of ERM-CZ120 were reconstituted in serum-free medium freshly and vortexed prior to use.

3.3.3. Cell culture

The human lung alveolar epithelium cell line A549 (CCL-185, American Type Culture Collection, Rockville, MD, USA) was used in this work. These cells were cultured in F12K medium supplemented with 10% (v/v) fetal bovine serum and 1% of penicillin-streptomycin (10,000 units/ml) at 37 °C in a humidified atmosphere of 5% CO_2 in the air. Prior to dose-response assays, cells were seeded in 6-well culture dishes (surface area/well 8.87 cm^2) and grown to confluence. Cultures incubated with particle-free serum-free medium, and serum-free medium containing 50 ng/ml TNF-α served as the negative and positive controls, respectively.

3.3.4. Exposure to particles/ particle fraction

Stock suspensions of particles, or water-insoluble particle fraction, at 1.25 mg/ml in serum-free medium were made fresh and vortexed for homogeneity. Serial dilutions were performed using the serum-free medium. Aliquots of solutions containing particles/particle fractions were then introduced to A549 cell cultures. For exposure to whole particles and insoluble fractions, the cells were incubated with particles suspended in 2 ml serum-free medium at dosages spanning 0 to 1250 μg/ml.

With respect to the water-soluble fraction, cell cultures were also incubated with the filtered supernatant of particle suspensions in 2 ml serum-free medium, where the dose of water-soluble fraction was calculated based on an equivalent dosage from 0 to 1250 μg/ml through knowledge that the original stock solution of the water-soluble fraction was obtained using ERM-CZ120 particles at 10 mg/ml, and was serial diluted using the serum-free medium.

3.3.5. Measurement of IL-6 and IL-8 concentrations in supernatants

Following the dose to the particles, the incubation period was 18 hours in duration, and then supernatants were collected and stored at –80°C until analysis. The concentrations of two pro-inflammatory mediators, IL-6 and IL-8, in the supernatants were quantified using ELISA kits (IL-6, model #900-M16, IL-8, model #900-M18, Cedarlane, Burlington, Ontario, Canada) as per the manufacturer's instructions. Each ELISA assay was performed in triplicate. The determined concentration of IL-6 and IL-8, mean and standard deviation (SD), were obtained through normalization against the positive and negative control, using the equation $s_{\mathrm{final}} = \frac{\mathrm{S-N}}{\mathrm{P-N}}$ (S: samples, N: negative control, P: positive control).

3.3.6. Trypan blue assay

After collection of the supernatant, each culture in a 6-well plate was washed three times with 2 ml PBS, and a trypan blue viability assay was immediately performed following the procedure of trypan blue exclusion test.[164] The numbers of viable and non-viable cells were counted using a hemacytometer (0.1 mm, Bright-Line™) and a bright-field microscope (TMS-F, Nikon), respectively. The percent viabilities of samples were normalized against negative controls.

3.3.7. Statistical analysis

The data acquired on cell viability, and the expression of IL-6 and IL-8 are reported as mean values ± standard deviation (1σ). The student t-test was used to compare the cell viability and cytokine expression between samples, and controls and samples. The threshold for statistical significance was set as $p < 0.05$, and when $p < 0.01$ was obtained it is reported.

3.4. Results and Discussions

The cytotoxicity of certified ambient particles ERM-CZ120, as well as their water-soluble and insoluble fraction, was measured as a function of the extent of stimulation of lung epithelial cell cultures, type A549. Mass concentrations of the dose in the

supernatant spanned 0 to 1250 µg/ml, the incubation period was 18 hrs, and the readouts were IL-6 and IL-8 by ELISA and cell viability by trypan blue assays.

For the whole particle and insoluble fraction, cell viability decreases with an increase in the mass of particles introduced to the culture medium (Figure 3.1). At the highest dosage used in this study, 1250 µg/ml, 30% of cells were viable after exposure to the whole particles or the water-insoluble fraction. There was no significant difference between the viability trends of the whole particle versus the insoluble particle fraction. The water-soluble fraction of ERM-CZ120 alone had no effect on cell viability up to the maximum dose accessed in this experiment, 1250 µg/ml.

Dose-dependent increases for IL-6 concentration were measured for both whole particles and insoluble fraction (Figure 3.2a). At the same mass dosages, the whole particle effected higher IL-6 expression versus the insoluble particle fraction, which suggests a non-additive effect is realized from the soluble fraction in the whole particle. Interestingly, these outcomes are cytokine specific as the IL-8 concentrations following exposure to the whole particle, or either of its fractions, were not differentiable from the negative control (Figure 3.2b). Similar dose-dependent correlation between doses of the whole particle, water-soluble and insoluble particle fraction and the cellular response has been reported by several previous studies.[142, 174, 178]

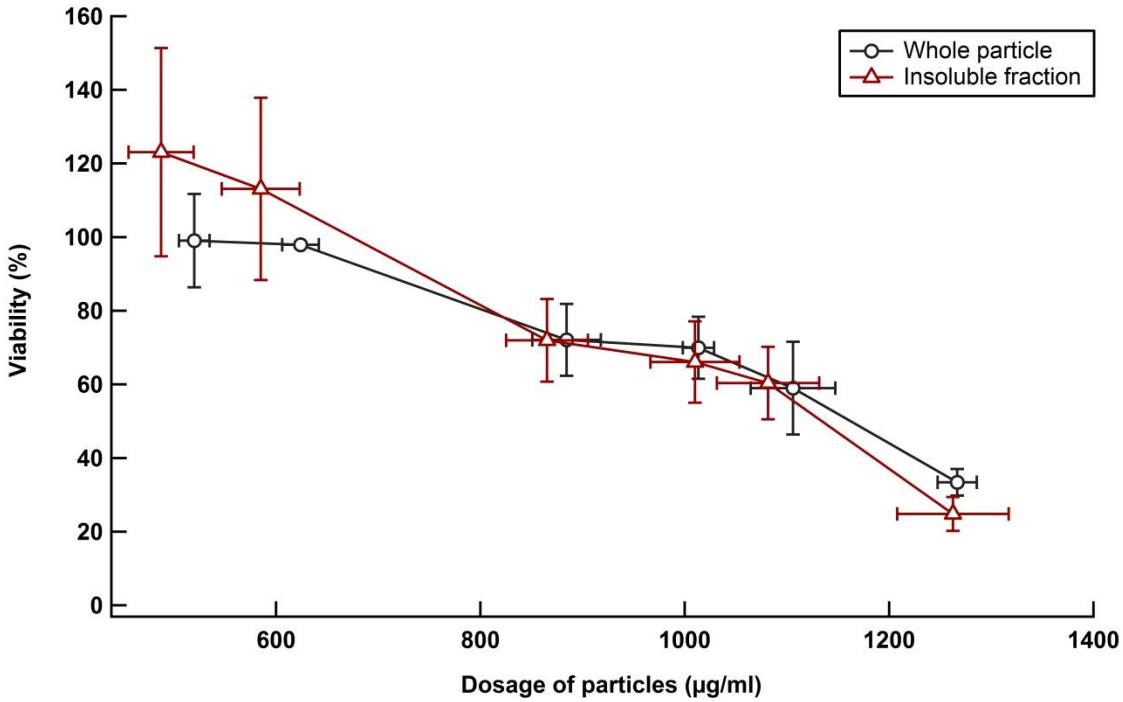

Figure 3.1 Normalized cell viability following 18 hrs incubation of A549 cells as a function of dose of particle type EMR-CZ120, and its water-insoluble fraction. Each data point corresponded to averages of more than three samples (n ≥ 3), and reported as mean values ± standard deviation (1σ). The x-axis and y-axis propagated uncertainties arose from standard deviations of the dosages and the cell viabilities of the samples, respectively.

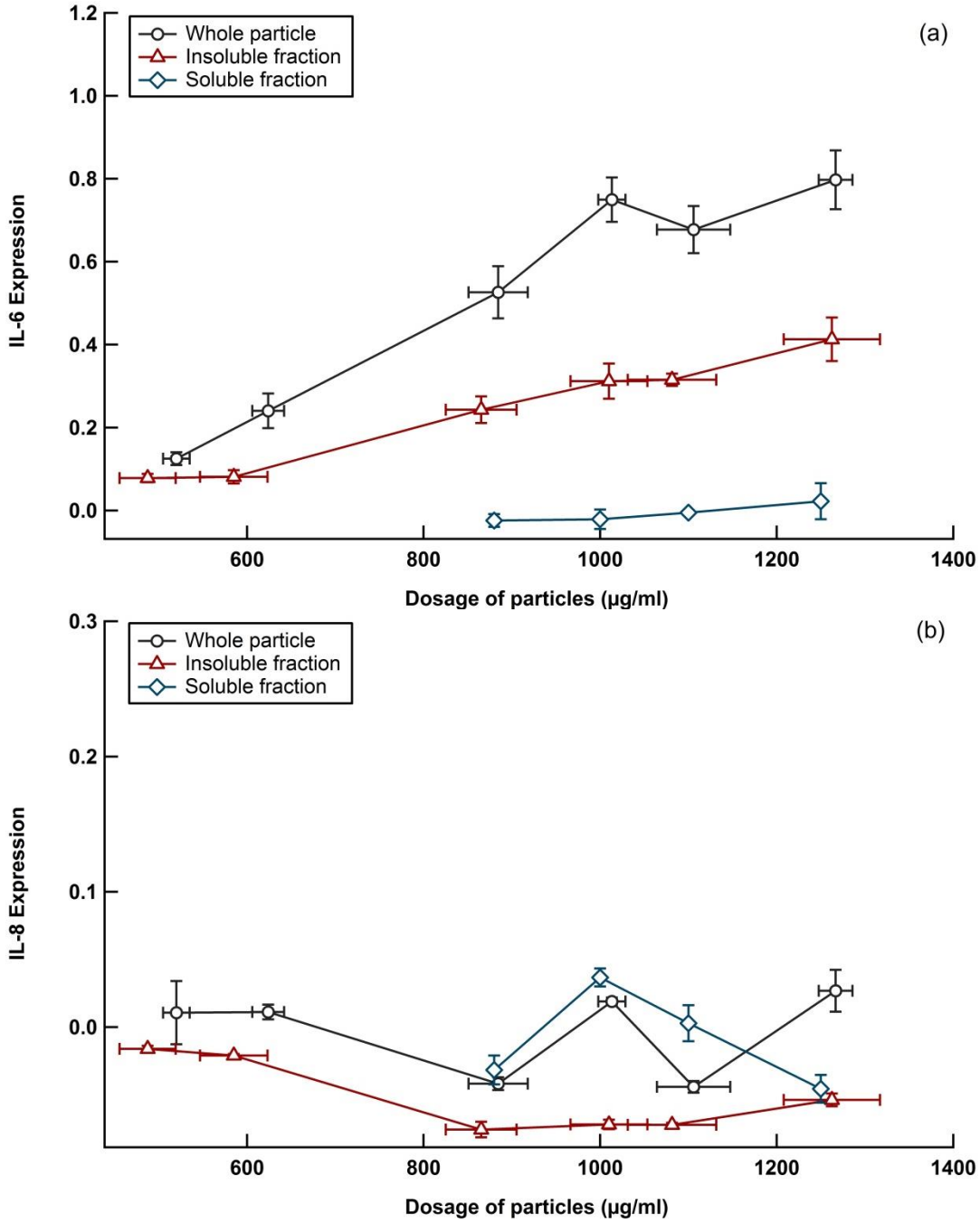

Figure 3.2 **Normalized a) IL-6 and b) IL-8 expression following 18 hrs incubation of A549 cell cultures as a function of dose of particle type EMR-CZ120, the water-soluble fraction and the insoluble fraction of EMC-CZ120. Each data point corresponded to averages of three or more samples (n ≥ 3), and reported as mean values ± standard deviation (1σ). The x-axis and y-axis propagated uncertainties are from standard deviations of the dosages, and the individual cytokine expression levels, IL-6 or IL-8, as a function of the dose, respectively.**

The A549 responses to doses of the whole particle, the water-soluble fraction, and the insoluble fraction of ambient particle type ERM-CZ120 illustrate the significant role of endocytosis in health outcomes due to particulate air pollution. The water-soluble fraction alone effects no differential expression of cytokines IL-6 and IL-8 relative to the negative control, yet clearly, it has an assignable role in the overall response of the whole particle type ERM-CZ120 (Figure 3.1 and Figure 3.2). This result, in general, agrees with other studies of insoluble and soluble fractions of ambient particle types, where cellular responses to the individual soluble plus insoluble fractions do not sum to the response from the whole particle.[142, 161, 169, 174, 176, 180] For instance, Fujii *et al.* investigated the cytotoxicity of ambient particle EHC-93 on human bronchial epithelial cells (HBECs), and measured dose-dependent trends for cytokine expression for the whole particle, whereas the soluble fraction of EHC-93 did not simulate differentiable cytokine expression relative to the control.[181] Jalava *et al.* investigated the inflammatory and cytotoxic effects of both fine and coarse particles, including their water-soluble and insoluble fraction, as well as the organic-solvent-soluble and insoluble fraction. In that study, the insoluble particle fraction effected the highest cellular response of the macrophage cell line used.[177] Huang *et al.* found that the cytotoxicity of both coarse and fine particles was dependent on exposure time and concentration. Soluble components such as inorganic ions (nitrates, sulfates, and ammonium) and organic components might cause the cytotoxicity synergistically or additively with metals.[174]

Numerous studies have measured the role of the water-soluble components such as metal ions for the purpose of investigating the hypothesis that the main contributor of the toxicity was attributable to the water-soluble particulate fraction.[170, 172-173] In fact, this hypothesis has been shown for compounds such as biologics, where a receptor is presented on the cell exterior that selectively recognizes the biologic compound, which triggers an immune response.[167, 175-178] Imrich *et al.* found that certain particle types readily adsorbed components such as endotoxin, a biologic, that itself effects strong cellular response.[175] Conversely, with respect to the results presented in this chapter for water-soluble metal ions, rather than inducing cytotoxicity directly, the water-soluble metals, and other soluble components that may present, do not effect A549 cellular response alone, but this fraction does effect synergistically cellular responses when introduced together with insoluble components. The most probable mechanism is that

the water-insoluble particle components play a role as carriers, via endocytosis, for the water/lipid-soluble components. In addition, the cell-particle interactions could cause cell membrane damage which can facilitate greater internalization of the water-soluble fraction compounds.[142] These reports, as well as the current study, emphasize the critical role of endocytosis when species that have no receptor expressed in the cell membrane are presented to intact viable cells.

3.5. Conclusion

Following 18-hour incubation period for A549 cultures with ambient particle type ERM-CZ120, pro-inflammatory cytokine IL-6 expression, and cell death was measured for both the whole particle and the water-insoluble fraction in a dose-dependent manner. No differential expression of cytokines and cell viability relative to negative control was effected by the water-soluble fraction alone. However, the whole particles lead to higher IL-6 expression than the insoluble fraction at the same mass dosages, suggesting that the soluble fraction does have an assignable effect but only when dosed together with the insoluble fraction. No differential expression of IL-8 relative to the negative control was measured for either the whole particle or any of its fractions. This data is the basis of our recommending studies that measure cellular responses to learn of interactions between different particle components to identify the most significant components of ambient particle types causing adverse effects on human health.

Chapter 4.

Human lung cell responses caused by insoluble particle types that are mimics of major particle types adjacent to roadways

4.1. Abstract

Three insoluble particle types, carbon black nanoparticles, crystalline silica particles, and nickel nanoparticles, and interactions between them have been measured as a function of dose, by mass, with respect to effecting lung cell responses *in vitro*. Responses measured were pro-inflammatory cytokines IL-6 and IL-8, and the extent of cell death. No differentially measurable effect on cell viability or cytokine expression was observed for nickel nanoparticles at dosages ≤ 100 μg/ml in the serum-free medium. Crystalline silica, at a nominal diameter ~ 2 μm, lead to the lowest cell viability and the greatest cytokine expression for a given total mass dosage as compared to CB alone, or a mixture of CB nanoparticles and crystalline silica. Mixtures of CB and crystalline silica, at three different mass ratios, were observed to effect additive mass effects with respect to decreased cell viability and increased IL-8 expression. Interestingly, a non-addictive lung cell response for IL-6 was measured for the mixture of CB plus crystalline silica in specific doses. These results illustrate that specific mixtures of particle types can generate cellular expression that is greater than an equivalent mass dose of either particle type alone, but this result certainly has limits/restrictions. Similarly, 10 μg/ml nickel nanoparticles plus crystalline silica induced significantly higher IL-6 expression at both low and high silica dosages as compared to crystalline silica alone.

4.2. Introduction

The ambient particulate matter has been correlated positively with adverse health effects through numerous, independent, epidemiology studies.[10, 15, 26, 28, 182-183] Traffic-related air pollutants, either a direct outcome of their chemical compositions and/or the fact that the concentrations of these pollutants are elevated adjacent to roadways, have a high correlation to adverse effects on human health.[183-184] Short-term exposure to roadside particles can lead to pulmonary inflammation and exacerbation of the respiratory/pulmonary diseases, such as asthma; whereas chronic exposure is associated with respiratory/pulmonary diseases, atherosclerosis, and cardiovascular diseases.[8, 10, 14, 183-185] Proximal to major roadways, ubiquitous particle types include soots from incomplete combustion of fossil fuels, vehicular wear materials (e.g., metals, brakes, and tires), re-suspended crustal dusts and road salts, particle types from proximal industrial related activities, as well as background particle types from distal emission sources.[10, 14] Of the traffic-derived PMs, diesel exhaust particles can comprise up to 90% of the particles in the world's largest cities.[186-187]

Results obtained using reference ambient particle type ERM-CZ120 indicate that the insoluble fraction of the particles induces IL-6 expression and cell death at high mass dosages. The insoluble fraction has an important role in particles' cytotoxicity, as has been well documented in the literature, but, in addition, it is becoming clear that the insoluble fraction plays a critical role of transporting soluble compounds into cells, via endocytosis (e.g. Chapter 3). In this chapter, three laboratory mimics of ambient particle types were used: CB nanoparticles to represent diesel soot, crystalline silica particles to represent re-suspended road dusts, and nickel nanoparticles to represent an insoluble metal particle type. The effects of dosing these particle types individually, as well as binary mixtures thereof, were studied by measuring select lung cell responses *in vitro*. Through the study of a single particle type dose, and then a binary particle type dose, two questions were investigated: is there a measurable differential role of a particle type's physical and chemical characteristics relative to another particle type, and is there a non-additive interaction between different particle types, as a function of total particle mass dose, as ascertained using specific cellular responses?

4.2.1. Background on Carbon Black

Carbon black is a commercially available commodity made through a highly defined and controlled partial combustion, thermal decomposition process of hydrocarbons. Hydrocarbon combustion, from lower molecular weight fuels to coal tars, in internal combustion engines rarely leads to complete combustion, and thus, worldwide, the study of soots is an environmentally important area involving many diverse themes of study.[56, 188-189]

CB is manufactured in the format of small elemental carbon particles. Primary particles, as being described as nodules, are roughly spherical with diameters varying from 5 to 500 nm.[56, 123, 188-189] Inside the particle, there is a relatively disordered nucleus oriented centrically with imperfect graphite layers. The carbon layers are generally parallel to each other, but their relative positions and sizes are irregular.[188-189] Through particle-particle collisions and the further deposition of carbon, primary particles can aggregate together into grapelike in appearance chains or clusters, termed aciniform aggregates.[56, 188-189] Approximately 99% of particulate carbon in CB is aciniform. In turn, aciniform aggregates may form agglomerates through van der Waals forces.[56] The surface area of CB varies widely, and it is dependent on its structure. For example, due to the large primary particle size and low degree of aggregation, coarse thermal black particles have surface area as small as 8 m^2/g, whereas pigment grade CB can have surface area up to ~ 1000 m^2/g.[188] CB having large surface area is the result of a porous structure, thus the aggregation tends to not affect the surface area and other characteristics of particles generated by particular modification.[56, 190]

CB composition does depend on its raw material, manufacturing process, and post-production processing.[56, 188-189] More than 80 wt% of CB is element carbon. It may also contain hydrogen, nitrogen, and sulfur, but the quantities of the impurities are usually minimal, each at less than ~ 1 wt%.[188] The presence of air in the manufacturing process and oxidative after-treatment leads to oxygen content up to 15 wt%. These oxidized CB particles have surface properties different from CB produced using other processes due to the oxygen atoms bound to their surfaces, which present acidic or basic functional groups depending on the conditions.[188] Other impurities include alkali and alkaline earth metal salts which are from the water used in the manufacturing process, and trace amounts of organic compounds that strongly adsorb on the surfaces

of the particles.[56, 188-189] It is reported that the soluble organic fraction of CB is less than 0.5 wt%.[188] The dominant organic compounds in this fraction are PAHs.[188-189] These organic compounds are usually biologically inactive, and can only be isolated by continuous extraction with strong organic solvents due to the large surface area of CB particles and their low organic loading.[56, 188, 191]

In vitro studies suggest that CB nanoparticles cause oxidative stress, pro-inflammatory effects, genotoxicity, and cell death.[123-124, 190-195] One of the mechanisms is the generation of reactive oxygen species through interactions between cells and the particle surfaces.[123-124, 191] Chuang *et al.* found that CB caused oxidative stress and DNA damage in rats. Particle surface area and chemistry are expected to be important regarding interactions with cells and generating self-mediated free radicals.[196] Hussain *et al.* measured a positive correlation between the oxidative stress and inflammatory effects of CB nanoparticles and the Brunauer–Emmett–Teller (BET) surface area of individual particles. Production of H_2O_2 was also observed, and it played an important role in the process of ROS generation.[190] In general, CB particles' ability to generate ROS is related to surface properties such as specific reactivity of available sites and their abundance (e.g., surface area). However, mechanistic details are not yet available.[123, 191]

CB nanoparticles can interact with expressed membrane proteins due to their strong absorption ability, which is generally thought to lead to complicated consequences.[123] These non-specific interactions can activate or inhibit proteins by causing denaturation and/or conformational changes on proteins, and as a result, lead to a variety of cell functions to be activated or disrupted. For instance, through interacting with enzyme and cytokines, CB particles have been documented to disturb cell metabolism and immune response.[123-124, 191, 197] Moreover, it is reported that nanoparticles can also interact with cytoskeletal or bind to intercellular junctional proteins, and induce alteration of cell signalling, migration, and autophagy.[124] Simultaneously, interactions between CB nanoparticles and proteins also affect the particle's surface properties, including reactivity and aggregation state, and thus influence the process of particle internalization and the particle's toxicity.[123, 198]

Both high levels of oxidative stress caused by excess ROS and the interactions between CB particles and cell proteins can initiate inflammation, cytotoxicity and

apoptosis.[123-124, 191, 199] Hussain *et al.* found that exposure to CB nanoparticles can lead to apoptosis of bronchial epithelial cells through a ROS dependent mitochondrial pathway. The process is known to involve H_2O_2 production, mitochondrial surface-potential perturbation, caspase activation, the release of pro-apoptotic factors and DNA fragmentation.[124] Mroz *et al.* suggest that CB nanoparticles can induce DNA single-strand breaks and pro-inflammatory transcription factors activation on A549 cells.[195]

As a nanoparticle, CB can cause adverse effects on the cardiovascular system directly by translocating to the bloodstream and/or interacting with platelets and the vascular endothelium, and/or indirectly through causing local inflammation which may lead to further tissue inflammation and potential destabilization of pre-existing atheromatous plaques.[123, 188, 191, 199-201] An *in vivo* study reported that rat exposed to a high dosage of CB with an exposure duration of 24 months developed increased lung tumor incidence, which was believed to be due to the inability to clear the lung when challenged by an excessive particle burden.[202] This phenomenon was summarized as "lung overload", and it is not restricted to CB nanoparticles as evidenced through rat exposure to high doses of any low-toxicity insoluble particle types.[188, 203-204] In contrast to the above-cited rat-based studies showing that insoluble particle types are toxic at high dosages, but related studies on humans having workplace compliance with safety regulations have shown that humans in the CB industry indicate no health hazards.[188-189, 204]

Generally, CB is viewed as an example of a low solubility, low toxicity particle type and due to its high purity, it has used as a reference material in studies investigating particle toxicity.[123, 188, 191, 204] Recall that CB without oxidative treatment is > 95% by mass is elemental carbon, and adsorbed on the CB surfaces are metals and organic compounds, whose overall toxicity is considered negligible.[188] In the report of IARC (international agency for research on cancer) in 2010, CB was classified as group 2B, which is defined as possibly carcinogenic to humans, based on the criteria that there is inadequate evidence in humans, but sufficient carcinogenic evidence in experimental animals as well as evidence on potential mechanisms for the carcinogenicity of CB.[204]

In this study, CB nanoparticles were adopted as a mimic of soots. However, there are many differences between soots and CB. As an unwanted by-product, soots are produced through uncontrolled partial combustion or pyrolysis of carbonaceous

materials, such as coal, gasoline and diesel fuels, wood, fuel oils, and waste oils.[55, 189] Soot physical and chemical properties, as overviewed in Chapter 1, are highly variable as they depend on the starting materials and the combustion conditions.[55, 189, 205] Generally, CB nanoparticles and soots are distinct in physical structure, chemical composition, and toxicity (Table 4.1).

Table 4.1 Differences between CB and Soots

	CB	Soots
Physical structure	Aciniform	aciniform carbonaceous microgel carbon cenospheres coke and char fragment
Chemical compositions	> 95 wt% elemental carbon, with trace quantities of ash (< 1 wt%) and SOF(< 0.5 wt%) [A]	< 60 wt% elemental carbon, with variable percentages of SOF, metals, and other components are viable[B]
Toxicity	Low toxicity, possibly carcinogenic to humans (Group 2B) [C]	High toxicity, carcinogenic to humans (Group 1)[C]

[A] Date from[188], [B] data from[56], [C] data from[204 206]. SOF = soluble organic fraction.

Although soots have similar generation processes as CB, including nucleation, aggregation, and surface growing process, their particle structure can range from amorphous to graphitic or even fullerenic due to different emission sources and thermal history.[55-56, 205] Aciniform carbon is predominant in diesel engine exhaust soots, and it has been reported that the particulate portion of diesel soot has similar carbon structure as CB.[207-208] Recall, as previously mentioned, approximately 99% of the particulate carbon in CB is aciniform, which can be characterized as colloidal size, grapelike aggregates of imperfect graphitic structure particles.[56, 189] However, the subsequent deposition of carbonaceous materials, such as crosslinked resins, can cement the aciniform carbon particles together, and form carbonaceous microgels (carbon or carbonaceous material embedded with spheroidal colloidal dimension carbon particles), termed xerogels that have large size distribution.[189, 207, 209] Additional types of carbon particles that are found in soots include carbon cenospheres (porous or hollow carbon spheres with diameters of 10-100 µm, formed by carbonization of liquid drops without shape change), coke and char fragments (fragments of carbonized wood or coal with dimensions from millimeters to micrometers).[56, 189, 207]

CB particles have ~ 95 wt% element carbon, whereas the mass fraction of elemental carbon in soots is less than 60 wt%.[56, 188] A larger percentage of soluble organic fraction (SOF) and inorganic impurities/ash can be found in soots relative to CB.[55-56, 189] For instance, diesel soot contains 20 to 40 wt% of organic compounds, among them, PAHs and their derivatives comprise approximately < 1 wt%, and PAHs are associated with adverse health effect. Nitrate, sulfate, transition metals, and other trace elements may also be found in diesel soot.[209] As a consequence, soots are much more toxic than CB.[55-56, 189, 206] For instance, numerous studies have demonstrated that soots effect adverse outcomes on humans, such as respiratory irritation, pulmonary inflammation, exacerbation of cardiovascular diseases and even cancer.[55-56, 189, 206, 209] IARC evaluated soots as carcinogenic to humans (group 1, defined as carcinogenic to humans).[55, 206]

4.2.2. Background on Silica

Silica and siliceous minerals are the major constituents of the earth's crust. 12-14 wt% of the lithosphere is quartz, which is one of the crystalline forms of silica.[210-211] In PM_{10}, silica is ubiquitous. Sources of airborne silica are construction activities, dust from paved roads and unpaved roads, agricultural operations, wind erosion, volcanic eruptions, and mining and quarrying.[212-213] Several amorphous and crystalline forms of silica are known.[212] The majority of the free silica (pure crystalline silica) is in the form of quartz. Other crystalline forms include tridymite and cristobalite.[146, 210, 212-213] In this study, quartz was selected for study due to its abundance in ambient particles. The phrase "crystalline silica" implies quartz unless another form of crystalline form silica is specified.

There are two dimorphs of quartz, α-quartz and β-quartz, which are temperature dependent. The structure of quartz is a three-dimensional helix framework that is composed of either three or six silicon tetrahedra along the trigonal c-axis. Below 573 °C, quartz is in the form of trigonal α-quartz, and above 573 °C, it converts to hexagonal β-quartz.[146, 213] Silicon tetrahedra are the basic structural units of quartz. In each unit, a silicon atom is surrounded by four oxygen atoms, and each oxygen atom is common to two tetrahedra.[5, 146, 210-211]

Generally, the purity of quartz is high, but the chemical compositions of quartz are affected by its sources. For commercial products, the preparation process may also affect their compositions.[146, 212-213] Major impurities include Al, Fe, Li, Na, K and Ca, yet their concentrations are usually below 1 wt%.[146, 149] Metal ions such as Al^{3+} and Fe^{3+} can substitute Si^{4+} in the tetrahedra, and at the same time introduce monovalent or divalent cations including Li^{+}, Na^{+}, K^{+}, Mg^{2+} and Ca^{2+} to the interstitial sites. Moreover, the metal ions can also form non-bridging oxygen sites in the lattices.[146, 210]

Inhalation of crystalline silica is associated with adverse health effects. At the cellular level, crystalline silica induces the generation of ROS, which in turn leads to the secretion of cytokines and pro-inflammatory mediators, which may cause membranolysis, lipid peroxidation, DNA damage, and cell death.[131, 214-215] It is believed that the surfaces of quartz, especially the silanol groups (Si-OH) and ionized silanol groups ($Si\text{-}O^{-}$) on the particle's surfaces, play an important role.[129-131] The quartz planes can be cleaved or fractured when the quartz is ground, and lead to homolytic and/or heterolytic cleavage of Si-O bonds, as a result, $Si^{\cdot}$ and $Si\text{-}O^{\cdot}$ radicals (for homolytic cleavage) and Si^{+} and $Si\text{-}O^{-}$ ions (for heterolytic cleavage) can be generated. [131] Generally, silanol and ionized silanol are viewed as the main "active sites" attributing to quartz toxicity.[149-150] Freshly fractured quartz is speculated to be more toxic than an aged one due to its relatively higher surface reactivity.[5, 129, 149] In aqueous environments, such as in lung lining fluid, those surface radicals can give rise to ROS including $OH^{\cdot}$ and H_2O_2 in the lung lining fluid. In the presence of water or H_2O_2, surface radicals of quartz can form silanol and $OH^{\cdot}$ through following reactions:

$$\text{-SiO(•)} + H_2O \rightarrow \text{-SiOH} + \text{HO(•)}^{-}$$

$$\text{-SiO}_2\text{(•)} + H_2O_2 \rightarrow \text{-SiOH} + \text{HO(•)} + O_2$$

$$\text{-Si}^{+}\text{O}_2\text{(•)}^{-} + H_2O_2 \rightarrow \text{-SiOH} + \text{HO(•)} + O_2$$ [109,110]

A silanol can bind to bio-macromolecules though hydrogen bonding. The binding can modify the particles' toxicity in several ways, for example, reduce the toxicity of the particles by preventing the direct contact between the particles and the molecules or enhance the toxicity by activating the immune system.[131, 215] Further, ionized silanol can interact with the cell membranes.[131]

In interacting with phagocytic cells, crystalline silica can also induce oxidative stress by stimulating a respiratory burst.[130] Phagocytosis of particles is capable of stimulating a sudden increase in oxygen consumption by the cells, and as a consequence, there is an increased production of ROS such as $O_2(\bullet)^-$ and H_2O_2, and NO.[129-130, 216] The reaction between NO and $O_2(\bullet)^-$ yield NO_2^- which is one of the important reactive nitrogen species (RNS).[129, 216] Both ROS and RNS are able to react with various biological targets directly, such as DNA, proteins, and lipids, and thereby cause damage to cells.[5] Fanizza *et al.* found that short-term exposure to α-quartz can induce direct oxidative DNA damage and cell death of A549 cells in a dose-related manner.[217] Chu *et al.* observed that cell damage caused by crystalline silica nanoparticles, which included mitochondrion multiplication and DNA fragmentation, was associated with an increased level of ROS in the cells.[214] Duffin *et al.*, in using DQ12 quartz, a commonly used commercial product in laboratory studies, measured increased chemokine expression and activation of an important pathway in inflammation, nuclear factor kappa beta (NF-κB), that depended on the particles' surface reactivity.[30] This type of cell damage leads to the apoptosis of the cells, spanning alveolar macrophages to epithelial cells, with subsequent further inflammation and fibrosis.[131, 216, 218]

One well-known occupational disease caused by exposure to crystalline silica is silicosis, caused by inhalation of respirable crystalline silica (crystalline silica particles with diameters < 10 μm), and can be categorized into four types: acute, chronic, accelerated, and complicated silicosis.[212-213] Silicosis is a fibrotic lung disease. Acute silicosis is exposure to very high concentrations of silica dust, and is usually fatal over a period of 1-3 years. Its cause is attributed to fluid accumulations from cell debris and surfactants in the upper and middle regions of the lung, inducing further damage in alveolar cells that manifest as shortness of breath and other symptoms characteristic of pulmonary edema. Chronic silicosis is the most common type of silicosis. It is caused by long-term exposure (≥ 10 years) to low concentrations of silica dust. The interaction between quartz particles and lung tissues also induce the recruitment and activation of pulmonary macrophages, that in turn leads to the secretion of fibrogenic factors such as interleukins and growth factors which stimulate the production of collagen. The collagen produces silicotic lesions through hyalinization. Further growth of silicotic lesions leads to fibrotic scars in the lung tissue, which is the main characteristic of chronic silicosis. The main symptoms include a dry cough, sputum production, and reduction of

pulmonary function. Accelerated silicosis is due to exposure to high levels of silica in a period shorter than chronic silicosis (around 5-10 years). It shares some symptoms with chronic silicosis, but the development processes are faster. Asymptomatic silicosis is described as early onset stage of the disease, but there is no symptoms present.[131, 212-213, 216]

In addition to silicosis, inhalation of silica can lead to other airway/lung diseases such as bronchitis, pulmonary tuberculosis, rheumatoid arthritis, and lung cancer.[212-213] IARC classified crystalline silica (quartz and cristobalite form) as group 1, which is defined as carcinogenic to human, suggesting that sufficient evidence in both animal and human exists.[146]

Metal impurities such as Al and Fe modify the toxicity of the quartz particles.[131, 149] Aluminum salts decrease the toxicity of quartz particles. Duffin *et al.* reported that the treatment of aluminium lactate on DQ12 quartz can reduce the generation of $HO^{\cdot}$ and thus decrease the damage of the cells.[30] Bégin *et al.* in using a sheep tracheal lobe model observed that quartz treated by aluminium lactate demonstrated less pathologic score than untreated quartz. It was suggested that aluminium salts can bind on the surfaces of the quartz particle, especially the “active sites” such as silanol, thus lower the bio-activity of the particles, and accelerate the clearance of the particles from the lung.[150] For iron, it appears more complicated. Iron ions can catalyze the generation of ROS through the Fenton reaction, however, metallic iron [Fe(0)] is reported to protect against the toxicity caused by quartz.[5, 129, 131, 149] Castranova *et al.* found that freshly milled quartz having high Fe contamination lead to higher ROS generation and stronger inflammatory effect as compared to quartz having low Fe contamination.[151] Cullen *et al.* investigated the effect of particulate and ionic iron on the toxicity of quartz *in vivo*. Only particulate iron showed the ability to decrease the inflammatory effect of quartz. No effect of ferrous/ferric iron on quartz surface radical production was observed. However, the mechanism of the protective effect is unclear yet.[152] In conclusion, iron is believed to react with the ROS generated by quartz particles in an indirect way, unlike aluminium which interacts directly with active sites on particle surfaces.

In this study, crystalline silica particle was chosen as a mimic of re-suspended road dust. In the environment, quartz is usually mixed with different kinds of particles and chemical components. Those particles and components in the mixtures may modify

the surface properties of quartz, and as a result, affect its toxicity in different ways. The average concentration of quartz in ambient air across 22 U.S. cities were measured by EPA Inhalable Particulate Network (IPN) in 1980, and the mass ratio of quartz ranged from 1.0% to 9.0% (avg. 4.9%) in coarse particles, and from 0% to 2.6% (avg. 0.4%) in fine particles.[212, 219] Near roadside, the main sources of quartz include the minerals used for road pavement, and dusts from unpaved roads and the shoulders of paved roads.[161, 212-213] Hetland *et al.* analyzed 4 types of road pavement minerals and roadside PM_{10} samples, and found that both the chemical components and the cytotoxicity of PM_{10} samples were similar to those of the minerals used for road pavement. The content of quartz in the roadside PM_{10} samples is 24%. Metal components such as Fe and the treatment during asphalt production may modify the toxicity of the mineral particles.[161]. In general, the interaction between quartz particles and other types of particles, or particle components, is not well characterized, and thus it should be investigated as it could be a significant source of the observed adverse effects on human health.

4.2.3. Background on Nickel

Nickel is a silver-white metal that occurs naturally in the earth' crust at an abundance ~ 0.009%.[220] Due to its ability to increase a metal solid's strength, corrosion/temperature resistance, and overall toughness when alloyed with other metallic elements, nickel is widely used in metallurgical, chemical processing and nanomaterials industry in the manufacturing of stainless steels, alloys, electroplating, catalysts, nickel-cadmium batteries, and pigments.[220-222]

Natural sources of atmospheric nickel include windblown dusts, volcanic emissions, rocks/soils weathering, and forest fires.[223-224] Anthropogenic sources include industrial processes spanning mining, melting, refining, to alloy production, combustion of fossil fuels, and waste incineration.[222-223] Tobacco smoking is also a source of nickel exposure.[224] Among the different sources, fossil fuel combustion, specifically coals and heavy oils, is reported as the main contributor of atmospheric nickel.[222] Ambient particles containing nickel deposit into surface waters and soils, and lead to the accumulation of nickel by plants and animals.[225]

Airborne nickel is predominantly in the particle phase, and the concentration varies depending on the source. It has been reported that the average airborne nickel

levels are 0.01-3 ng/m^3 in remote areas, 3-30 ng/m^3 in urban areas without metallurgical industries, and 0.07-0.77 µg/m^3 in industrialized areas that utilize Nickel.[224] Based on a survey conducted in 11 Canadian urban cities and one rural site from 1987 to 1990, the annual mean concentration of nickel was 1 ng/m^3 for the rural site, and ranged from 1 to 20 ng/m^3 for urban areas, with maximum values from 6 to 77 ng/m^3.[226] A point source study indicated that the background annual mean nickel concentrations in Canadian Shield and Great Lakes region range from 0 to 1.46 ng/m^3, while the nickel concentrations measured close to the nickel/copper smelters in Sudbury are 46-151 ng/m^3, which accounted for approximately 0.67% of the total PM_{10}.[227] For the general population, food and water uptake is the main exposure route of nickel instead of inhalation. It is reported that, for non-smoking urban residents, the daily uptake of nickel is below 0.0008 mg through inhalation, while it is ~ 0.1-0.3 mg via food. However, for occupational exposure to nickel, inhalation is the primary route.[225] An occupational study of nickel exposure in a nickel refinery in Norway indicated an average concentration of nickel ≤ 0.7 mg/m^3 in the breathing zone for all workers.[228] Dermal contact is another pathway for both occupational and general exposure.[224]

Inhalation of nickel involves the following forms: particles of insoluble nickel compounds, aerosols derived from soluble nickel solutions, and gases containing nickel species (e.g. nickel carbonyl).[224] The different chemical formation and physical properties, such as solubility, do affect the species toxicity. Soluble nickel species dissolved in the mucus are cleared rapidly from tissues through ciliary transport. However, less soluble nickel particles can enter cells by phagocytosis, and slowly dissolve inside the cells and in so doing provide an extended exposure period to high cellular levels of Ni^{2+}.[222, 224-225, 229] Generally, the less soluble species, including nickel oxides and sulfides, are more carcinogenic than the soluble nickel species, such as nickel chloride or nitrate.[222]

Inhalation exposure to nickel has been associated with various adverse health effects. Short-term high-dose exposure can induce nasal cavity damage, lung irritation, hyperplasia of pulmonary cells, fibrosis, pneumonia, and emphysema. Chronic exposure is speculated to contribute to respiratory disorders such as asthma and bronchitis, pneumoconiosis and lung cancer.[222-223, 230] It has been reported that nickel refinery workers have a significantly higher risk of pulmonary and nasal cavity cancers as compared to a control population. Higher mortality due to non-cancerous lung diseases

has also been observed.[230] The International Agency for Research on Cancer (IARC) has classified nickel compounds as group 1 (carcinogenic to humans).[222]

The mechanism of nickel's toxicity is not yet fully understood. It has been suggested that Ni could be involved in Fenton chemistry, and lead to the generation of ROS in the presence of strong oxidizers such as H_2O_2 and ascorbate in the cytosol and nucleus.[5, 229-230] Note that Ni^{2+} does not directly participate in redox cycling reactions. However, through chelation with biological ligands, the reduction potential of Ni^{2+} can be altered, thus allowing the oxidation of Ni^{2+} to Ni^{3+} by a strong oxidant.[5] Intracellular glutathione depletion and oxidative damage including lipid peroxidation and DNA depurination induced by Ni have been observed.[229-232] As a carcinogen, Ni can also interfere with cellular metabolism, and cause genotoxicity by replacing essential metals such as Fe(II), Mg(II) and Ca(II) in enzymes and proteins, or binding to cellular compounds including nuclear proteins and DNA.[224, 229-230] Salnikow *et al.* found that exposure of A549 cells to Ni^{2+} lead to the production of ROS and the activation of Hypoxia-inducible factor (HIF) -1 transcription factor, which is associated with cell survival and lung cancer. The activation of HIF-1 was proposed due to the substitution of iron by nickel in the oxygen sensor.[233] Through complexing with heterochromatin, Ni is implicated in methylation of DNA, gene silencing and chrome condensation. The mechanism is not clear, but the replacement of magnesium by nickel in the DNA backbone is proposed to be a factor.[229] Through interactions with repair enzymes, Ni can also inhibit DNA repair.[234] A former colleague of our group has studied the cellular response to soluble nickel plus amorphous silica particle at a mass ratio of 5,000 ppm using co-culture of THP-1 cell and A549 cell. No differential IL-6 or IL-8 expression was measured for cells dosed with Ni^{2+} plus amorphous silica particles relative to the response of cells dosed with amorphous silica particles alone.[235] In this study, nickel nanoparticle was chosen as a representation of insoluble metal particle.

4.3. Methodology

4.3.1. Reagents used in culturing

The culture medium, Nutrition Mixture F12 HAM Kaighn's modification (model: F-12K, Lot #N3520), human tumor necrosis factor-α (Lot #H8916), sodium bicarbonate (bioreagent, Lot #S5761, 99.5%-100.5%) and trypan blue solution (Lot #T8154) were

purchased from Sigma–Aldrich (Oakville, Ontario, Canada). Phosphate-buffered saline (PBS, Lot #OXBR0014G), fetal bovine serum (FBS, Lot #12483) and trypsin-EDTA solution (0.05%, phenol red, Lot #25300-054) were obtained from Fisher Scientific/Life Technologies (Pittsburgh, PA, USA).

4.3.2. Particles and compounds

Commercially available crystalline silica (model: Min-U-Sil® 5) was provided by the U.S. Silica Company (Berkley Springs, WV, USA). It is declared as high purity, inert, white crystalline silica derived from a natural source. According to the vendor, ~ 98-99% of the particles are SiO_2 with a median diameter of 1.7 μm. 92% of these particles have diameters ≤ 5μm. The main impurities include aluminium oxide (< 1%), iron oxide (< 0.1%) and titanium oxide (< 0.1%) which may also contribute to the toxicity of the quartz particles. Previous studies suggest that aluminium salts and metallic iron can decrease the toxicity of quartz particles by coating the active sites at the particle-air interface as well as the iron ions are capable of catalyzing ROS production by way of Fenton reaction.[30, 131, 149-152]

Carbon black nanoparticles (Lot #1211NH，100 nm) was purchased from Nanostructured & Amorphous Materials Inc. (Houston, USA). The purity of CB nanoparticles is 88.1%, and impurities include ash (5.8%) and water (1.06%). Nickel nanoparticles (Lot #577995, < 100 nm) were purchased from Sigma-Aldrich (Oakville, Ontario, Canada). The purity of nickel nanoparticles is ≥ 99% based on the trace metals analysis.

In this study, CB nanoparticles and crystalline silica particles were adopted as laboratory mimics of two insoluble particle types that are in roadside ambient particles, diesel soot, and re-suspended roadside dusts, respectively. As outlined above in the Introduction section, it is noted that CB nanoparticle and diesel soot are distinct with respect to chemical compositions and toxicity. Thus, the particle chemical compositions and the interactions between different particle types/components are much more complicated in the ambient environment than with the CB used here in these laboratory studies.

4.3.3. Cell culture

The human lung alveolar epithelium cell line A549 (CCL-185, American Type Culture Collection, Rockville, MD, USA) was used in this work. These cells were cultured in F12K medium supplemented with 10% (v/v) fetal bovine serum at 37 °C in a humidified atmosphere of 5% CO_2 in the air. Prior to dose-response assays, cells were seeded in 6-well culture dishes (surface area/well 8.87 cm^2) and grown to confluence. Cultures incubated with particle-free serum-free culture medium, and serum-free medium containing 50 ng/ml TNF-α served as the negative and positive controls, respectively.

4.3.4. Exposure to particles

Stock suspensions of particles (1 mg/ml in serum-free medium) were made fresh and vortexed for homogeneity. Serial dilutions of stock solutions were performed using the serum-free medium. Aliquots of solutions containing particles were then introduced to A549 cell cultures. For exposure to a single particle type, the cells were incubated with particles suspended in 2 ml serum-free medium at dosages from 0 to 700 μg/ml for CB nanoparticles and crystalline silica, and from 0 to 100 μg/ml for Ni nanoparticles. For doses involving a mixture of CB nanoparticles and crystalline silica particles, the mass ratios of CB nanoparticles to crystalline silica particles used were fixed at 0.7, 1.4 and 2.8, with a total mass dosage range from 0 to 700 μg/ml in 2 ml serum-free medium. Regarding dosages of crystalline silica particles plus Ni nanoparticles, silica was used from 62.5 to 125 μg/ml, and Nickel nanoparticles from 10 to 40 μg/ml. All samples were run in duplicate per experiment. Three or more independent experiments with the same dose were performed throughout.

4.3.5. Measurement of IL-6 and IL-8 concentrations in supernatants

Upon introducing the dose of particles to the cell cultures, the incubation period was 18 hours in duration, at the end of which the supernatants were collected and stored at –80°C until analysis. The concentrations of two pro-inflammatory mediators, IL-6 and IL-8, in the supernatants were quantified using ELISA kits (IL-6, model #900-M16, IL-8, model #900-M18, Cedarlane, Burlington, Ontario, Canada) as per the manufacturer's instructions. The ELISA assays were performed in triplicate. The determined

concentration of IL-6 and IL-8, mean and standard deviation, were obtained through normalization against the positive and negative control, using the equation $s_{\text{final}} = \frac{S-N}{P-N}$ (S: samples, N: negative control, P: positive control).

4.3.6. Trypan blue assay

After collection of the supernatant, each separate culture in a 6-well plate was washed three times with 2 ml PBS, and a trypan blue viability assay was immediately performed following the procedure of trypan blue exclusion test.[164] The numbers of viable and non-viable cells were counted using a hemacytometer (0.1 mm, Bright-Line™) and a bright-field microscope (TMS-F, Nikon), respectively. The percent viabilities of samples were normalized against negative controls.

4.3.7. Statistical analysis

The data acquired on cell viability, and the expression of IL-6 and IL-8 is reported as mean values ± standard deviation (1σ). The student t-test was used to compare the cell viability and cytokine expression between samples, and controls and samples. The threshold for statistical significance was set as $p < 0.05$, and when $p < 0.01$ was obtained it is reported.

4.4. Results and Discussions

4.4.1. CB nanoparticles

Figure 4.1 presents the measured cell viability as a function of the dosage of CB nanoparticles. Generally, as the dosage of the particles increased, cell viability decreased. 95% of the cells are non-viable when the dosage is ≥ 500 µg/ml. Two cytokines, IL-6 and IL-8, were adopted to indicate trends in cell response (Figure 4.2), because both are known as important pro-inflammatory mediators. As the dose of the CB nanoparticles increased, the IL-6 and IL-8 expression increased, to a maximum, for both IL-6 and IL-8, at a dosage of ~ 230 µg/ml. With further increases in the total mass dose of particles, cell cytokine expression decreased. The dosage 230 µg/ml corresponds to cell viability ~ 40% (Figure 4.1). The death of a large fraction of the cells provides an explanation for why the IL-6 and IL-8 expression decreases at dosages >

230 μg/ml. The elevation of IL-6 and IL-8 expression due to exposure to CB nanoparticles indicates a dose-dependent correlation between CB nanoparticle exposure and its ability to induce inflammation in A549 cells.

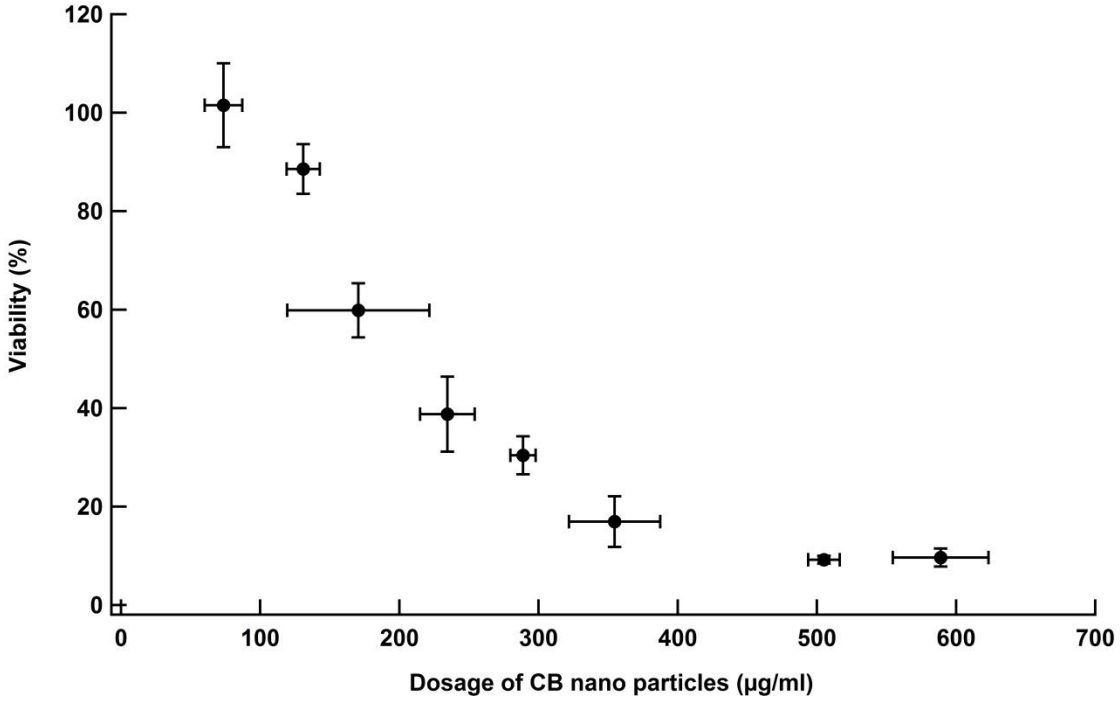

Figure 4.1 Normalized cell viability after 18 hrs incubation of A549 cells as a function of dose of CB nanoparticles. Each data point corresponded to averages of more than three samples (n ≥ 3), and reported as mean values ± standard deviation (1σ). The x-axis and y-axis propagated uncertainties arose from standard deviations of the dosages and the cell viabilities of the samples, respectively.

CB nanoparticles contain a trace amount of metal salts and organic compounds.[56, 188-189] As such, they are classified as an example of low toxicity particle which mainly induces cytotoxicity through interactions of particle surfaces with cells.[124, 188-189] However, previous studies have generated results that were interpreted that CB nanoparticles cause oxidative stress, pro-inflammatory effect, genotoxicity, and cell death.[124, 188-189, 191, 204] Val *et al.* investigated the inflammatory process caused by CB and TiO_2 nanoparticles on human bronchial epithelial cell lines and found that CB nanoparticles were able to induce several kinds of pro-inflammatory cytokines in a dose-dependent manner, including IL-6, TNF-α and granulocyte-macrophage colony-stimulating factor (GM-CSF). They also suggested that the ability for nanoparticles to absorb cytokines could affect the evaluation of the pro-inflammatory potential of the particles.[198] The work of Mroz *et al.* demonstrated that CB nanoparticles induced DNA

single-strand break and pro-inflammatory transcription factors activation on A549 cells. Oxidative stress pathways were involved in the process.[195] Hussain *et al.* found that exposure to CB nanoparticles lead to apoptosis of bronchial epithelial cells through a ROS dependent mitochondrial pathway. In review, two pathways, the generation of ROS, and the interactions between particulate surfaces and cell proteins, are believed as main contributors of CB's cytotoxicity. CB solid-air interface properties such as surface area and reactivity appear to play important roles in the process.[124] However, the detailed mechanisms are not fully understood yet. Our results are in general agreement with the measurements made in previous studies, that CB induces pro-inflammatory mediator expression and cell death in a dose-dependent relationship.

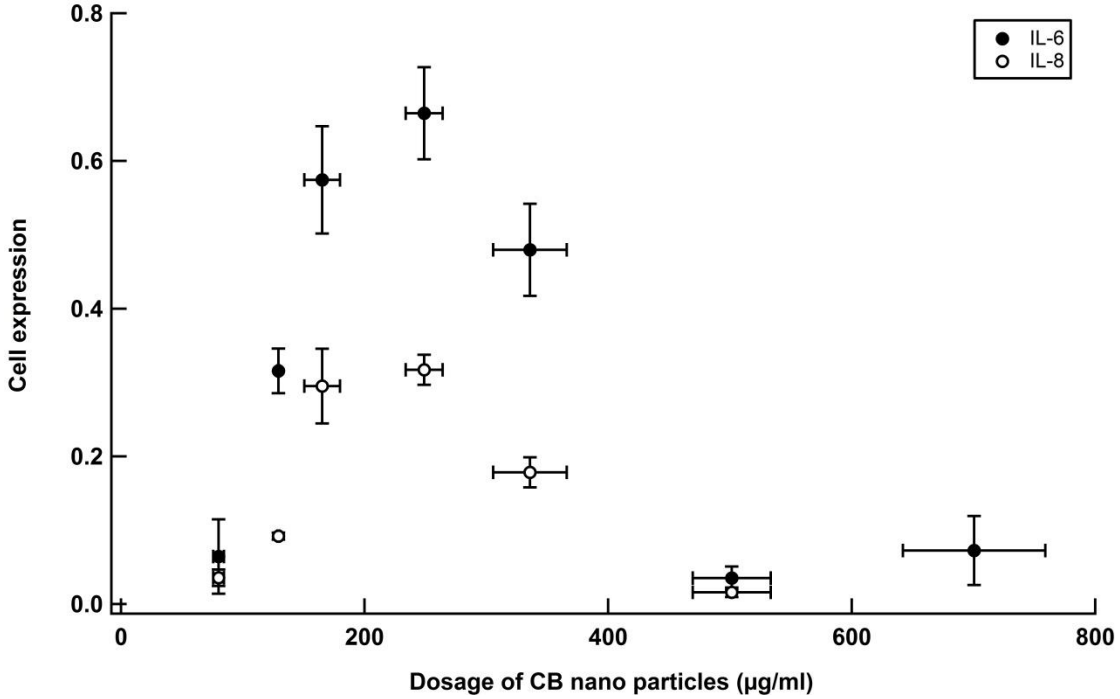

Figure 4.2 Normalized IL-6 and IL-8 expression after 18 hrs incubation of A549 cell cultures as a function of dose of CB nanoparticles. Each data point corresponded to averages of more than three samples (n ≥ 3), and reported as mean values ± standard deviation (1σ). The x-axis and y-axis propagated uncertainties arose from standard deviations of the dosages and the IL-6 or IL-8 expression of the samples, respectively.

4.4.2. Crystalline silica

Figure 4.3 and 4.4 show the cell viability, and selected cytokines expression, IL-6 and IL-8, as a function of the dosage of crystalline silica, respectively. The dose-

dependent results for silica have similarity to that was measured using CB nanoparticles. For instance, cell viability decreases as the mass dosage of crystalline silica increases. At dosages ≥ 360 μg/ml, the culture is non-viable. Also, regarding both IL-6 and IL-8 expression, at low mass doses, silica caused increased cytokine secretion up to maxima, but, with further increases in particle mass dosage, the concentrations of cytokines measured in the supernatant decreased steadily to become non-differentiable relative to the negative controls. The measured maximum for interleukin secretion corresponded to a trade-off between maximal stimulation of the cells versus minimal cell death. The highest IL-6 and IL-8 expressions were observed at a dosage of 130 μg/ml and 250 μg/ml respectively, which correspond to viabilities of ~ 50% and ~ 15%, respectively.

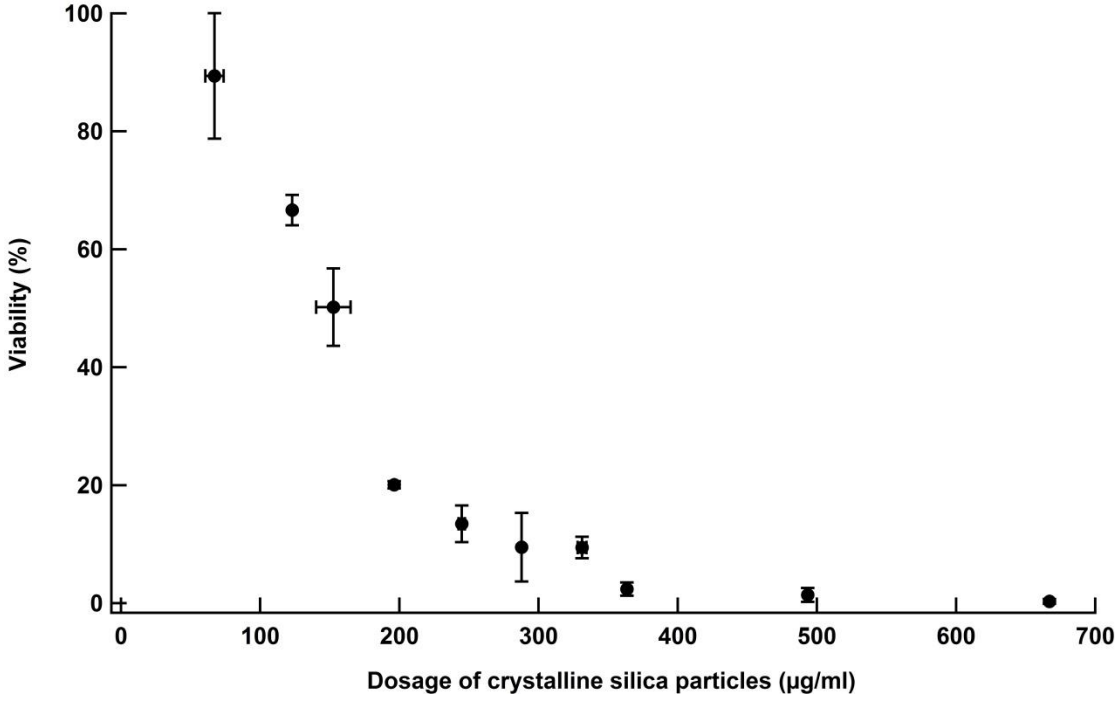

Figure 4.3 Normalized cell viability after 18 hrs incubation of A549 cells as a function of dose of crystalline silica. Each data point corresponded to an average of more than three samples (n ≥ 3), and reported as mean values ± standard deviation (1σ). The x-axis and y-axis propagated uncertainties arose from standard deviations of the dosages and the cell viabilities of the samples, respectively.

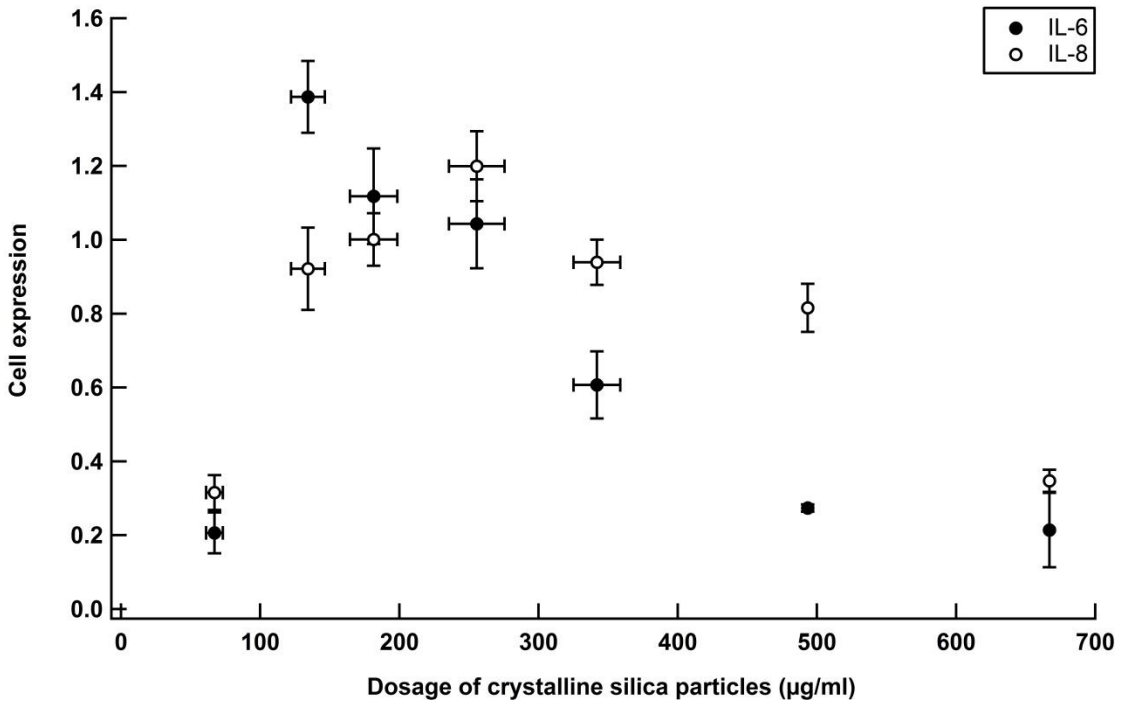

Figure 4.4 Normalized IL-6 and IL-8 expression after 18-hour incubation of A549 cell cultures as a function of dose of crystalline silica. Each data point corresponded to an average of more than three samples (n ≥ 3), and reported as mean values ± standard deviation (1σ). The x-axis and y-axis propagated uncertainties arose from standard deviations of the dosages and the IL-6 and IL-8 expression of the samples, respectively.

On the cellular level, the toxicity of crystalline silica mainly depends on the surface properties, especially the "active sites" with silanol groups.[129-131] Either by directly producing ROS at the particle surfaces, and/or stimulating the respiratory burst of the cells and inducing ROS/RNS indirectly, quartz particles are capable of generating oxidative stress, triggering pro-inflammatory cytokine expression, and causing cell apoptosis.[131, 212, 215] The study of Fanizza *et al.* indicated that short-term exposure of α-quartz induced direct-oxidative DNA damage and cell death of A549 cells in a dose-related manner.[217] Herseth *et al.* investigated the cytotoxicity of silica using both mono-culture (alveolar macrophages) and non-contact co-culture (alveolar macrophages and endothelial cells). Pro-inflammatory cytokine response, i.e. the release of IL-1β, IL-6, and IL-8, can be observed for both monoculture and co-culture. IL-1β is known to have an important role in triggering the release of other cytokines.[236]

4.4.3. Nickel nanoparticles

A dosage range from 0-100 μg/ml was selected and adopted for nickel nanoparticles. At this range, nickel nanoparticles induced no differentiable cytokine expressions from negative controls (Figure 4.5). Also, there was no obvious effect on cell viability was observed, but at dosage ≥ 40 μg/ml, transparent vacuoles were observed inside the A549 cells (Figure 4.6). Abnormal cellular morphology induced by nickel has been reported.[223] Ahamed's study on the toxic response of A549 cells exposed to nickel nanoparticles indicated significant toxicity of Ni nanoparticles in which the generation of oxidative stress plays an important role.[231]

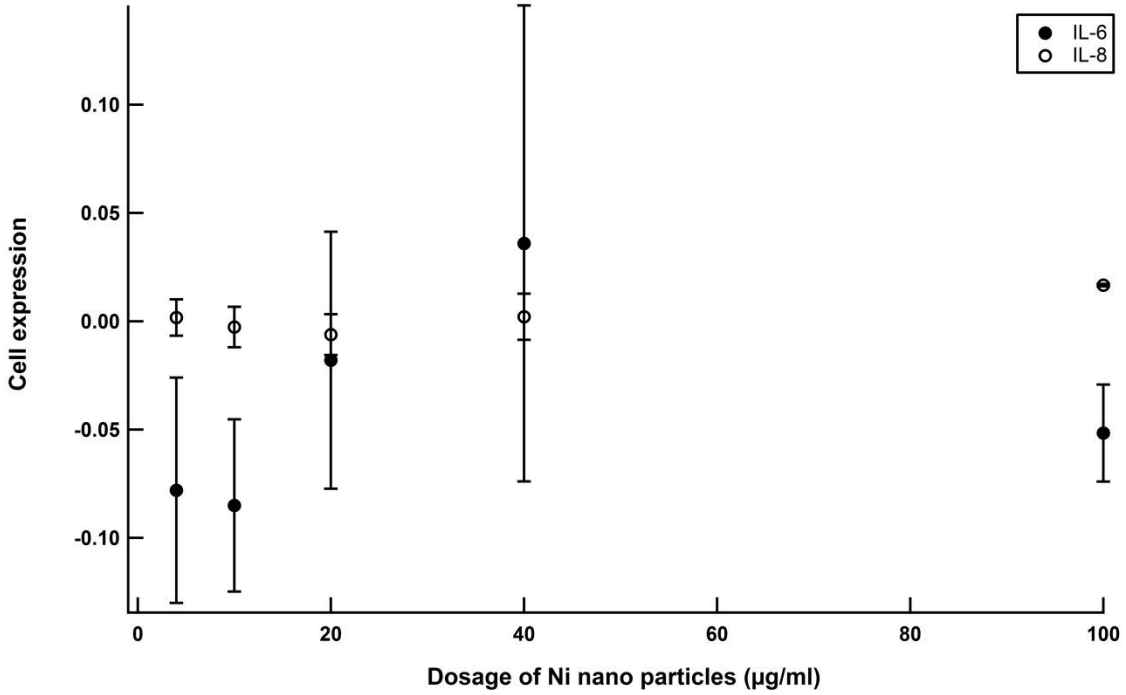

Figure 4.5 Normalized IL-6 and IL-8 expression after 18 hrs incubation of A549 cell cultures as a function of dose of nickel nanoparticles. Each data point corresponded to averages of more than three samples (n ≥ 3), and reported as mean values ± standard deviation (1σ). The y-axis propagated uncertainties arose from standard deviations of the IL-6 and IL-8 expression of the samples, respectively.

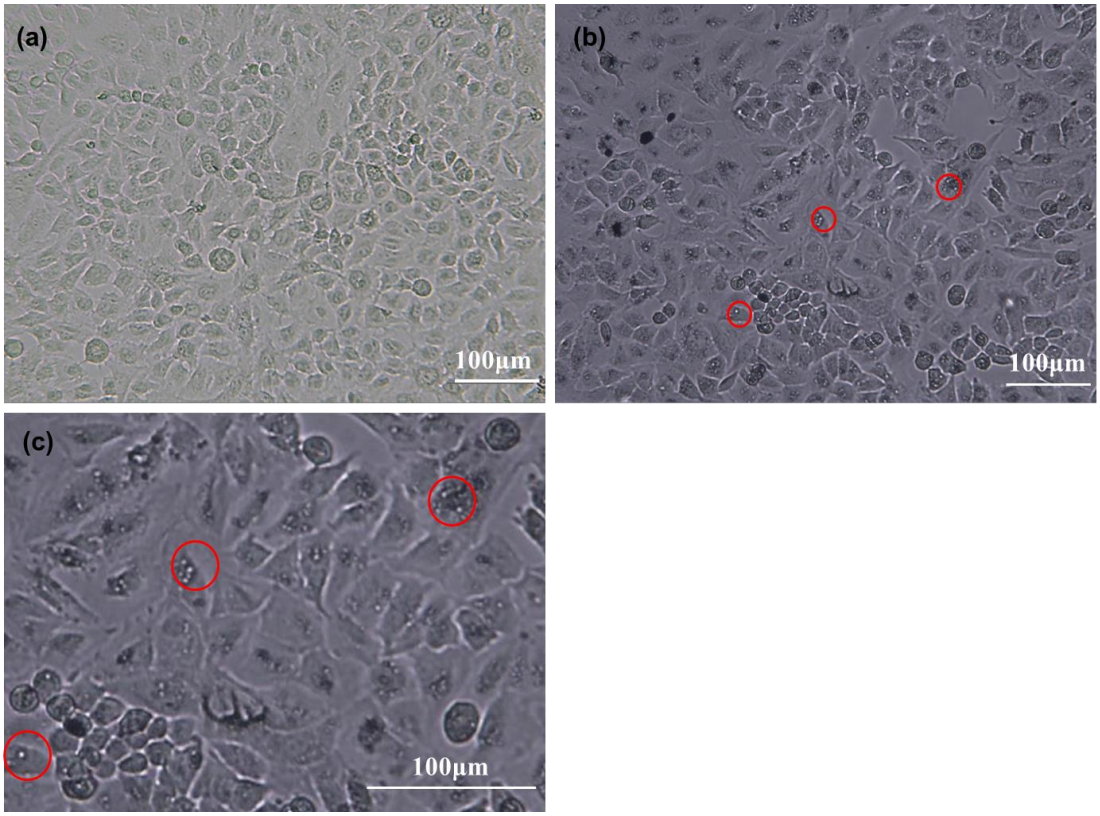

Figure 4.6 A549 cells as viewed after an 18 hrs incubation period (a) without any particles/particle components (negative control) (b) with 100 µg/ml nickel nanoparticles. (c) close-up image of the area with circles. Images were obtained using a bright-field microscope, at 100X magnification. Circles show transparent vacuoles inside the A549 cells caused by dosage of nickel nanoparticles

Prior work by our group with soluble nickel, $Ni(NO_3)_2 \cdot 6H_2O$, which used a co-culture of THP-1 cell and A549 cells, indicated that Ni^{2+} can induce significant higher expression of both IL-6 and IL-8 than negative controls when the dosage ≥ 20 µg/ml.[235] The different effects of nickel, spanning soluble nickel salts to insoluble nickel nanoparticles indicate that the cytotoxicity of nickel depends on the cellular concentration of bioavailable nickel ions.[224-225, 229] Additional differences in the results involving doses of nickel are likely due to different methodology (e.g., cell types used), exposure time, and molecules measured in assessing the cellular response. For insoluble nickel nanoparticles, the surface sites and overall particle charge are likely important factors, with additional experimental investigation required to further delineate.

4.4.4. Is there a synergy between different particle types?

4.4.4.1 CB nanoparticle plus crystalline silica

For particle mixtures of CB nanoparticles plus crystalline silica particles, different mass ratios (the mass dosages of CB nanoparticles over mass dosages of crystalline silica) as 0.7, 1.4, and 2.8 were used. Cell viability (Figure 4.7), IL-6, and IL-8 expression (Figure 4.8) are plotted out as a function of the dosage of the particle mixtures with different mass ratios, respectively. For both cell viability and cytokine expression, there was no measurable difference between cells dosed with CB nanoparticles plus crystalline silica at different mass ratios. This mass ratio dose data was also averaged and plotted out (Figures 4.9 and 4.10).

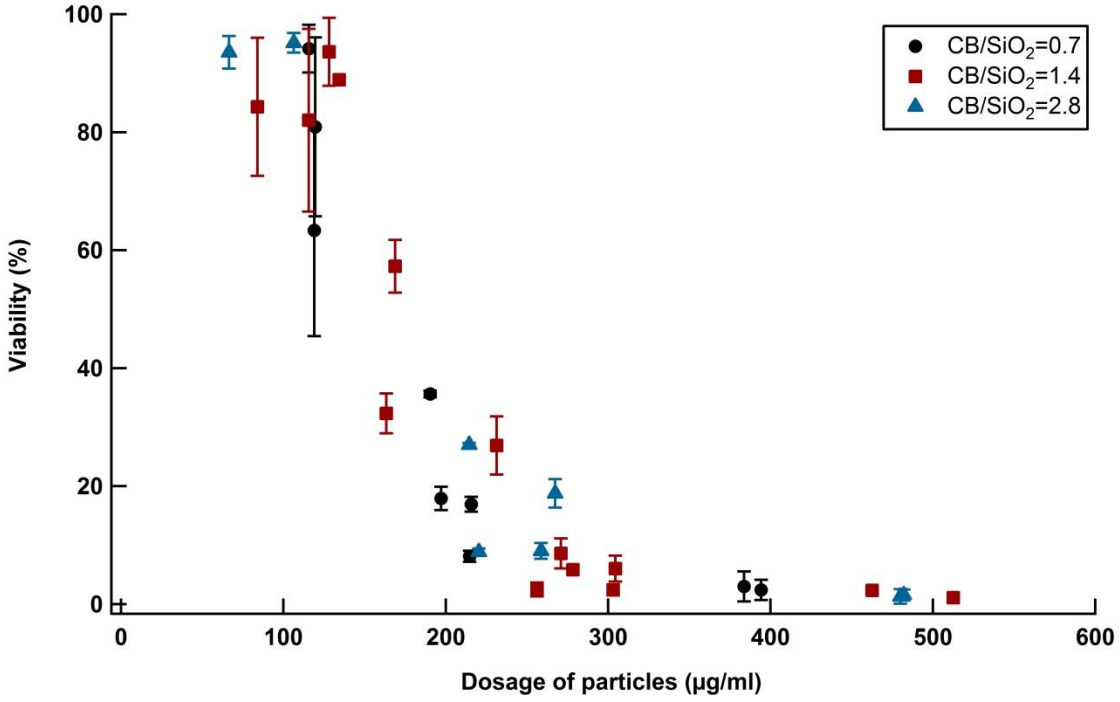

Figure 4.7 Normalized cell viability after 18 hrs incubation of A549 cells as a function of dose of CB nanoparticles plus crystalline silica at different mass ratios. Each data point corresponds to an average of more than three samples (n ≥ 3), and reported as mean values ± standard deviation (1σ). The y-axis propagated uncertainties arose from standard deviations of the cell viabilities of the samples.

The trend for all of the particle doses (CB nanoparticles, crystalline silica particles, and mixtures of CB nanoparticles plus crystalline silica particles) is that cell viability decreased with increased mass of particles introduced (Figure 4.9). At the same

mass dosage, CB nanoparticles led to highest cell viability, whereas crystalline silica and mixtures of CB nanoparticles and crystalline silica induced similar cell viabilities, both lower than CB nanoparticles. Note that all of these particles induce > 95% cell death at mass loadings ≥ 500 µg/ml. Figure 4.10a and 4.10b plot IL-6 and IL-8 concentrations, respectively, as a function of the dosage of different types of particles. The trends for these two cytokines are similar, with low mass dosage of the particles inducing increased cytokine secretion up to a maxima, and, then with further increases in particle mass dosage, the concentrations of cytokines measured in the supernatant decreased steadily to, at mass doses > 700 µg/mL, equivalent to negative controls. The maxima in the interleukin secretion correspond to a trade-off between maximal stimulation of the cells (Figure 4.10) versus cell death (Figure 4.9), as the maxima of interleukin secretion occurred at cell viability ~ 30%.

In comparing cellular responses to crystalline silica particles versus CB nanoparticles that were used in this study, the cytokine response to crystalline silica is greater at an equivalent mass dose, a significant difference was observed with respect to IL-8. Regarding cells dosed with CB nanoparticles and crystalline silica mixtures, the IL-6 expression is generally the same at < 150 µg/ml doses, but greater than for cells dosed with crystalline silica particles alone for doses > 150 µg/ml. For example, IL-6 at 230 µg/ml particle dose, was measured as having significantly higher cell expression for the mixture of CB nanoparticles and crystalline silica versus CB nanoparticles or crystalline silica alone (Figure 4.10b). This outcome illustrates that, for certain mixtures of particle types and mass loadings, greater cellular expression can be measured for the equivalent mass dose of either particle type alone. Conversely, for the IL-8 concentrations measured, though the CB alone gave a significantly lower response at all doses, the crystalline silica versus the mixtures of crystalline silica and CB were not measurably different, suggesting that the IL-8 response was effected predominantly by mass of the crystalline silica in the dose. This hints at the potential complexity of understanding cellular responses when presented with ambient particulate matter that is heterogeneous in composition and size.

Several pathways have been implicated regarding the toxicity of CB nanoparticles and crystalline silica.[5, 123, 237] The particles can interact with cell membrane proteins and activate or inhibit signalling pathways. Internalization of particles can lead to lysosomal destabilization or accumulation.[123] For silica, it is believed that the siloxyl

radicals on its surfaces can generate ROS such as hydrogen peroxide, hydroxyl and superoxide radicals in an aqueous environment.[5, 237] CB nanoparticles and crystalline silica can each participate in intercellular reactions and lead to the further generation of ROS which is related to the particle surface area and reactivity.[5, 123] Our results suggest that, certain mixtures of particle types may stimulate one or more pathways, which would account for the observed greater cellular expression of mixtures than measured for the equivalent mass dose of either particle type alone. Conversely, a study by Borm *et al.* on coal mine dust and coal fly-ash indicated that, the quartz in the particle mixtures was not as bio-active as the pure samples at equivalent doses both *in vitro* and *in vivo*.[238] The difference between their results and ours may due to the differences between different methods, e.g., cell line, particle compositions, and readouts used. Regardless of the details, our results specifically suggest interactions between different particle types, mass loadings, and chemical compositions, play critically important roles in the summative toxicity of each dose, with obvious health implications on ambient particle exposures.

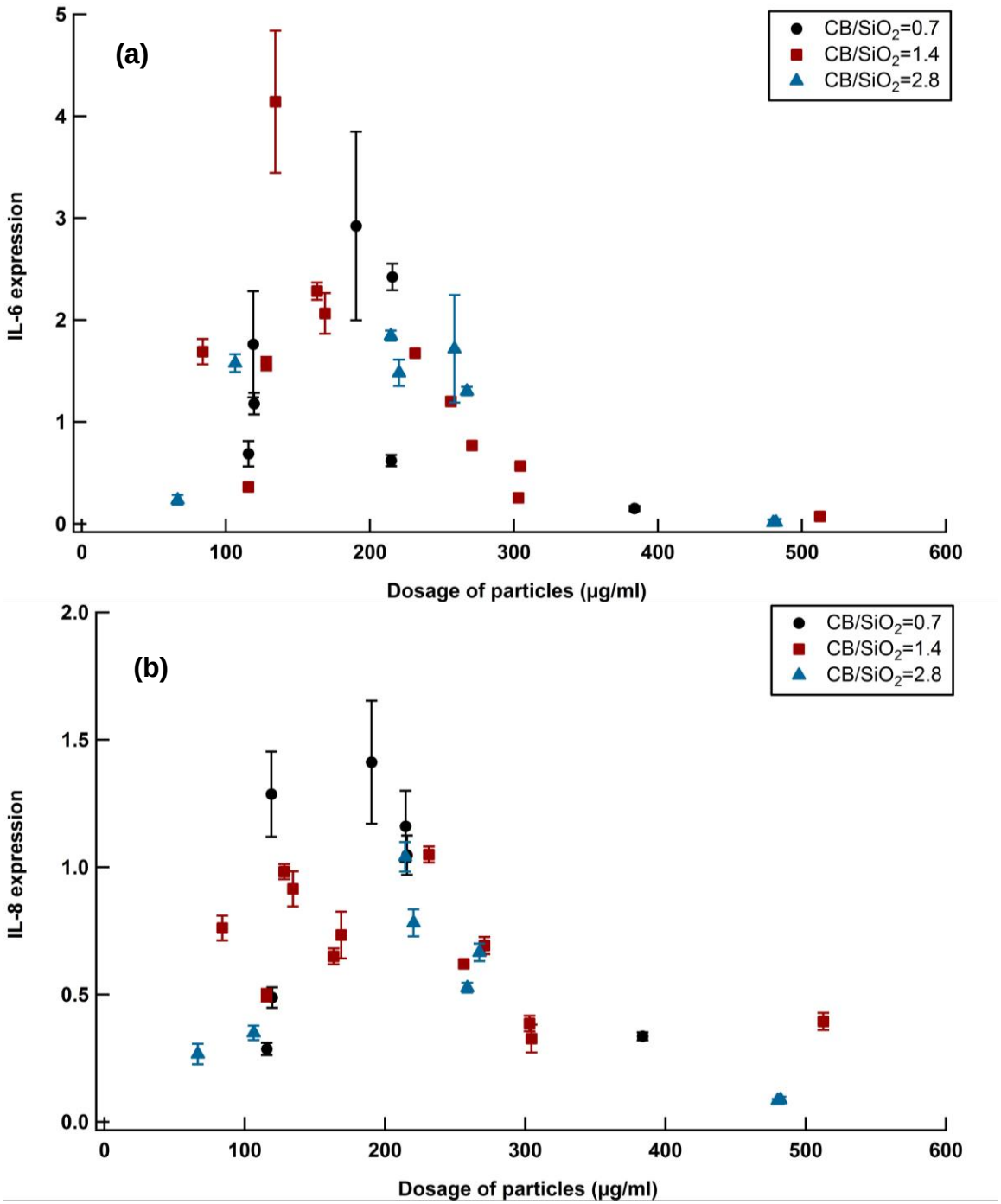

Figure 4.8 **Normalized a) IL-6 and b) IL-8 expression after 18 hrs incubation of A549 cell cultures as a function of dose of CB nanoparticle plus crystalline silica at different mass ratios. Each data point is an average of more than three samples (n ≥ 3), and reported as mean values ± standard deviation (1σ). The y-axis propagated uncertainties arose from standard deviations of the IL-6 and IL-8 expression of the samples, respectively.**

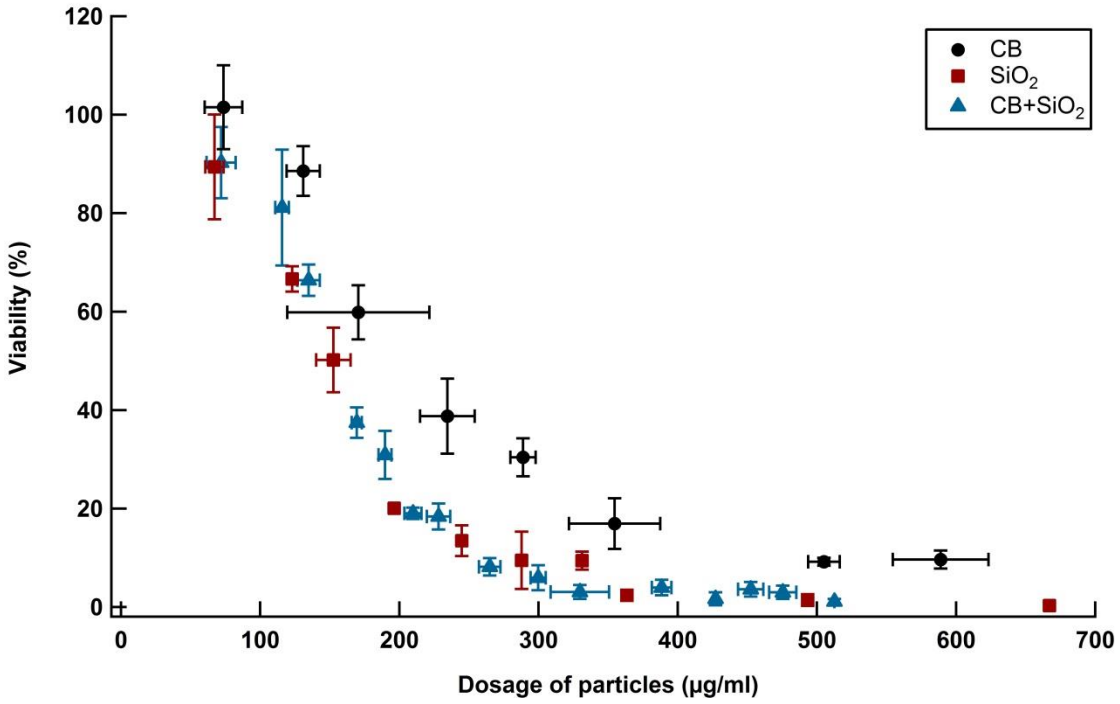

Figure 4.9 Normalized cell viability after 18 hrs incubation of A549 cells as a function of dose of CB nanoparticles, crystalline silica, and CB nanoparticles plus crystalline silica. Each data point is an average of more than three samples (n ≥ 3), and reported as mean values ± standard deviation (1σ). The x-axis and y-axis propagated uncertainties arose from standard deviations of the dosages and the cell viabilities of the samples, respectively.

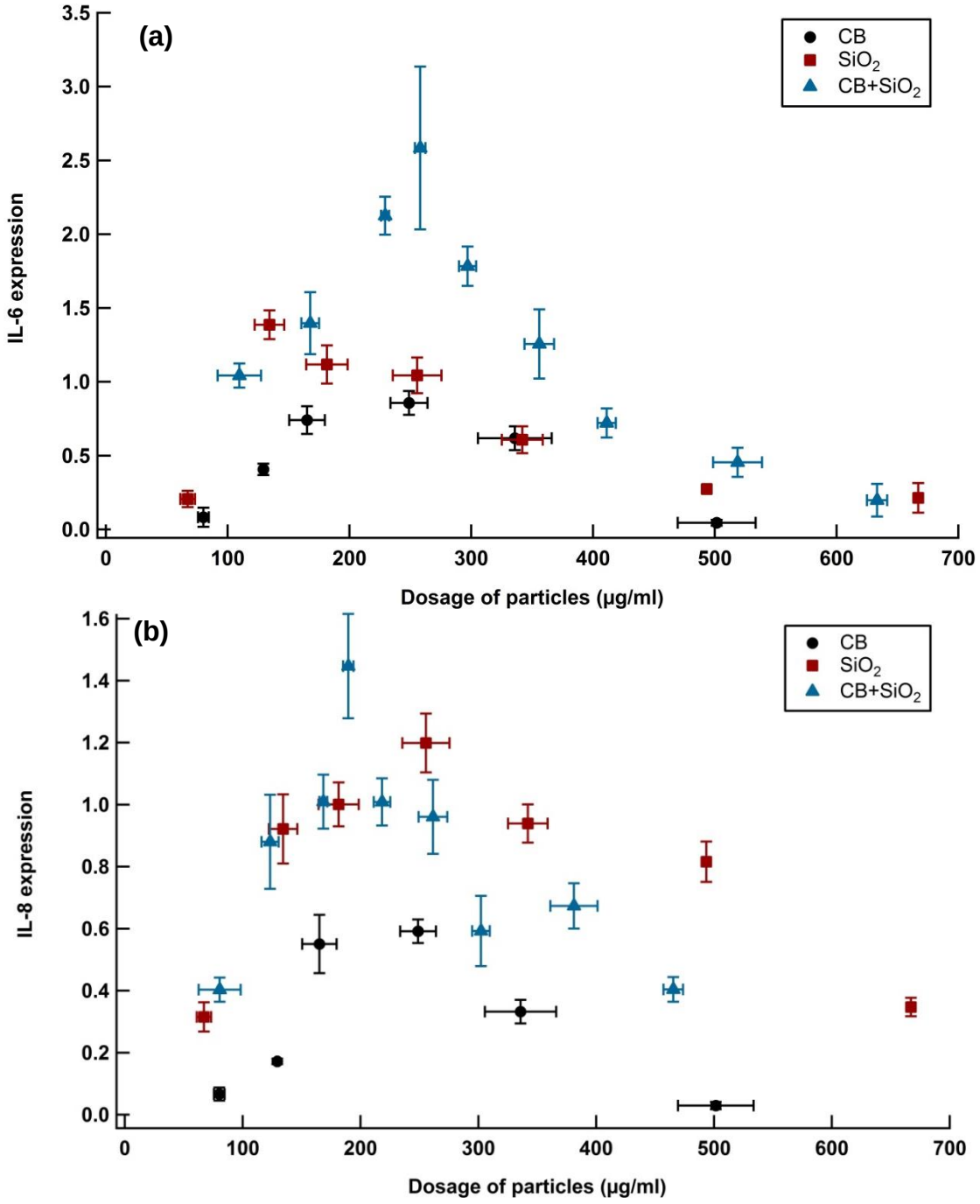

Figure 4.10 Normalized a) IL-6 and b) IL-8 expression after 18 hrs incubation of A549 cell cultures as a function of dose of CB nanoparticles, crystalline silica, and CB nanoparticles plus crystalline silica. Each data point corresponded to averages of more than three samples (n ≥ 3), and reported as mean values ± standard deviation (1σ). The x-axis and y-axis propagated uncertainties arose from standard deviations of the dosages, and the IL-6 and IL-8 expression of the samples, respectively.

4.4.4.2 Nickel nanoparticle plus crystalline silica

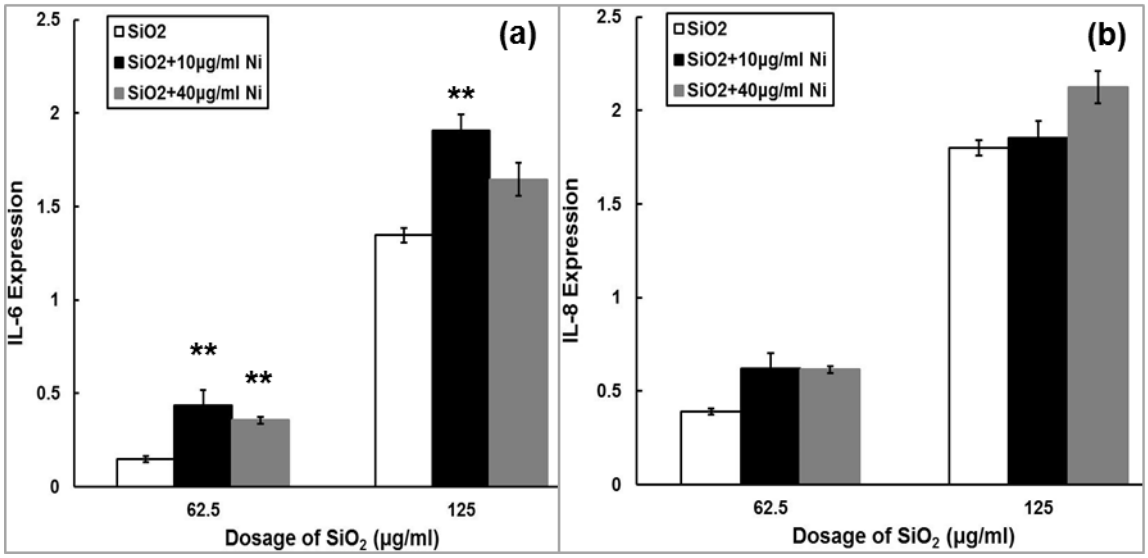

Figure 4.11 Normalized a) IL-6 and b) IL-8 expression after 18 hrs incubation of A549 cell cultures as a function of dose of nickel nanoparticles plus crystalline silica. The data are reported as mean values ± standard deviation (1σ), with the number of samples ≥ 3. Asterisk symbols indicate the difference between the cytokine expression of the cells dosed with nickel nanoparticles plus crystalline silica and that of the cells dosed with crystalline silica alone is statistically significant. A single asterisk symbol (*) represents $p < 0.05$, two asterisks represent $p < 0.01$.

The effect of combined doses of nickel nanoparticles with crystalline silica was characterized by varying the concentrations of nickel nanoparticles, at 10 and 40 µg/ml, together with crystalline silica particles at 62.5 and 125 µg/ml (Figure 4.11). Compared with crystalline silica alone, 10 µg/ml nickel nanoparticles plus crystalline silica induced significant higher IL-6 expression at both low and high silica dosages, whereas no difference with respect to cell viability was observed. However, when the dosage of nickel increased to 40 µg/ml, the measured IL-6 expression levels of nickel nanoparticles plus crystalline silica were lower than that for the respective lower mass nickel doses, because many cells were no longer viable at the end of the 18-hr exposure (Figure 4.12). For IL-8, a mass dosage-dependent relationship between the dosage of particle mixture and IL-8 expression was measured.

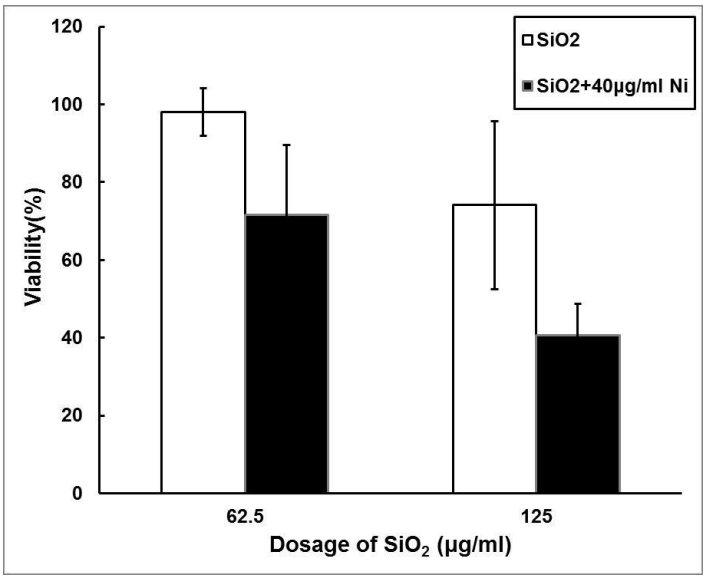

Figure 4.12 Normalized cell viability after 18 hrs incubation of A549 cells as a function of dose of nickel nanoparticles plus crystalline silica. The data are reported as mean values ± standard deviation (1σ), with the number of samples ≥ 3.

Nickel nanoparticles alone at both 10 and 40 µg/ml following incubation with A549 cells did not induce IL-6 or IL-8 expression differential from the negative control. When combined with crystalline silica at both low and high dosages, increased cellular response was measured. However, both IL-6 and IL-8 of the crystalline silica alone versus the crystalline silica and nickel nanoparticle were not measurably different at the same total mass dosage (Figure 4.4 and 4.11). Further, our results suggest that the mass of crystalline silica in the dose is a primary factor in the cellular response, but yet added nickel does alter the response, which suggests more than one biological pathway mechanisms could be involved. Silica particles have been proposed as cytotoxic dependent on the solid-aqueous interface's siloxyl radicals and silanol groups to generate ROS, and trigger the expression of pro-inflammatory cytokines and chemokines.[5, 237] Nickel can generate ROS through Fenton chemistry in the presence of strong oxidizers such as H_2O_2 and ascorbate in cytosol and nucleus. The ROS generated by crystalline silica could be providing the oxidizer to active a Fenton reaction.[5, 230] It is reported that metallic nickel and nickel oxide nanoparticles are involved in the regulation of inflammation signalling pathways such as NF-κB pathway.[239-241] Multiple inflammation signalling pathways triggered by silica particles and nickel nanoparticles, respectively, may work synergistically and lead to an increase of IL-6 expression.

4.5. Conclusion

To investigate the toxicity of insoluble fraction of ambient particles, three typical particle types near the roadside, i.e. CB nanoparticles representing diesel soots, crystalline silica particles representing re-suspended road dusts, and nickel nanoparticles, have been chosen. A549 lung cell responses following incubation with these particle types were studied *in vitro*. Dose-dependent correlations between particle exposure and cell viability and pro-inflammatory cytokine expressions have been measured for CB nanoparticles, crystalline silica and mixtures of them at the mass dosage range varies from 0 to 700 μg/ml. Generally, cell viability decreased with increased mass of particles introduced. At mass loadings > 500 μg/ml, > 95% cell death was measured. The trends for IL-6 and IL-8 were similar. The low mass dosage of the particles induced increased cytokine secretion up to a maxima, and, then with further increases in particle mass dosage, the concentrations of cytokines measured in the supernatant decreased steadily to, at mass doses > 700 μg/ml, equivalent to negative controls. The maxima in the interleukin secretion correspond to a trade-off between maximal stimulation of the cells versus their death. No obvious effect on cell viability or cytokine expression has been observed for nickel nanoparticles alone at dosages ≤ 100 μg/ml.

For mixtures of CB nanoparticles and crystalline silica particles, all different particle mass ratios generated dose-dependent cell viability and cytokine expression trends that were similar to the individual particle type. The small differences observed were, CB nanoparticles lead to highest cell viability and lowest cytokine expression at the same mass dosage as either crystalline silica or mixtures of crystalline silica plus CB nanoparticles. Mixtures of CB nanoparticles and crystalline silica particles lead to increased cellular expression for IL-6 as compared to equivalent mass doses of either particle type alone. This result illustrates that certain mixtures of particle types can lead to greater cellular expression as compared to an equivalent mass dose of either particle type alone. 10 μg/ml nickel nanoparticles plus crystalline silica induced significantly higher IL-6 expression at both low and high silica dosages than crystalline silica alone. For both the mixtures of CB nanoparticles and crystalline silica particles, and those of nickel nanoparticles and crystalline silica particles, the mass of crystalline silica in the dose effect the cellular response predominantly.

Though our studies did not investigate cellular mechanisms, the mechanisms are not clear yet, but in drawing information from other studies we assume that the surface chemistry of the particles plays an important role. Ambient particle surfaces could be activated from the sources, or through heterogeneous radical chemistry in the troposphere or deactivated through homogeneous and heterogeneous chemistry. For instance, crustal dusts like silica could be deactivated through sorption of humic materials through processes prior to their introduction to the troposphere. Conversely, various organic compounds, such as natural organic matter (NOM), would sorb strongly (e.g. multi-chelation) to the pH-dependent negatively charged, or polar, the particle-air interface of silica. Thus, NOM could passivate the silica interface. In our case, the interactions between different particle types could possibly modify chemistry on the particle-air interface and thus modify the toxicity of the whole mixtures of particles. Future studies need to be done to confirm this assumption.

Several general conclusions can be drawn based on our results. The insoluble fraction of the particles, CB and crystalline silica particles are able to induce the secretion of pro-inflammatory cytokines and cell death. At the same mass dosage, crystalline silica particles (nominally < 5 μm diameter) lead to higher cytokine expression and more cell death than CB or nickel nanoparticles (each nominally 100 nm diameter). At the same mass dosage, the total surface area of CB nanoparticles can be more than 10^6 times larger than that of crystalline silica particles. It illustrates that particle size and surface area do not pre-determine the cytotoxicity of the particles. Previous studies have shown particle types of all size and composition, e.g. crystalline silica and CB nanoparticles, effect different cellular responses.[5, 123, 237] Results presented in this chapter agree well with previous conclusions that the total mass of the particle types is important, and from that, there was no measurable synergy between the different particle types studied. Other factors including chemical composition, and especially surface chemistry of the particles, should be taken into consideration when assessing the overall toxicity of a given sample of ambient particles.

Chapter 5.

Human lung cell responses measured after incubation with particles plus soluble metal ion salts

5.1. Abstract

Soluble compounds commonly measured on ambient particle types, including ammonium nitrate, and soluble salts of zinc, lead, and iron were dosed onto human lung cells *in vitro*, either alone, or with commercially available crystalline silica or carbon black nanoparticles. The responses of A549 cultures to these doses were measured to be dependent on the chemical composition of the dose. Ammonium nitrate effected no differentiable cellular response relative to the negative control, either alone or in combination with particles. The soluble transition metal salts, introduced alone at 100 µM to the culturing medium, had no differential effect on cytokines IL-6 and IL-8 expression relative to negative controls. However, when combined with particles, Zn or Fe each effected cytoprotectant behavior. In contrast, Pb plus SiO_2 induced a non-linear increase in expression of these cytokines. The experiments yielded the following specific outcomes. For cells dosed with 125 µg/ml crystalline silica plus Fe^{2+}, measurably different responses comparing against cells dosed with crystalline silica alone occurred at [Fe^{2+}] > 10 µM with respect to both IL-6 and IL-8. The analogous threshold for 175 µg/ml CB nanoparticles was [Fe^{2+}] > 100 µM. For Pb^{2+}, the IL-6 threshold to observe a non-linear effect with 62.5 µg/ml silica was at 10 µM, and for 125 µg/ml silica it was 1 µM. For IL-8, the threshold for differential response due to crystalline silica particles plus Pb^{2+} was 10 or 100 µM for the combined dose with 62.5 or 125 µg/ml silica, respectively. High dosages of ferrous chloride (500 µM) and lead chloride (1000 µM) alone lead to a significant decrease of cell viability, and an increase of cytokine expression, but obvious precipitates were observed in these solutions so the outcomes were a combined effect of amorphous precipitates plus soluble metal ions. High cell viability and low IL-6 and IL-8 expression was observed for cells exposed to a ternary mixture of 100 µM Fe^{2+} and Pb^{2+} plus 125 µg/ml crystalline silica. With this measured outcome, Fe^{2+} clearly plays an important role with respect to cell response.

5.2. Introduction

Components measured in ambient particles span a wide range of source materials, including water-soluble metals, acids, polyaromatic hydrocarbons, insoluble particles, and biogenic compounds such as endotoxin. Each of these components has been the subject of extensive dose-response investigation, and most of these compounds/materials are classified as individually having considerable negative effect on human health through several mechanisms.[5, 10, 14, 26]

Water-soluble metals typically range in concentration on ambient particles from 10 ng/m^3 to ~10 µg/m^3.[14, 242] Redox-active transition metals, such as Fe, are capable of generating reactive oxygen species directly through redox-cycling in lung tissues, specifically mitochondria, where the ensuing emergence of oxidative stress markers themselves factor in inflammation and pathogenesis of chronic respiratory diseases.[5, 10, 14-15, 26, 28] Non-redox-active metals, such as Zn and Pb, can influence the toxicity of the particles by either decreasing or increasing oxidative stress, as well as through direct interactions with functional groups on biological molecules. For example, Pb influences the nervous system, and interacts directly with enzymes that are involved in hemoglobin manufacture.[5, 31-32, 100, 243-245]

Other particle components, nitrates and sulfates, are main contributors of the total particle mass, but these anions alone are not considered toxic. Conversely, it has been proposed that NO_x and SO_x following atmospheric oxidation, lower the pH of ambient particle surfaces or aqueous phase, and also change the bioavailability of other particle components. These gaseous emissions, therefore, induce an indirect, negative, health effect.[246-247]

Based on these select examples of individual water-soluble components on ambient particles exerting toxic effects, the general consensus is that each particle component plays a role in a subsequent inhalation health outcome.[248] Further elucidation of particle toxicity, especially regarding interactions between the water-soluble species on particles and the insoluble components of ambient particles, is the subject of this chapter.[8, 10, 14-15, 26, 28, 143, 179, 249] Our earlier study on reference ambient particle type ERM-CZ120 suggests an assignable role to the water-soluble fraction, but only when dosed with particles, regarding the overall response of A549 cells to doses of the whole

particle (Chapter 3). In this chapter, several soluble particle components, including ammonium nitrate, and soluble salts of zinc, lead, and iron, and their respective interactions with two insoluble particle types, CB nanoparticle and crystalline silica particle, are studied with respect to effecting lung cell responses *in vitro*. Two questions guided the experimental design for this study i. what is the respective role of a particle's chemical components when introduced individually? ii. How do water-soluble and insoluble particle components interact with respect to either increasing or decreasing the overall response of the cells?

Different pathways have been reported for the toxicity of CB nanoparticles and crystalline silica particles.[5, 123, 237] CB particles interact with cell membrane proteins, and in so doing non-specifically activate or inhibit cell signalling pathways. The internalization of CB nanoparticles can lead to lysosomal destabilization or accumulation.[123] For crystalline silica, it is believed that the silanol groups on the particle's solid-liquid interface are capable of generating ROS, such as hydrogen peroxide, hydroxyl and superoxide radicals in aqueous environments.[5, 237] Soluble compounds co-administered with these insoluble particle types are expected to have no effect, have an additive effect, or a negative effect with respect to effecting cellular response.

5.2.1. Background on ammonium nitrate

Ammonium nitrate is classified as a secondary component of ambient particles, meaning it is formed through chemical reactions in the atmosphere as compared to other materials emitted directly from a primary source. Generally, ambient nitrogen oxides (NO_x) can be converted to gaseous nitric acid by homogeneous reaction with hydroxyl radical or ozone, through a series of reactions, to nitrate radical and dinitrogen pentoxide. Nitric acid, and analogously formed sulfuric acid, reacts with alkaline gaseous substances, usually ammonia (NH_3), in the atmosphere to form salts (NH_4NO_3).[250-251] The salts then homogeneously condense as condensation nuclei or precipitate on existing particles, depending on the local environmental conditions. Nitrogen oxides and ammonia are introduced to the troposphere from both natural and anthropogenic sources. The dominant anthropogenic source of NO_x is high-temperature combustion, which accounts for 54% of total NO_x. 85% of total NH_3 is from agricultural emissions.[250, 252] On-road vehicle emission also happens to be another main source of atmospheric ammonia. Nowadays, most automobiles are equipped with three-way catalysts that help

to reduce nitrogen oxide emissions, by oscillating the air-to-fuel ratio between oxidation and reduction conditions in the engine. Ammonia is one of the by-products generated under reducing conditions.[252]

Ammonium nitrates are present in both fine and coarse size ambient particles. Based on source appointment studies across the United States, the contributions of secondary nitrates vary from 2% to 36.6% for $PM_{2.5}$, and for PM_{10} the range is from 0 to 33.4%.[253] Another report found ammonium salts account for 10-30% of the fine particle mass in a polluted urban area. [254] According to the data obtained from the U.S. EPA Aerometric Information System (AIRS) 2004, the average annual concentration of nitrates in $PM_{2.5}$ of 25 largest U.S. cities was 2.1 $\mu g/m^3$, which accounted for 14% of the total $PM_{2.5}$ mass. Note the range of nitrates in $PM_{2.5}$ spans 5% to 38%).[250] Harrison *et al.* collected and analyzed both $PM_{2.5}$ and PM_{10} in the urban background and roadside locations in the UK. Their results suggested that there was no obvious difference between the annual concentrations of ammonium nitrates in background sites versus roadside sites. In that study, ammonium nitrates accounted for 9.1% and 14.5% of the total mass of $PM_{2.5}$ and PM_{10} respectively in background sites, and 5.7% and 8.5% of the total mass of $PM_{2.5}$ and PM_{10} at roadside sites.[255]

At most locations, nitrates and sulfates are significant contributors to the total particle mass. Compared to sulfates, toxicity studies involving nitrates is limited. Based on published epidemiological and laboratory studies, there appears to be no obvious adverse health effect due to sulfates and nitrates at ambient levels.[250-251] However, several postulates regarding how nitrates and sulfates could factor in ambient particle toxicity, especially the strong acids generated have been proposed.

Lipfert *et al.* have suggested that nitrate was a potential contributor to the mortality of male U.S. military veterans during 1997-2002, because a statistically significant relation had been found between mortality and nitrate concentration, based on the results of their single-pollutant model. However, automobile density, which is highly related to the nitrate concentration, has been found to be the most important factor, but when it was added as a covariate to the model, the nitrate risk coefficient was only elevated but was not significant.[256] A hypothesized mechanism of nitrate and sulfate-containing particles' toxicity is the acidity of either the whole particles for liquid particles, or the surface layer for solid particles. Several studies discussed the possibility

that (a critical mass of) inhaled acidic particles would generate an adverse effect by altering the local pH and changing the properties of the tissue on which they deposit.[257-259] At doses less than a critical mass of acid to alter pH in lung tissues and fluids, the acidity of particles would be neutralized by respiratory ammonia and airway fluids.[250-251, 259]

Several theories regarding the potential for indirect health effects due to particulate nitrates/sulfates have been proposed. Jang *et al.* observed that an acidic surface layer on particles can lead to a multifold increase of secondary organic aerosol (SOA) mass.[247] The acidic layer can also lead to an increase in the quantity of organic components, such as organic peroxides, sorbed onto the particles, and thus an increase in the overall toxicity of these particles. Friedlander *et al.* suggested that the hygroscopic property of ammonium sulfates/nitrates can increase the quantity of gaseous peroxides and other soluble reactive species to be retained in the particle phase. Particle-phase peroxides can be transported into human cells by endocytosis and thereby effect a more severe outcome relative to an exposure to gaseous peroxides at similar quantities.[246]

5.2.2. Background on zinc

Zinc metal is lustrous blue-white in appearance, but it is not found in this form in nature due to its relatively high activity.[260-261] Zinc metal has a high reduction potential (-0.76 V), and the only oxidized form of zinc found in nature is plus two oxidation state (Zn^{2+}).[262] Zinc metal reduces many metal ions to their metallic state. Based on this capability, zinc is usually used to protect metals such as iron from corrosion.[260] For instance, zinc can be used as an anode/coating by galvanizing, electrodeposition, or zinc dust paints, and corrodes sacrificially to protect other metals. Zinc plates are bolted to the keels or hulls of marine vessels. Other important applications of zinc metal include the production of alloys, die casting, and manufacturing brass and bronze products.[244, 260, 263]

Zinc is the 24th most abundant element in the planet's crust, at an average concentration in the earth's crust of 65 g/t (0.0065%).[261] The zinc concentration in the waters, soils, and atmosphere of this planet is highly variable. The main natural sources of zinc in the atmosphere are soils, volcanic emissions, forest fires, biogenic emissions, and sea sprays. Anthropogenic sources of zinc in the atmosphere include zinc mining,

electroplating, smelting, iron/steel production, facilities utilizing zinc in their product production, fuel and coal combustion, zinc-containing fertilizers and pesticides, corrosion of galvanized solids, and waste disposal and incineration.[244, 260-261, 263] In the atmosphere, zinc is in, or adsorbed to, particles. It has been reported that the mass median diameter of zinc-containing particles is ~1.5 μm for both rural and urban sites.[264] Generally, the natural background concentration of atmospheric zinc is ≤ 300 ng/m^3. In urban areas, the zinc concentrations in the atmosphere are generally < 1 μg/m^3.[244, 260-261] A survey of the National Air Surveillance Network showed that the mean zinc atmospheric concentration was 0.02 to 0.16 μg/m^3 for urban areas, 0.01 to 0.05 μg/m^3 for rural areas, and 0.003 to 0.027 μg/m^3 for remote areas in the United States from 1977 to 1979.[244] In Europe, the zinc atmospheric concentration ranged from 0.4 to 300 ng/ m^3 in the rural air, and 10 to 2400 ng/ m^3 in the urban air. In samples taken over the Atlantic Ocean, remote areas (depending on respective recent atmospheric transport histories), the atmospheric zinc concentration range was 0.3 to 27 μg/m^3.[263] Regarding regulations, the province of Ontario, Canada has an ambient air quality criteria, averaged over a 24 period, of Zn < 120 μg/m^3.[265]

Zinc is an essential trace element. Zinc in organisms, is present as Zn^{2+}, and is a component in over 300 enzymes and proteins. The zinc ion is, thus, involved in many cell processes, including DNA synthesis, membrane stability, cellular signalling, cell proliferation, metabolism, differentiation and apoptosis.[245, 266] Approximately 50% of zinc is localized in the cytosol and cell membranes, and 30 to 40% is in the nucleus. [32] With respect to health implications from particulate air pollution, a function of Zn^{2+} is cellular protection from oxidative stress. As a non-redox metal, zinc itself is not directly involved in free radical reactions, rather the Zn^{2+} role is as an antioxidant through several indirect mechanisms. It is an essential structural component of superoxide dismutase (SOD), and the primary inducer of the metal-binding protein metallothionein (MT).[32, 266] Both of these proteins are free radical scavengers. Metallothioneins are potent scavengers of heavy metals, including cadmium, mercury, and copper.[266] Zinc can also reduce the generation of free radicals by replacing redox-active transition metals such as copper and iron from biomolecules.[267] It is reported that the increase of intracellular zinc concentration can reduce the hydroxyl radical driven DNA damage by replacing iron ions from the nucleoproteins.[268] In addition, zinc stabilizes cell membrane structure, and prevents lipid peroxidation.[266]

At moderate extracellular zinc concentration, zinc is an inhibitor of cell apoptosis and protects cells against oxidative stress. Exposure to elevated concentrations of zinc is toxic. The zinc homeostatic system can fail in instances when extracellular zinc concentration is high, and cause the accumulation of intracellular zinc, trigger pro-apoptotic molecules and in turn cell death.[244, 266] The impact of zinc on cell apoptosis is complex, and it remains ambiguous due to contradictory results.[32, 266] High concentrations of zinc prompt interaction with other metal ions, including copper, iron, and calcium, that have similar properties as zinc, and compete for the same protein binding sites.[263] As a result, it can lead to a nutritional deficiency of other essential metals. Copper deficiency and interfering of iron metabolism caused by excess zinc have both been reported.[32, 245, 263] Negative effects due to zinc deficiency are not discussed here.

Acute and chronic toxicity due to inhaled zinc is usually associated with occupational exposure. It is well-documented that intense exposure to zinc oxides can lead to metal fume fever (MFF), a risk in certain occupational situations such as zinc smelting and welding. The symptoms include fever, chest pain, cough, nausea, dyspnea, fatigue, and pulmonary function impairment. Generally, those effects are reversible and will not develop further into a chronic lung disease.[244-245, 269] Inhalation of small zinc oxide particles (< 1 μm) may cause inflammation, an increase of bronchiolar leukocytes, and tissue damage.[32, 244, 263] The zinc concentration that triggers MFF is not clear yet due to a limited number of studies.[32] Adult respiratory distress syndrome (ARDS), and human death, as a result of smoke bomb explosions that have high concentrations of zinc, zinc chloride vapor, plus other constituents, such as zinc oxide, hexachloroethane, and calcium silicate, have been reported in several cases.[270-272] Nevertheless, the evidence is not unequivocal to prove zinc's toxicity on humans. The LCT_{50} (lethal concentration and time, 50%) of zinc chloride in mice is 11800 mg/min/m^3.[273]

There are only a few studies that consider a chronic outcome due to inhaled zinc. Ishiyama *et al.* investigated the toxicity of zinc hydroxide and zinc sulfate using single intratracheal instillation. Rat lung morphological alterations have been observed after being treated with 1 mM of zinc hydroxide for 7 days, while no effect was found for zinc sulfate.[274] Hirshon *et al.* have suggested that there was an association between the high ambient air $PM_{2.5}$ zinc level and the increasing emergency department (ED) visits and hospital admissions for children having asthma the following day. In that study, a limited

number of particle components, including zinc, had been measured. The zinc concentration in ambient particles was ≥ 8.63 ng/m^3 and generally less than 1 µg/m^3, which does not compare to the occupational exposure level of zinc of 0.26 to 0.29 mg/m^3 in order to lead to an outcome of clinical disease. [244, 266, 275] This association is not, however, validation of zinc concentrations in ambient particles as being the cause of increased risk for asthma.

5.2.3. Background on lead

Lead is a rare metal, its mean abundance in the earth's crust is 16g/t (0.0016%).[276] It forms two series of compounds, having valence states of +2 and +4. Generally, Pb(II) compounds are ionic, while Pb(IV) compounds are covalent.[277] As a lustrous metal, the surfaces of metallic lead is bluish white when freshly cut, but undergoes oxidation rapidly to form an insoluble grey surface layer that resists corrosion from oxygen in the air, water, and soil. It was this property, the resistance to corrosion, that was the rationale behind using lead plumbing and piping.[276-277] Besides resistance to corrosion, metallic lead has other properties of commercial importance, such as high malleability, softness, low melting point, high density, and ductility. As such, metallic lead is widely used in different industries, including automotive, battery, pigments, coatings, ceramic glazes, ammunition, alloys, gasoline additives, and radiation shields.[100, 276-278] The single largest industrial use of metallic lead is in batteries.[100]

Natural sources of lead in the atmosphere include volcanic activity, forest fires, earth's crust weathering, sea sprays, and radioactive decay of radon.[278-279] However, human activities are the predominant sources of lead emissions into the atmosphere. Emission from vehicles using leaded gasoline had been the main source of ambient atmospheric lead for several decades following World War II,[278] but this source has been significantly reduced with the world-wide switch to unleaded gasoline for automobiles.[100] Other anthropogenic sources include smelting and refining of lead, manufacturing involving lead, and combustion of coal, biomass, and incineration of lead-containing wastes.[277-279]

With the persistence of lead in the environment, re-mobilization in sediment, soil, and water, is a risk.[279] Roadside dusts, and lake beds that have received roadside runoff, contain lead. Atmospheric lead is predominantly found in particles < 1 µm

diameter. It is reported that the concentration of atmospheric lead is 0.000076 μg/m^3 in remote areas, yet > 10 μg/m^3 proximal to stationary sources. According to the data from the EPA National Air Quality Monitoring Program, the average atmospheric lead concentration of United States was < 0.05 μg/m^3 in 2002.[278] In European cities, the average atmospheric lead levels were 0.15 to 0.5 μg/m^3 in urban areas, and < 0.15 μg/m^3 in nonurban areas.[280] Environment Canada's National Air Pollution Surveillance (NAPS) program has measured the ambient air concentrations of lead in $PM_{2.5}$ nationwide. Between 1984 to 2008, ambient air lead concentrations in Canada were consistently below 0.02 μg/m^3.[281]

Lead is a well-known toxin. It affects human body systems including central nervous, hematopoietic, hepatic, cardiovascular, renal, and reproductive system, and causes disorders of many functions, such as brain damages, delay growth for children, anemia, nephropathy, cardiac and vascular damage, hypertension, infertility, and miscarriage. Some of these adverse effects are irreversible.[31, 100, 278, 281-283] The route for lead internalization in humans is either through respiratory or gastrointestinal systems. Regarding inhalation, approximately 30-40% of the lead will enter the bloodstream, and then disperse to other tissues.[284] Lead toxicity is now diagnosed through blood concentration. Blood lead concentrations > 10 μg/dl are considered toxic. [267] Acute exposure, such as lead concentrations at up to 100-120 μg/dl for a short period of time, can lead to gastrointestinal disturbances, damage of hepatic and renal systems, hypertension and neurological effects including malaise, drowsiness, and encephalopathy, convulsions and even death. Chronic exposure at concentrations of 40-60 μg/dl, which is more common, can cause anaemia, nephropathy, cardiac and vascular damage, interference of reproductive systems and neurological disturbances such as lethargy, convulsions, and paralysis.[31, 279, 283] IARC has classified inorganic lead compounds as group 2A, as probably carcinogenic to humans, meaning there is limited evidence in humans but sufficient evidence in experimental animals to characterize inorganic lead compounds these compounds as carcinogenic.[278]

Induction of oxidative stress is a prominent mechanism in the toxicity of lead. Though it is a non-redox-active metal, lead has also been reported to generate ROS, such as hydroperoxides, hydrogen peroxides, and singlet oxygen directly.[31, 285] Through inhibition of sulfhydryl-dependent enzymes, and replacement of zinc ions that serve as co-factors in these antioxidant enzymes, lead can reduce the cellular antioxidant pools

including glutathione, SOD, and catalase (CAT), and thereby effect indirect stress on cellular oxygen homeostasis.[5, 31, 267, 285] Through binding to phosphatidylcholine in cellular membranes, lead can also induce changes in the biophysical properties of the membrane, such as lipid peroxidation.[284-286]

Lead also affects several intracellular system functions, from metabolism, inflammation, apoptosis, and intracellular movement, by replacing cations such as Ca^{2+}, Zn^{2+}, and Na^{+}.[31, 282] For example, it has been reported that lead can interfere with calcium fluxes, and it replaces Ca^{2+} in proteins. In calcium-binding proteins such as calmodulin, Pb^{2+} has a higher affinity, with an outcome that calcium-regulated activities are disrupted.[282, 284] Chelation of this nature may in part explain the observed lead transport across the blood-brain barrier, which is known to cause damage to the nervous system.[31, 100] Lead can also outcompete sodium, and seriously impair the Na^{+} dependent cellular functions.[31]

5.2.4. Background on iron

Iron is the fourth most abundant element in the earth's crust.[287] Its industrial use is extensive. Pure iron is a relatively soft silvery-white metal, and thus often alloyed with other elements, such as carbon, nickel, or concrete, for commercial applications.[287-288] However, iron is usually found in oxygen and/or sulfur-containing compounds as oxides, hydroxides, carbonates and sulfides in nature, with valences of +2 and +3.[287, 289] The main industrial application of iron is to manufacture steel, which is an iron-carbon alloy, usually containing 0.3-2% of carbon and small amount of other additive elements, and is widely used as a basic material in the construction and manufacturing of buildings, railways, bridges, ships, automobiles, aircraft, spacecraft, machinery, pipes, household appliances, furniture, tools, and weapons.[290] Other applications of iron include pigments in plastics and coatings, coagulants in water treatment, and nutritional supplies as an essential trace element.[289]

Natural processes such as weathering of the earth crust weathering, volcanic eruptions, forest fires, and sea sprays are the predominant sources of atmospheric iron. An estimated 95% of the globally averaged atmospheric iron budget is from mineral aerosol sources, and the largest sources are the North African deserts.[289, 291] Anthropogenic sources including industrial emissions, combustion of fuels and coal, and

biomass burning contribute to the remaining 5% of the budget.[291-292] Generally, the ambient level of iron in the air is around 1.3 μg/m^3 in urban areas, up to 12 μg/m^3 near stationary emission sources such as iron and steel manufacturing plants, and 50-90 ng/m^3 in remote areas.[289] M. Oakes *et al.* investigated the iron components in $PM_{2.5}$ for both urban and rural sites in Atlanta, United States. The total 24-hr average iron concentrations in the $PM_{2.5}$ ranged from 52.6 to 1743 ng/m^3 for the urban sites, and from 15.4 to 78.0 ng/m^3 for the rural sites. The fractional iron solubility was between 2 to 38% for all the sites. Iron was presented as a mixture of Fe(II) and Fe(III) in atmospheric particles, with a majority (estimated 74%) as Al-substituted Fe-oxides. The Fe(II) content ranged from 5 to 35% with an average of 25%.[293] B.J. Majestic *et al.* investigated iron content in both coarse and fine particles sampled from three urban sites. The total 24-hr average iron concentrations ranged from 58.2 to 241.0 ng/m^3 (mean: 152.1 ng/m^3) in $PM_{2.5}$, and from 16.2 to 417.8 ng/m^3 in PM_{10} (mean: 158.9 ng/m^3). The soluble fraction accounted for 1% to 20% of the total iron. The majority of both insoluble and soluble iron was in the form of Fe(III) in all the particle size fractions.[294]

Iron is an essential trace element for humans, which involves several fundamental activities, including oxygen transport, DNA synthesis, and energy metabolism.[295] The minimum iron nutritional requirement ranges from 10 to 50 mg/day depending on age, sex, and physiological status.[289] Approximately 65% of all internalized iron is bound to haemoglobin, another 10% is an integral component of enzymes, cytochromes, and myoglobin, and the remainder is sequestered by iron storage proteins such as hemosiderin and ferritin, or bound with transport proteins, such as transferrin.[296] In instances when these storage pathways are overwhelmed, free redox-active iron can generate cellular damage mainly through inducing oxidative stress. In the presence of hydrogen peroxide, iron can catalyze the production of hydroxyl radicals via a Fenton reaction. Hydroxyl radicals are extremely active, and attack almost every constituent in the cell, causing lipid peroxidation, DNA damage, and even cell death. In addition, iron is a redox-active metal and the free ion reacts with lipid hydroperoxides directly which results in lipid peroxidation.[127-128, 296-297]

A protective pathway of cells to eliminate oxidative damage caused by exposure to excess iron is to sequester the iron within lysosomes, with subsequent removal through lysosome-mediated biliary excretion. Interestingly, a hypothesis that an overload of iron which leads to excessive accumulation of iron within lysosomes that causes

lysosomal fragility and function impairment has been proposed. With this hypothesis, the speculation is that the sequestered iron, and hydrolytic enzymes, will be released to the cytoplasm and induce cellular injury.[127]

Exposure to high doses of iron can lead to depression, shallow and rapid respiration, respiratory failure, convulsions, and coma.[289] Several pathological conditions, including heart and liver diseases, neurodegenerative disorders, diabetes, immune system abnormalities, and hormonal abnormalities have been reported.[296] Iron accumulation, ~10 mg per lung in hamsters, after exposure to 40 mg/m^3 ferric oxide dust, for 30 hours per week for 100 weeks. In these hamsters, pulmonary fibrosis has been observed. For humans, inhalation exposure to high doses of iron/iron compounds is usually restricted to occupational exposure risk.[298] However, no relationship has been found between the occupational exposure to free iron or iron compounds, and neither lung function damage or mortality of steelworkers by epidemiological studies.[299] Iron and its compounds are classified as possible human carcinogens, but rather in the situation of causing human lung cancer, it is probable that other dust and compounds aerosolized during iron and steel manufacturing processes, including quartz dust, polycyclic aromatic hydrocarbons, and non-ferrous metals, are responsible.[299-300]

5.3. Methodology

5.3.1. Tissue Culture Reagents

The culture medium, nutrition mixture F12 HAM Kaighn's modification (model: F12K), human tumor necrosis factor-α (Lot #H8916-10), sodium bicarbonate (bioreagent, Lot #S5761, 99.5%-100.5%) and trypan blue solution (Lot #T8154) were purchased from Sigma–Aldrich (Oakville, Ontario, Canada). Phosphate-buffered saline (PBS, Lot #OXBR0014G), fetal bovine serum (FBS, Lot #12483) and trypsin-EDTA solution (0.05%, phenol red, Lot #25300-054) were obtained from Fisher Scientific/Life Technologies (Pittsburgh, PA, USA).

5.3.2. Reagents, Particles, and Compounds

Commercially available crystalline silica (model: Min-U-Sil® 5) was used as provided (U.S. Silica Company, Berkley Springs, WV, USA). This material is declared as

high purity, inert, white crystalline silica from a natural source, having particles with a median diameter of 1.7 μm, and 92% of the silica particle diameters are reported as ≤ 5 μm. Carbon black (CB) nanoparticles (100 nm diameter，Lot #1211NH) were purchased from Nanostructured & Amorphous Materials Inc. (Houston, USA). The purity of CB nanoparticles is 88.1%, and impurities include ash (5.8%) and water (1.06%). Reagent grade soluble salts [NH_4NO_3, $FeCl_2$, $FeCl_3$, $Zn(NO_3)_2$, and $PbCl_2$] with purity ≥ 99% were purchased from Sigma–Aldrich (Oakville, Ontario, Canada).

5.3.3. Cell culture

The human lung alveolar epithelium cell line A549 (CCL-185, American Type Culture Collection, Rockville, MD, USA) was used for dose-response studies. The cells were cultured in F12K medium supplemented with 10% (v/v) fetal bovine serum (growth medium) at 37 ˚C in a humidified atmosphere of 5% CO_2 in the air. Cells were seeded in 6-well culture dishes (surface area per well 8.87 cm^2, Lot #83.1839.300, Sarstedt, Nümbrecht, Germany) and grown to confluence prior to dose-response assays. Cultures incubated with 2 ml particle-free serum-free medium, and 2 ml serum-free medium containing 50 ng/ml TNF-α, served as the negative and positive controls, respectively.

5.3.4. Cell exposure to particles and soluble salts

All particle stock solutions were made in serum-free medium fresh daily and vortexed homogeneously prior to their use. For CB nanoparticles and crystalline silica, the stock solution concentration used was 1 mg/ml. Stock solutions of 100 mM of NH_4NO_3, $FeCl_2$, $FeCl_3$, $Zn(NO_3)_2$, and 10 mM of $PbCl_2$ were prepared in sterilized deionized water. Serial dilutions of stock solutions were performed using the serum-free medium.

Aliquots of solutions containing particles and/or different soluble salts were then introduced to A549 cell cultures. For exposure to a single particle type, the cells were incubated with particles suspended in 2 ml serum-free medium at dosages from 0 to 175 μg/ml for CB nanoparticles, and 0 to 125 μg/ml for crystalline silica. For combination of insoluble particle and soluble salts, dosages of particles are 0, 87.5, and 175 μg/ml for CB nanoparticles, and 0, 62.5, and 125 μg/ml for crystalline silica, and soluble salts concentrations used were 0.234 and 0.937 μM for NH_4NO_3, 100 μM for $FeCl_3$ and

$Zn(NO_3)_2$, from 0 to 1000 µM for $FeCl_2$, and from 0 to 500 µM for $PbCl_2$ in 2 ml serum-free medium in binary model. In the ternary model, 100 µM Fe^{2+} and 100 µM Pb^{2+} plus 125 µg/ml crystalline silica was adopted. All samples were run in duplicate per experiment. Three or more independent experiments with the same dose were performed throughout.

5.3.5. Measurement of IL-6 and IL-8 concentrations in supernatants

Following exposure of the culture to the dose that was 18 hours in duration, supernatants were collected and stored at –80°C until analysis. The concentrations of two pro-inflammatory mediators, IL-6 and IL-8, in the supernatants were quantified using ELISA kits as per the manufacturer's instructions (IL-8, model #900-M18, and IL-6, model #900-M16, Cedarlane (Burlington, Ontario, Canada). The ELISA assays were performed in triplicate. The determined concentration of IL-6 and IL-8, mean and standard deviation (SD), were obtained through normalization against the positive and negative control, using the equation $s_{\mathrm{final}} = \frac{\mathrm{S-N}}{\mathrm{P-N}}$ (S: samples, N: negative control, P: positive control).

5.3.6. Trypan blue assay

After the collection of the supernatants, cultures were washed three times with 2 ml PBS per single culture in a 6-well plate. A trypan blue viability assay was performed immediately thereafter following the procedure of trypan blue exclusion test.[164] The numbers of viable and non-viable cells were counted using a hemacytometer (0.1 mm, Bright-Line™) and a bright-field microscope (TMS-F, Nikon), respectively. The viabilities of cells were calculated as viability (%) = $\frac{\text{total number of viable cells per ml of aliquot}}{\text{total number of cells per ml of aliquot}} \times 100\%$, then normalized against negative controls.

5.3.7. Statistical analysis

The data acquired on cell viability, and the expression of IL-6 and IL-8 is reported as mean values ± standard deviation (1σ). The student t-test was used to compare the cell viability and cytokine expression between samples, and controls and samples. The

threshold for statistical significance was set as $p < 0.05$, and when $p < 0.01$ was obtained it is reported.

5.4. Results and Discussions

5.4.1. Ammonium nitrate

Based on reported ambient particulate concentrations of ammonium nitrates, ~15% of the total particle mass, two dosages were adopted. Cultures were bathed with either 0.23 or 0.94 μM ammonium nitrate, which corresponds to 13% and 38% of the total particle mass, respectively, used later in this work. This study, involving ammonium nitrate, was performed because it is, by mass and by prevalence, a significant component of ambient particles. The assumption made was that ammonium nitrate can influence or change the physical and/or chemical properties of the ambient particles and, therefore, have a role in their cytotoxicity.

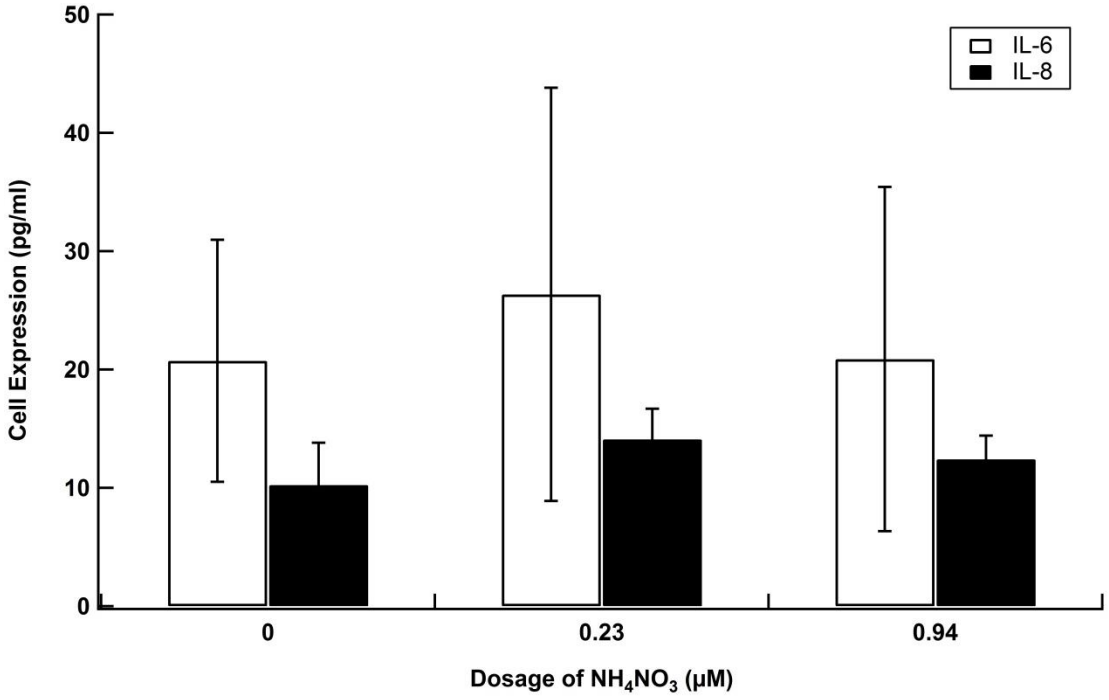

Figure 5.1 IL-6 and IL-8 expression of A549 cells after 18 hrs exposure to 0.23 and 0.94 μM NH_4NO_3. The data are reported as mean values ± standard deviation (1σ), with the number of samples ≥ 3.

Ammonium nitrate alone at either high and low dosages induced no differentiable cytokine expressions from negative controls (Figure 5.1). Also, there was no obvious

effect on cell viability observed. Figure 5.2 indicates the effect of combined doses of ammonium nitrate at either 0.23 or 0.94 µM plus a particle type, either crystalline silica or CB nanoparticles, at 125 µg/ml. In comparing the results from cells exposed to the particles alone, the addition of ammonium nitrate as a secondary component caused no change on the cell expression for both IL-6 and IL-8, for both the low and high concentrations of ammonium nitrate used. This result is consistent with previous studies of inhaled nitrates that have indicated that there was no measurable adverse effect from nitrate on ambient particles.[250-251] An interpretation of this result is that, for water-soluble particle components, the mass dosage is not as important as chemical composition, unlike the results presented in Chapter 4 that indicated ambient insoluble particle types induce cytokine expression in a dose-dependent manner.

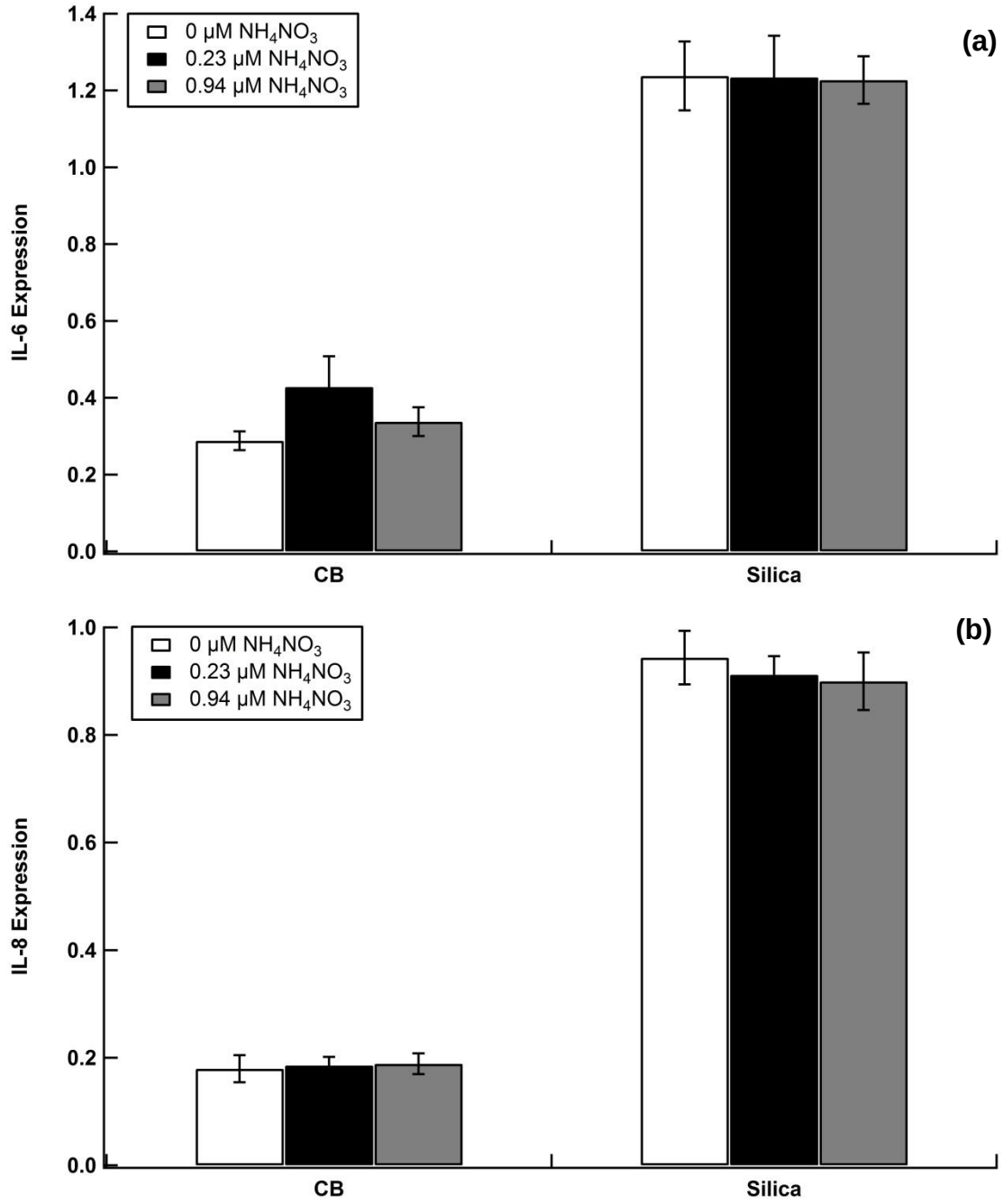

Figure 5.2 Normalized (a) IL-6 and (b) IL-8 expression after 18 hrs incubation of A549 cell cultures as a function of dose of NH_4NO_3 + 125 μg/ml of either CB nanoparticle or crystalline silica. The data are reported as mean values ± standard deviation (1σ), with the number of samples ≥ 3.

5.4.2. Zinc

Zinc nitrate alone at 100 μM induced no differentiable cytokine expression relative to negative controls in A549 cultures. The cells were then dosed with zinc ions plus particles, at 62.5 or 125 μg/ml for crystalline silica, and 87.5 or 175 μg/ml for CB nanoparticles, respectively. The cell expressions measured are plotted in Figure 5.3. Generally, in comparison to cells dosed with crystalline silica particles alone, the addition of Zn^{2+} together with crystalline silica reduced supernatant concentrations for both IL-6 and IL-8, with statistical significance measured for IL-8. In contrast, no measurable differential effect was found between cells dosed with CB nanoparticles alone versus cells exposed to Zn^{2+} together with CB nanoparticles.

Zinc has been reported to protect the cell from free radicals by several mechanisms, such as serving as a cofactor of enzymes that are believed to act as protectants.[5, 29, 245, 266, 301-302] Its possible activity as an antioxidant could explain the reduction of cytokine expression of cells exposed to zinc plus crystalline silica. Another possible mechanism is through hydrolysis of zinc on silica particle surfaces to generate $Zn(OH)^{+}$. The $Zn(OH)^{+}$ would be retained on the particle surfaces and thus reduce the surface reactivity of these particles.[149, 303] Of the pathways that zinc may be involved in, they do not appear to alter the toxicity of CB, because no significant effect in introducing Zn^{2+} with CB nanoparticles was measured.

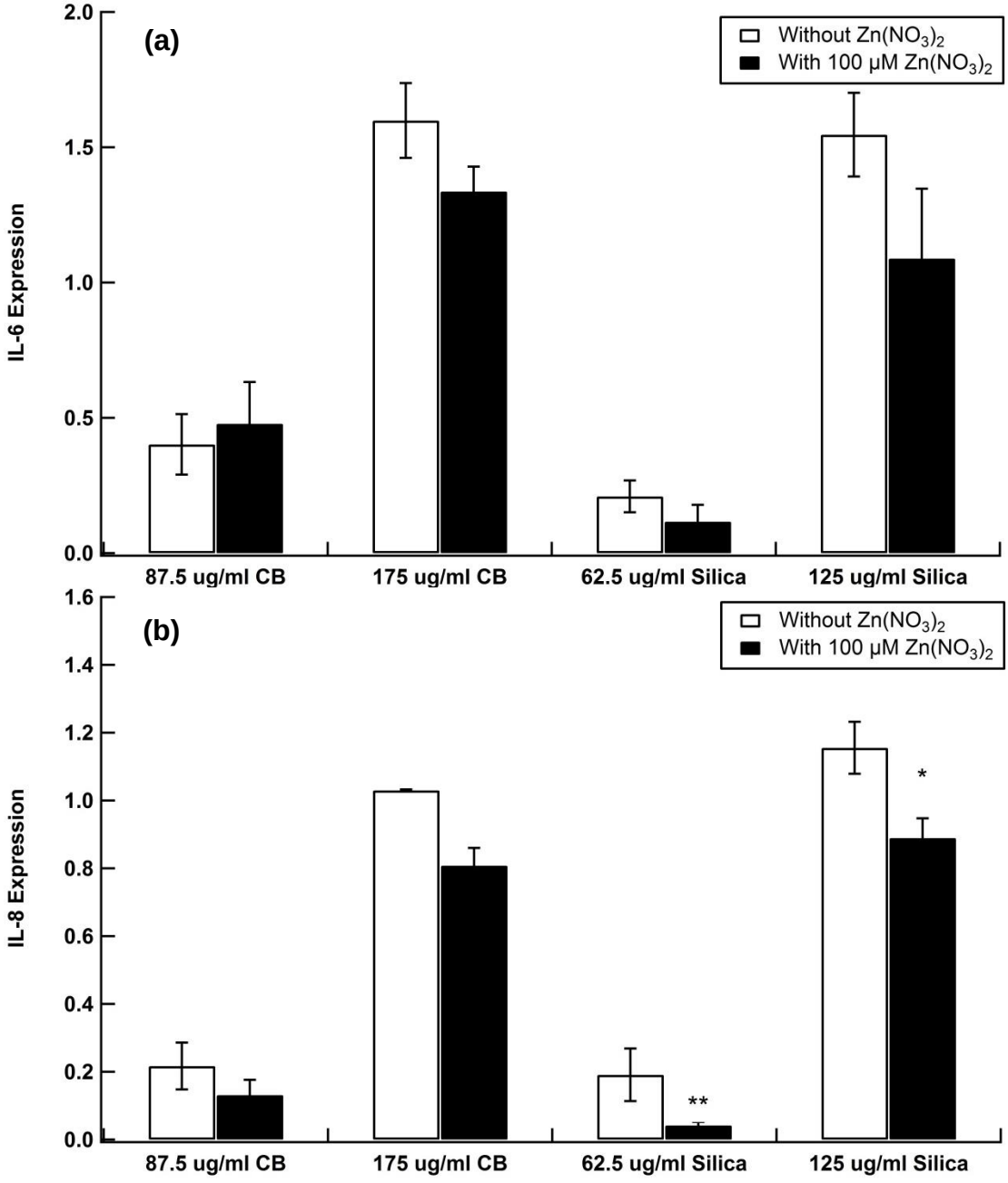

Figure 5.3 Normalized (a) IL-6 and (b) IL-8 expression after 18 hrs incubation of A549 cell cultures as a function of dose of CB nanoparticle/ crystalline silica + 100 μM $Zn(NO_3)_2$. The data are reported as mean values ± standard deviation (1σ), with the number of samples ≥ 3. The asterisks indicate statistical difference between the viability of the cells dosed with particles plus 100 μM $Zn(NO_3)_2$ and that of the cells dosed with particles alone. A single asterisk (*) represents $p < 0.05$, two asterisks (**) represent $p < 0.01$.

5.4.3. Lead

A549 cell cultures were exposed to 100 μM Pb^{2+} plus low and high dosages of particles, 62.5 or 125 μg/ml crystalline silica, 87.5 or 175 μg/ml for CB nanoparticles, respectively. Compared to cell cultures dosed with particles alone, Pb^{2+} plus either crystalline silica or CB nanoparticles, at the respective lower mass dose for each of these particle types, effected non-additive increases for both IL-6 and IL-8 expression relative to cells dosed with these particles alone (Figure 5.4). Cell viability measurements for the same doses are plotted in Figure 5.5. Lead chloride alone at 100 μM induced no differentiable cytokine expressions of A549 cultures as compared to the negative control (Figure 5.6). Statistically significant increases in both IL-6 and IL-8 was measured for the dose of the lower concentration used for silica plus lead ions. For doses at the higher concentration of silica used plus Pb^{2+}, the measured cytokine expression levels were lower than that for the respective lower mass silica doses. This result is rationalized with the measurement that many cells in the culture were no longer viable at the end of the 18-hr exposure (Figure 5.5). The trend for CB plus Pb^{2+} was similar as crystalline silica plus Pb^{2+} with respect to cytokine expression, except differential cell death was not measurable.

The effect of combined doses of Pb^{2+} with crystalline silica was further characterized by varying the concentration of Pb^{2+}, from 0 to 500 μM, and dosed with crystalline silica particles at 62.5 or 125 μg/ml (Figure 5.6). Lead chloride alone induced no differentiable cytokine expression and cell viability relative to negative controls until the dosage concentration of Pb^{2+} was 500 μM. At 500 μM lead chloride alone, precipitates were observable in the solutions. This result suggests that there are different pathways responsible for the cytotoxicity of soluble and insoluble lead, respectively. For cells exposed to crystalline silica plus Pb^{2+}, generally, as the dosage of Pb^{2+} increases, the concentration of the specific cytokines measured increased. With respect to IL-6, cells dosed with crystalline silica plus Pb^{2+}, as compared against the cells dosed with crystalline silica alone, measurably different responses occurred at ~10 and ~1 μM Pb^{2+} for combined doses with crystalline silica particles at 62.5, and 125 μg/ml, respectively (Figure 5.6a). For IL-8, the threshold for differential response due to the addition of Pb^{2+} to crystalline silica particles was ~10 and ~100 μM Pb^{2+} for combined doses with 62.5 or 125 μg/ml silica, respectively (Figure 5.6b). At [Pb^{2+}] = 500 μM, plus particles, the

measured cytokine expression levels were as low as the negative controls with respect to IL-6, because most cells in the culture were no longer viable.

The interaction between crystalline silica particles and lead measured here, and interpreted as a non-linear outcome, has also been measured by Chun-Feng Lu *et al.* using 10 μg/ml of nano-SiO_2 particles plus 100 μM lead acetate [$Pb(AC)_2$], with neither dose of silica or Pb^{2+} alone being cytotoxic. They suggested that the silica particles functioned as a carrier, and provided a route for the soluble, hydrophilic, lead cations to gain access to the interior of cells.[243] In our study, larger silica particles at higher concentrations were used, which appear to have a similar function. Recall the cytotoxicity of silica particles themselves has been proposed as being directly associated with the generation of ROS by the siloxyl radicals on its solid-liquid interface.[5, 237] Though a non-redox-active cation, Pb^{2+} has been reported to induce oxidative stress through multiple ways. It can catalyze peroxidative reactions, lead to lipid hydroperoxide production, generate ROS, and reduce the production of antioxidant compounds by inhibiting sulfhydryl-dependent enzymes.[5, 243, 285-286, 302, 304] Lead, internalized via endocytosis of carrier particles, can itself affect and stimulate additional intracellular functions, including inflammatory pathways and apoptosis by substituting for cations such as Ca^{2+}, Zn^{2+} and Na^{+}.[31, 282] Therefore, it is reasonable to assume that the addition Pb^{2+} enhances the level of oxidative stress induced by crystalline silica particles through different pathways, and/or enhancing these pathways.[305-307]

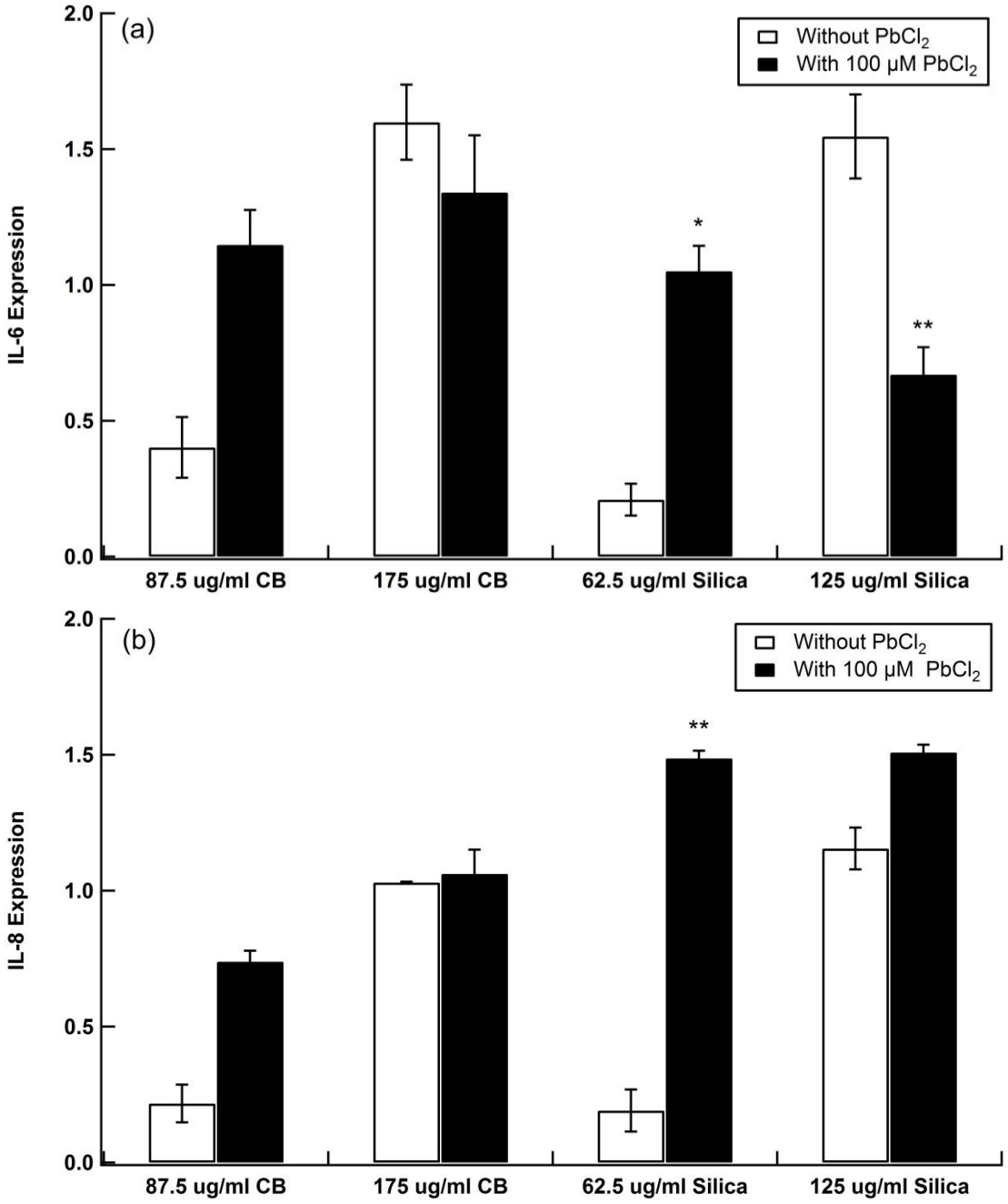

Figure 5.4 Normalized (a) IL-6 and (b) IL-8 expression after 18 hrs incubation of A549 cell cultures as a function of dose of CB nanoparticles or crystalline silica alone, or plus 100 μM $PbCl_2$. The data are reported as mean values ± standard deviation (1σ), with the number of samples ≥ 3. Asterisks indicate statistical difference between the viability of the cells dosed with particles plus 100 μM $PbCl_2$ versus that of the cells dosed with particles alone. One asterisk (*) represents $p < 0.05$, two asterisks (**) represent $p < 0.01$.

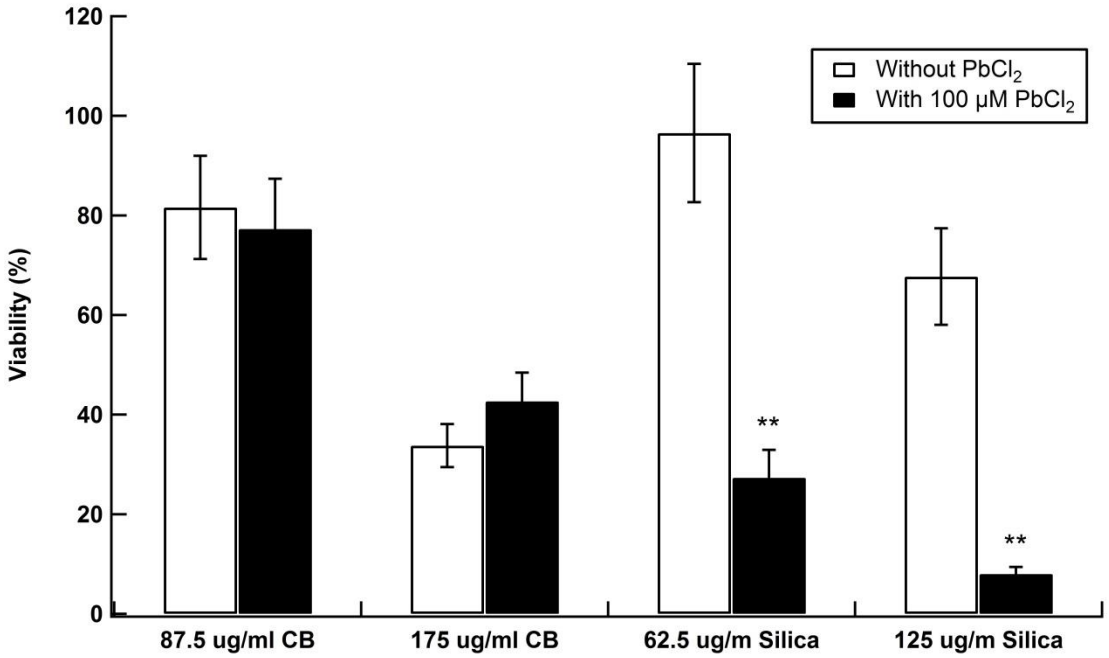

Figure 5.5 Normalized cell viability after 18 hrs incubation of A549 cells as a function of dose of either crystalline silica or CB nanoparticle alone, or with 100 µM $PbCl_2$. The data are reported as mean values ± standard deviation (1σ), with the number of samples ≥ 3. Asterisks indicate statistical difference between the viability of the cells dosed with particles plus 100 µM $PbCl_2$ versus cells dosed with particles alone. One asterisk above (*) represents $p < 0.05$, two asterisks (**) represent $p < 0.01$.

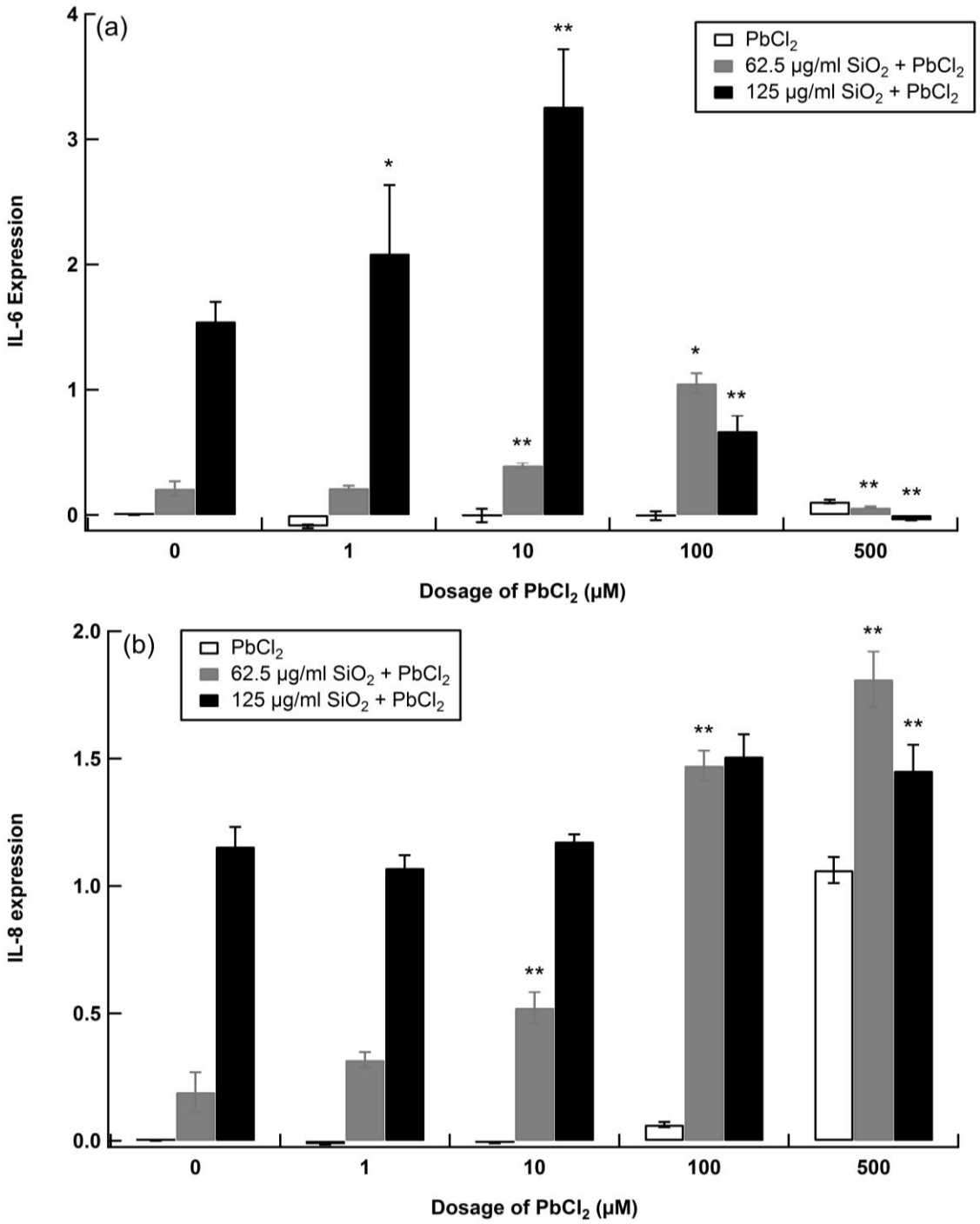

Figure 5.6 Normalized (a) IL-6 and (b) IL-8 expression after 18 hrs incubation period for A549 cell cultures as a function of a low and a high dose of crystalline silica, and the same dose plus varying concentrations of $PbCl_2$. The data are reported as mean values ± standard deviation (1σ), with the number of samples ≥ 3. Asterisks indicate the difference between the cytokine expression of the cells dosed with crystalline silica plus $PbCl_2$ and versus cells dosed with crystalline silica alone are statistically significant. One asterisk (*) represents $p < 0.05$, two asterisks (**) present $p < 0.01$.

5.4.4. Iron

The effect of either Fe(II) or Fe(III) ions on cellular expression have been investigated and results are plotted in Figure 5.7 and 5.8, respectively. Cells exposed to Fe^{2+} plus crystalline silica particles or CB nanoparticles at different particle dosages all effected a significant reduction in IL-6 and IL-8 expression levels. The cytokine expression level measured for all of the Fe^{2+} plus particles groups dosed dropped to the level of the negative controls (Figure 5.7). Regarding ferric iron, cells dosed with 62.5 µg/ml crystalline silica plus Fe^{3+}, the cytokine expressions were not differentiable from those of the cells dosed with 62.5 µg/ml crystalline silica alone. At higher silica doses, the Fe^{3+} plus 125 µg/ml silica resulted in an outcome similar to that measured for Fe^{2+}, with a significant reduction measured for IL-8. However, for both IL-6 and IL-8, the reduction of cytokine expression was not as large for ferric iron as it was for ferrous iron (with silica). For cultures dosed with Fe^{3+} plus CB nanoparticles at either concentration, effected a reduction of cytokine expression, but the reduction was significant only with respect to IL-8 (Figure 5.8).

In further measurements of the effect of ferrous iron, varying the concentration of Fe^{2+} from 0 to 1000 µM was studied in dosing the cell cultures (at constant volume of aliquot used), and also, the effect of combined doses of Fe^{2+} with 125 µg/ml crystalline silica or 175 µg/ml CB nanoparticle was measured. Ferrous chloride alone induced no differentiable cytokine expressions and cell viability from negative controls for doses < 1000 µM (Figure 5.9). At the dosage of 1000 µM, precipitates were observable in this solution, and ferrous chloride alone lead to a significant decrease of cell viability (61%) and an increase of IL-6 expression in comparison to negative controls. Similar phenomena were measured at high concentrations of lead chloride. These results at high concentrations of a soluble species, in which the solubility has been exceeded, clearly illustrate the significance of particulates in providing a route to the interior of cells via endocytosis for soluble, ionic, species.

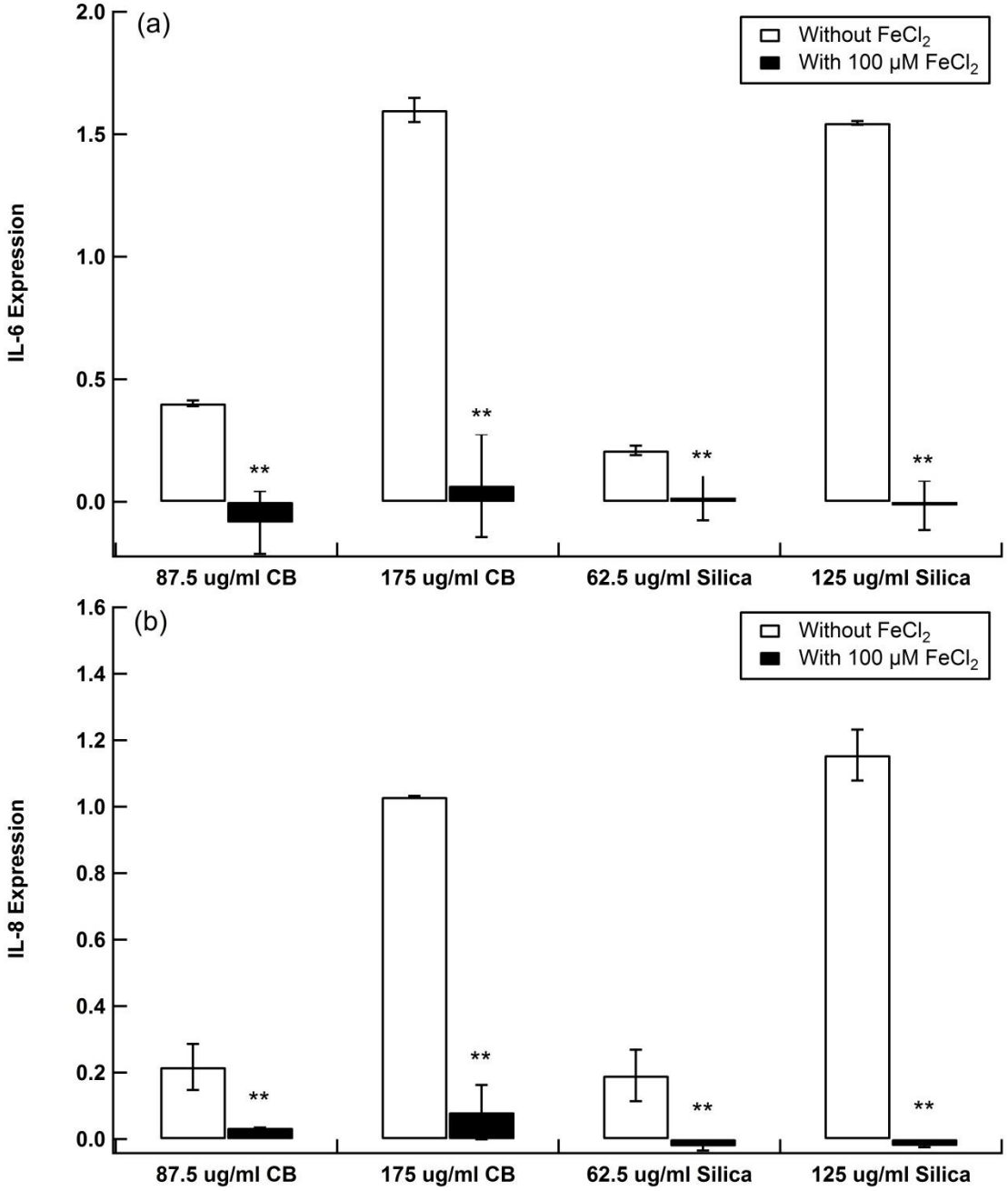

Figure 5.7 Normalized (a) IL-6 and (b) IL-8 expression after 18 hrs incubation period for A549 cell cultures with either CB nanoparticles or crystalline silica alone, and together with 100 μM $FeCl_2$. The data are reported as mean values ± standard deviation (1σ), with the number of samples ≥ 3. Asterisks indicate statistical difference between the viability of the cell cultures dosed with particles plus 100 μM $FeCl_2$ versus cell cultures dosed with particles alone. One asterisk (*) represent $p < 0.05$, two asterisks (**) represent $p < 0.01$.

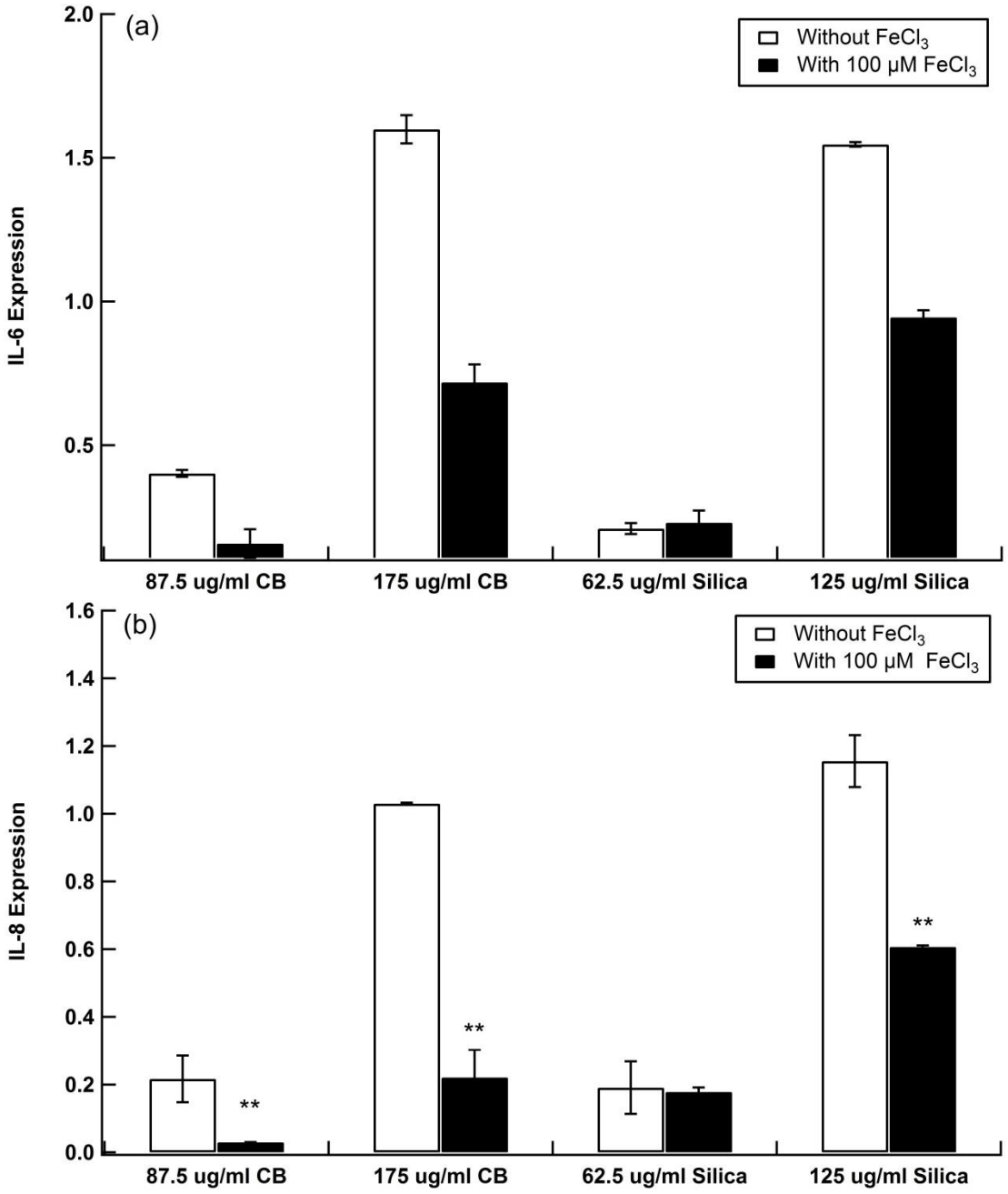

Figure 5.8 Normalized (a) IL-6 and (b) IL-8 expression after 18 hrs incubation of A549 cell cultures as a function of dose of CB nanoparticle or crystalline silica particles alone, and together with 100 μM $FeCl_3$. The data are reported as mean values ± standard deviation (1σ), with the number of samples ≥ 3. Asterisks indicate statistical difference between the viability of the cell cultures dosed with particles plus 100 μM $FeCl_3$ versus cell cultures dosed with particles alone. One asterisk (*) represents $p < 0.05$, two asterisks (**) represent $p < 0.01$.

Cell cultures exposed to increased concentrations of ferrous iron, up to [Fe^{2+}] = 100 μM, plus fixed concentration of CB nanoparticles or crystalline silica particles, responded with decreased abundance of cytokines (Figure 5.9), and increased cell viability (Figure 5.10), relative to the responses measured for the same mass dose of particles alone. This trend continued at [Fe^{2+}] = 1000 μM for IL-8, but not for IL-6, which was measured at high concentration, likely due to the increased fraction of cells becoming non-viable. As compared to the same mass of particles alone, the threshold for statistically reduced response for ferrous ion plus particles was 10 μM Fe^{2+} for both IL-6 and IL-8 with silica particles, and 100 μM Fe^{2+} with CB particles, while for cell viability, it was 100 μM Fe^{2+} with silica or CB particles.

Iron, under normal physiological conditions, is sequestered and thus considered inactive by iron storage proteins such as hemosiderin and ferritin.[296] Only when these storage pathways are overwhelmed is free redox-active iron available to cause cellular damage mainly through inducing oxidative stress. Previous studies have suggested that iron can introduce oxidizing species directly through redox-cycling in lung tissues and increase the production of ROS through Fenton reactions.[5, 308-309] With the presence of hydrogen peroxide, iron can catalyze the production of hydroxyl radicals by Fenton reactions.[128, 297] The quantity of hydroxyl radicals can be significantly affected by the concentrations of intracellular antioxidants, such as ascorbate, citrate, and glutathione.[310] Wilson *et al.* found that the addition of both Fe^{2+} and Fe^{3+} enhanced ROS generation by ultrafine CB particles in cell-free media. However, no increase of inflammation was observed due to the addition of either Fe^{2+} or Fe^{3+} *in vitro.* They suggested that the added ferric iron was sequestered by storage proteins, such as ferritin.[311] Ferrous iron is likely acting directly as a reducing agent, prior to being sequestered by ferritin. In addition, the generation of ROS may not directly correlate to the expression of pro-inflammatory cytokines.[312-313] In a study by Øvrevik *et al.* on mineral particles' cytotoxicity, no correlation was observed between ROS generation and cytokine expression or cell apoptosis, or in particular, the iron content of the particles.[314] Hydrolysis products of iron, including $Fe(OH)^{+}$ and $Fe(OH)^{2+}$, can interact with the silanol group/ionized silanol groups on the active site of silica particles, thus lowering the surface reactivity of the particles.[149, 303, 315] Experimental factors that have been proposed include the surface reactivity of the particles, regulation pathways involving Fe and how they can be affected, the concentration of storage/transport/receptor proteins, and

antioxidants. Additional experimentation is necessary to ascertain the validity of proposed mechanisms of oxidative stress and cytokine expression that exist in the peer-reviewed literature.

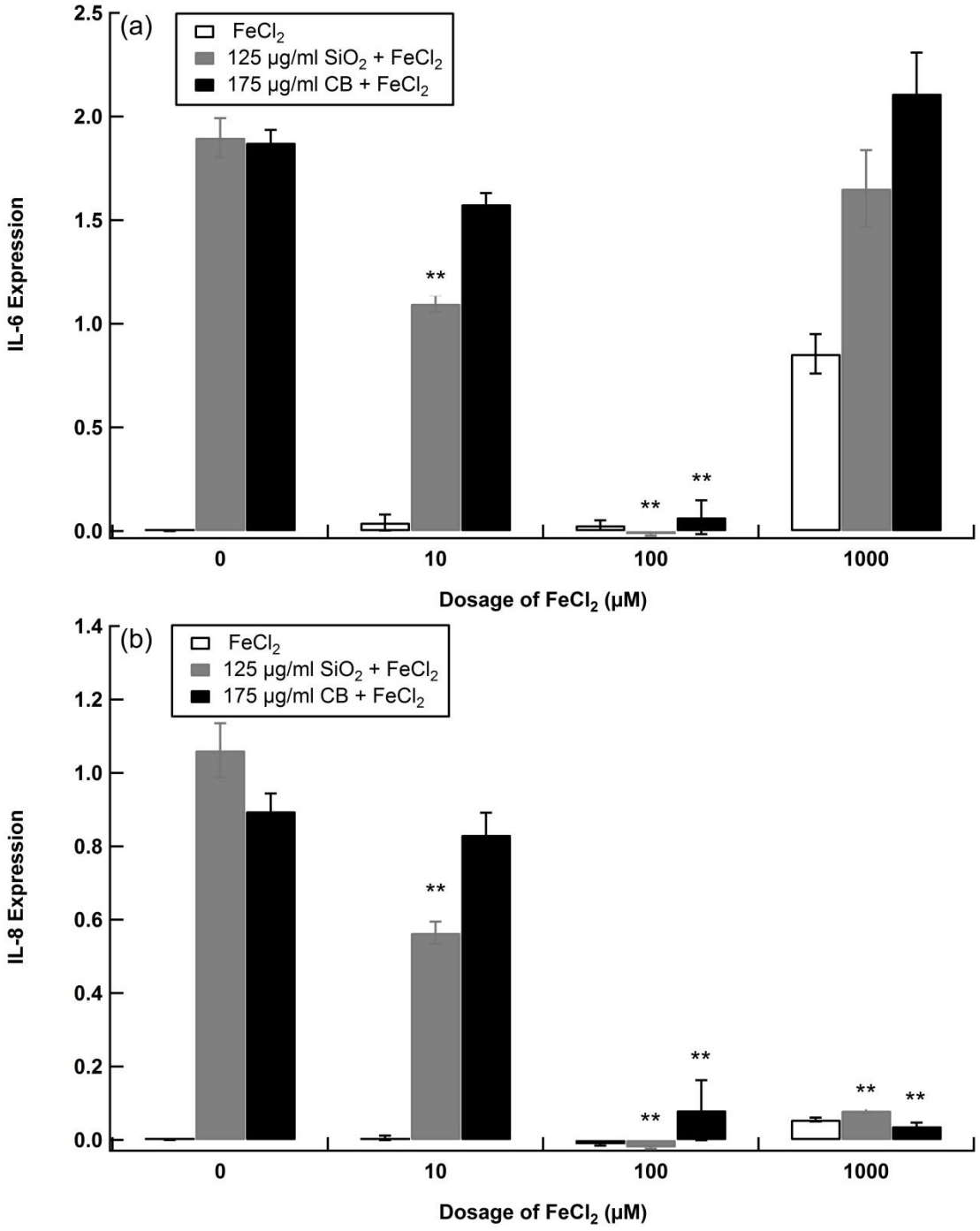

Figure 5.9 Normalized (a) IL-6 and (b) IL-8 expression after 18 hrs incubation of A549 cell cultures as a function of [$FeCl_2$] plus CB nanoparticles or crystalline silica particles. The data are reported as mean values ± standard deviation (1σ), with the number of samples ≥ 3. Asterisks indicate statistical difference between the cytokine expression of the cells dosed with $FeCl_2$ versus $FeCl_2$ plus crystalline silica or CB nanoparticles. One Asterisk (*) represents $p < 0.05$, two asterisks (**) represent $p < 0.01$.

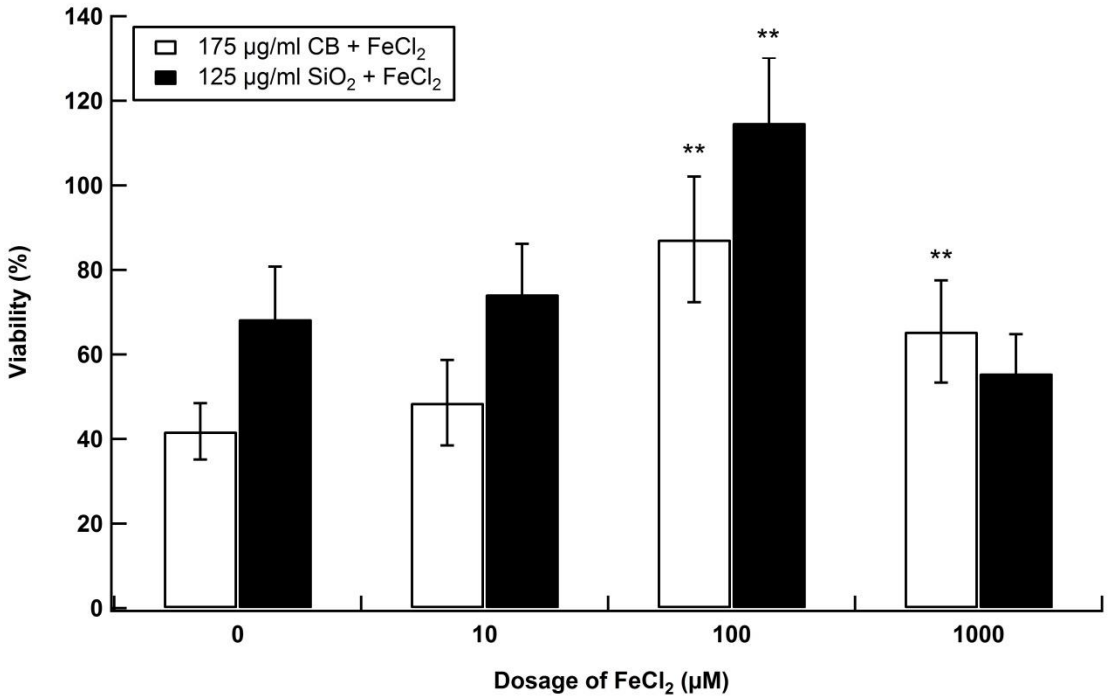

Figure 5.10 Normalized cell viability after 18 hrs incubation of A549 cell cultures as a function of [$FeCl_2$] plus crystalline silica particles or CB nanoparticles. The data are reported as mean values ± standard deviation (1σ), with the number of samples ≥ 3. Asterisks indicate statistical difference between the cytokine expression of the cells dosed with $FeCl_2$ plus crystalline silica particles or CB nanoparticles versus cells dosed with either particle type alone. One asterisk (*) represents $p < 0.05$, two asterisks (**) represent $p < 0.01$.

5.4.5. Combined doses using iron and lead

To further investigate the effect of iron(II) and lead ions, a ternary model using 100 µM Fe^{2+} and 100 µM Pb^{2+} plus 125 µg/ml crystalline silica particles was studied. The cell viability measurements are plotted in Figure 5.11a. The addition of 100 µM Fe^{2+} to the mixture of Pb^{2+} plus crystalline silica leads to an increase of cell viability relative to the responses measured for doses of particles alone and Pb^{2+} plus crystalline silica. Both Fe^{2+} plus crystalline silica and the mixture of Fe^{2+}, $Pb^{2+}$and crystalline silica lead to a cell viability of approximately 100%. In comparison to cell cultures exposed to crystalline silica alone and Pb^{2+} plus crystalline silica, Fe^{2+} plus Pb^{2+} and crystalline silica particles effected significant decreases in both IL-6 and IL-8 expression levels. The measured cytokine expression level is, however, higher than that of cells dosed with Fe^{2+} plus crystalline silica particles, where the latter is as low as the negative controls (Figure 5.11b).

Recall that results presented earlier in this chapter for Fe^{2+} with silica effected cytoprotectant behaviour, whereas Pb^{2+} with silica-induced a non-linear additive cell expression. An explanation for this result is that the insoluble crystalline silica particles function as carriers and provide access to cell interiors for the water-soluble particle components, such as iron and lead. Based on our results, Fe^{2+} is likely acting as a sacrificial reducing agent, whereas Pb^{2+} induces oxidative stress and stimulates inflammatory pathways and apoptosis through multiple pathways.[31, 282, 285-286] However, when Fe^{2+}, Pb^{2+}, and crystalline silica particles combine together, the presence of Fe^{2+} in the dose appears to dominate the cytotoxicity of this ternary mixture, as assessed using cell viability, and IL-6 and IL-8 expression. It is possible that more Fe^{2+} than Pb^{2+} was adsorbed on the surface of crystalline silica particles and carried into the cells. If a similar amount of Fe^{2+} and Pb^{2+} was transported into the cells, then these results suggest that the generation or reduction of ROS plays an important role in determining overall cell response and reduced redox species, such as Fe^{2+}, may play an important role in protecting the cell from oxidative stress. In addition, the ternary mixtures induced significant higher cytokine expression than the combination of ferrous ions and silica. It is possible that a certain amount of lead has been carried into the cells, which could be highly toxic. However, the biomarkers that have adopted in this study are very general pro-inflammatory cytokines, and may not be necessarily sufficient to indicate the cytotoxicity of lead under this condition.

As a mixture, traffic-derived particles consist of assorted insoluble particle types and water-soluble components. Riley *et al.* studied the interactions between combustion-derived metals, Zn with Cu or V or Ni, and found that the mixtures could either lead to a decrease or increase of the toxicity of the mixture as compared to the toxicity of Cu or V or Ni alone. Fe lead to the lowest toxicity amongst the metal ions of V, Zn, Cu and Ni, where the TC_{50} (toxic concentration, 50%) was used to provide quantitative information.[29] Studies focusing on measuring cellular outcomes using multiple particle types/components model should be pursued in the future to provide an improved understanding of the interaction between the components on a particle and the particles, and assist in identification of toxins/important particle components in the mixture.

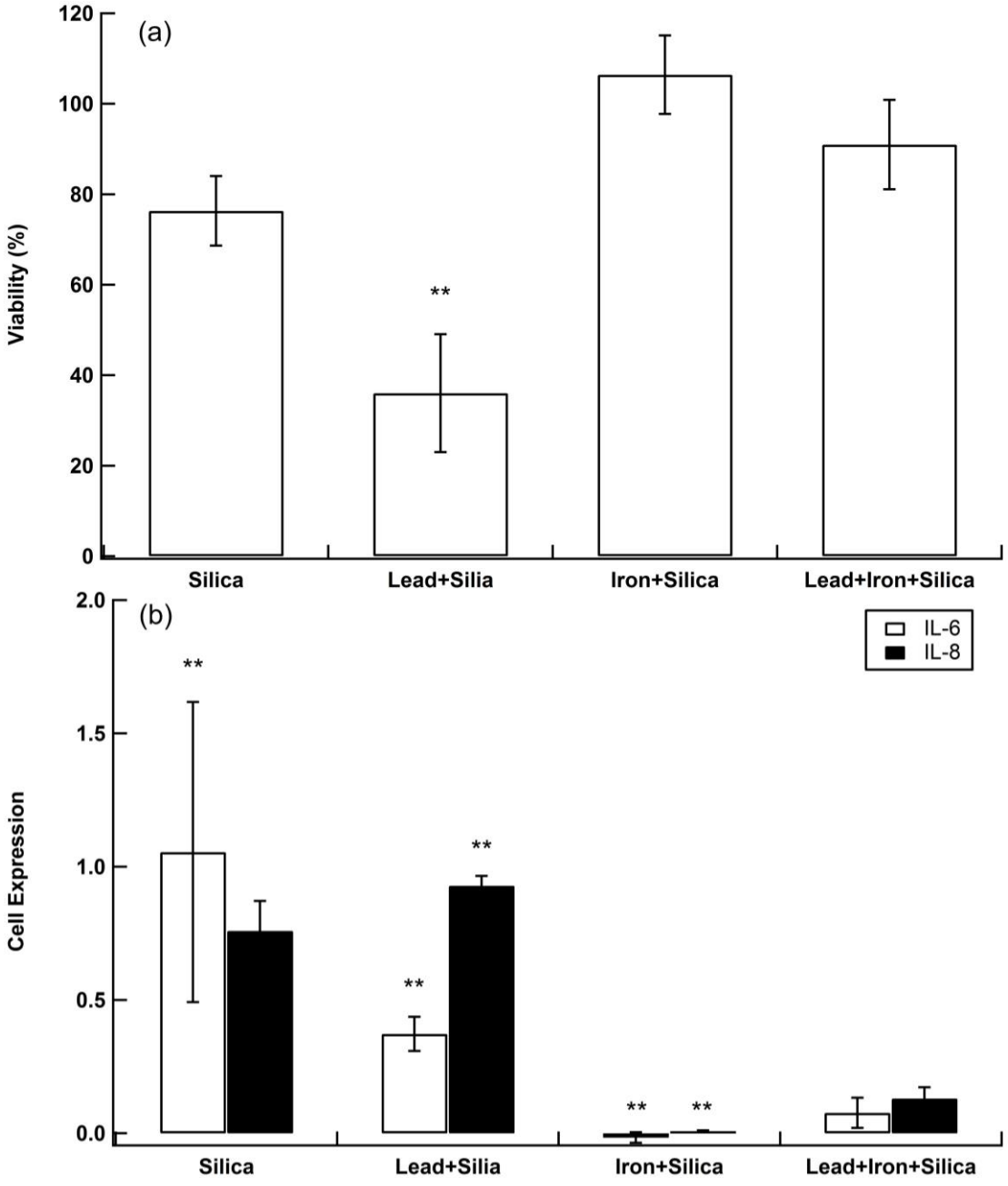

Figure 5.11 Normalized (a) cell viability (b) IL-6 and IL-8 expression after 18 hrs incubation of A549 cell cultures as a function of 100 µM $FeCl_2$ and 100 µM $PbCl_2$ plus 125 µg/ml crystalline silica. The data are reported as mean values ± standard deviation (1σ), with the number of samples ≥ 3. Asterisks indicate statistical difference between the viability or cytokine expression of the cells dosed with $FeCl_2$ and $PbCl_2$ plus crystalline silica versus cells dosed with crystalline silica alone or either $FeCl_2$ or $PbCl_2$ plus crystalline silica. One asterisk (*) represents $p < 0.05$, two asterisks (**) represent $p < 0.01$.

5.5. Conclusion

The combinations of particles plus various salts cause different cellular outcomes. There was no measurable effect with ammonium nitrate as a secondary component. Particles dosed with Zn or Fe each effected reduced cytokine expression. For cells dosed with 125 µg/ml crystalline silica particles plus Fe^{2+}, as compared against the cells dosed with crystalline silica particles alone, measurably different responses were at ≥ 10 µM of Fe^{2+} with respect to both IL-6 and IL-8. The analogous threshold for differential cytokine expression due to the addition of Fe^{2+} plus 175 µg/ml CB nanoparticles was ≥ 100 µM (Figure 5.9). Conversely, Pb^{2+} with crystalline silica particles induced a non-linear additive expression of cytokines. The lead salt concentration threshold to observe the non-linear additive effect with respect to IL-6 were at ~10 and ~1 µM of Pb^{2+}, for combined doses with crystalline silica particles at 62.5 and 125 µg/ml, respectively (Figure 5.6a). For IL-8, the threshold for differential response due to the addition of Pb^{2+} plus crystalline silica particles was 10 and 100 µM (Figure 5.6b) plus 62.5 and 125 µg/ml silica, respectively. The ternary combination of 100 µM Fe^{2+} and 100 µM Pb^{2+} plus 125 µg/ml crystalline silica leads to near 100% cell viability (Figure 5.11) and low IL-6 and IL-8 expression (Figure 5.12). Based on these results, it is concluded that Fe^{2+} plays an important role in the mixture with respect to lowering cytokine expression and maximizing cell viability.

The incubation of individual metal ions together with particles illustrates the importance of endocytosis in assessing how particle composition affects overall cellular responses. Ferrous chloride and lead chloride alone induced no differentiable cytokine expression and cell viability from negative controls until the dosages were as high as 1000 µM and 500 µM, respectively, at which concentrations, obvious precipitates were observable. At these high dosages, both ferrous chloride and lead chloride lead to a significant decrease of cell viability, and elevated cytokine expression. Under this condition, endocytosis provided a facile pathway for metal ions to access intracellular space. It also indicates that even for the same particle component, different regulation pathways may be activated by its soluble versus insoluble forms.

For an insoluble particle type plus water-soluble particle component system, particles can function as carriers, and provide the pathway for the soluble, hydrophilic, components to gain admission to the interior of cells. For example, the silanol group and

ionized silanol groups on silica particles will be negatively charged, and their interaction with soluble particle components in solution act to neutralize the surface charge of the particles, and thus enable bound ions, and others in the electrical double layer surrounding the particles, to be transported via endocytosis into the interior of cells. It has been reported that the cation concentration in the Stern layer of silica nanoparticles can be elevated by factors of ~10 - ~20 because of the silica particle's surface charge in electrolyte solution of pH ~7 (surface potential ranges from -200 to -400 mV).[47] Once internalized by a cell, the pH drop to 4~5 within a lysosome would be expected to displace metal cations bound in the Stern layers of a particle's solid-liquid interface. This is one mechanism for how soluble components alone are not toxic to cells, yet when presented with particles, are cytotoxic.

At similar solution conditions (i.e. pH 7 in F12 medium), the surface potential of CB nanoparticle with the diameter of 95 nm was measured as -5 mV, which could lead to a lower concentration factor for metal ions in the Stern layer.[190] Thus, in comparison to crystalline silica, fewer metal ions could be transported by CB nanoparticles. This assumption is supported by our results that show CB plus solutes, Pb^{2+} or Fe^{2+}, effected analogous, but smaller, cellular response than silica plus Pb^{2+} or Fe^{2+}. Further, the greater surface area of the CB nanoparticles versus the micrometer silica particles was therefore a non-factor in this experiment. Rather, this outcome points to the particle surface properties for a given set of experimental conditions is important.

Our studies support the conclusion that varied different cellular outcomes are resultants followed by dosage with different combinations of particles plus various salts, and other compounds on ambient particles. Related, Ghio *et al.* has suggested that sulfate can increase the mobilization of metal ions, by functioning as new ligand in the cell competing with physiological ligands, and thus contribute to the cytotoxicity of particles in an indirect way.[316] By extension, cellular responses to doses of whole ambient particles are the summative outcomes of the respective species and their abundances in causing injury to the cells. Future investigations that extend this basic methodology can be done, to study more particle components and varied particle types and their interactions. Results of that nature would likely elucidate more clearly if there are specific particle components that contribute disproportionately to the cytotoxicity of the whole system. This type of information is needed to inform policy development regarding air quality.

Chapter 6.

Summary and Future work

6.1. Summary

To investigate the toxic effect of traffic-derived ambient particles, an *in vitro* methodology using human lung alveolar epithelium cell line A549 was adopted in this work. Certified reference material ERM-CZ120, an ambient particle type collected in a high traffic volume automobile tunnel, was used to illustrate the relative roles of the water-insoluble and water-soluble fractions of ambient particulate matter. Laboratory mimics of several insoluble particle types and water-soluble particle components that are commonly measured in locations at or near major automobile roadways were adopted to evaluate their health effect. In this study, the emphasis was on learning about the interactions between different particle types and components as assessed using specific cellular readouts (i.e. cell viability, and expression of two pro-inflammatory cytokine IL-6 and IL-8), and thus add to the understanding of how such interactions affect the cytotoxicity of whole particles.

Following 18-hour incubation periods of A549 cultures with ERM-CZ120 (whole particle), its water-insoluble fraction, and the water-soluble fraction at mass concentrations in the supernatant spanning 0 to 1250 μg/ml, a dose-dependent pro-inflammatory cytokine IL-6 expression and cell death was measured for both the whole particle and the water-insoluble fraction, with the former effecting higher levels of IL-6. No differential expression of cytokines and cell viability relative to negative control was effected by the water-soluble fraction alone. IL-8 was also measured, but there was no expression differentiable from the negative control. These results suggest that, for the particle type ERM-CZ120, the insoluble fraction is the primary, mass dependent, factor that determines the overall cytotoxicity, and the water-soluble fraction has an assignable effect but only when dosed together with the insoluble fraction. Endocytosis clearly plays an important role in this process.

Carbon black nanoparticles, crystalline silica particles, and nickel nanoparticles were chosen as laboratory mimics of the insoluble fraction of diesel soots, a re-

suspended roadside dust type, and an insoluble metal particle type, respectively. Dose-dependent correlations between particle exposure and cell viability and cytokine expressions (both IL-6 and IL-8) have been measured for CB nanoparticles, crystalline silica and the mixture of them at the mass dosages range varies from 0 to 700 μg/ml. In comparison to crystalline silica, and mixtures of CB nanoparticles and crystalline silica, crystalline silica particles lead to lowest cell viability and greatest cytokine expression at the same mass dosage. Additive mass effects were observed for mixtures of CB and crystalline silica at three different mass ratios with respect to cell viability and IL-8 expression, while non-addictive lung cell response for IL-6 was measured in specific doses. No differentially measurable effect on cell viability or cytokine expression was observed for nickel nanoparticles at dosage ≤ 100 μg/ml. 10 μg/ml nickel nanoparticles plus crystalline silica induced significantly higher IL-6 expression at both low and high silica dosages than crystalline silica alone. In these particle mixtures, the mass of crystalline silica in the dose effect the cellular response predominantly.

Several water-soluble particle components, including ammonium nitrate, and soluble salts of zinc, lead, and iron, and their interaction with two insoluble particle types, CB nanoparticle and crystalline silica particle, have been studied on effecting lung cell responses *in vitro*. No cellular response was caused by ammonium nitrate either alone or in combination with particles. 100 μM of soluble metal salts alone had no differential effect on both IL-6 and IL-8 compared to negative controls. However, cellular outcomes dependent on the chemical composition of the dose were observed for the combination of metal salts at the same concentration (100 μM) plus particles. Combination of particles (CB nanoparticles or crystalline silica particles) with Zn or Fe each effect cytoprotectant behavior, whereas Pb with crystalline silica induced a non-linear additive expression of both IL-6 and IL-8. For cells exposed to 125 μg/ml crystalline silica plus Fe^{2+}, measurably different responses relative to crystalline silica alone occurred at $[Fe^{2+}]$ > 10 μM with respect to both IL-6 and IL-8, and the analogous threshold for CB nanoparticles at 175 μg/ml was $[Fe^{2+}]$ > 100 μM. For Pb^{2+}, the IL-6 threshold to observe a non-linear additive effect was 10 μM with 62.5 μg/ml crystalline silica, and 1 μM with 125 μg/ml crystalline silica, while the IL-8 threshold was 10 and 100 μM when combined with 62.5 or 125 μg/ml crystalline silica, respectively. High dosages of $FeCl_2$ (500 μM) or $PbCl_2$ (1000 μM) alone lead to a significant decrease of cell viability, and an increase of cytokine expression. Obvious precipitates were observed in these solutions, which

suggested that the cellular response was caused by a combined effect of amorphous precipitates plus soluble metals. The ternary mixture of 100 µM of Fe^{2+} and Pb^{2+} plus 125 µg/ml crystalline silica lead to a significantly lower IL-6 and IL-8 expression and higher viability relative to crystalline silica alone or Pb^{2+} plus crystalline silica. Further, the ternary combination had a higher level of cytokine expression but similar viability which is around 100% as compared to cells exposed to Fe^{2+} plus crystalline silica. Fe^{2+} plays a significant role in these doses with respect to lowering cytokine expression and maximizing cell viability.

6.2. Future work

6.2.1. Method modification: co-culture, new biomarkers, and data analysis

In this study, human lung alveolar epithelium cell line A549 was dosed with mimics of traffic-derived ambient particles. While this study illustrated that mixtures of particle components lead to cellular outcomes that were not linear summations of responses to the same components that were individually dosed onto the cells. The methodology is a simply mono-culture system, and as such, it has a limitation in reflecting the complexity of an organismal respiratory system and the interaction between inhaled particles and the respiratory system. For instance, in the case of particles depositing in the AI region, alveolar epithelial cells interact with particles and in response secrete pro-inflammatory cytokines/chemokines that function to recruit phagocytic cells. Alveolar macrophages clear the particles from the lung through phagocytosis.[5] During this process, a complex network of multiple extracellular and intracellular signalling pathways can be activated that involves different types of cells.[5, 109] In addition, the pulmonary endothelial cells has also been reported to interact with inhaled particles and contribute to both the local pulmonary injury and the systemic effect.[87, 93-95] Adopting a co-culture of alveolar epithelial cells, macrophages, and/or pulmonary endothelial cells, and possibly using air-liquid interface supports, could be used to provide better mimicry of particle-cell interaction in the AI region.

Non-linear additive cellular expression, possibly by the involvement of more than one biological pathway, has been measured following doses of a combination of certain particle types and components. For instance, endocytosis possibly plays an important

role for water-insoluble particle fraction, and water-soluble particle components effected different outcomes. The biomarkers, IL-6, IL-8 and cell viability, that were adopted to assess the cellular response in this study, however, are insufficient to address the underlying mechanisms by which particles interact with the cells. To enable a better investigation of the biological outcomes following doses with different particle components/types, especially to confirm the proposed mechanisms, other factors/techniques are needed for the future study. For example, the scanning electron microscope (SEM) and/or confocal microscopy can be used to observe the internalization of particles. And special endocytosis assay can be applied to further investigate the different pathways of particle internalization. The Intracellular level of glutathione versus that of its oxidized state, glutathione disulfide, is a possible indicator for evaluating the cellular oxidative stress.[317] Biomarkers for specific biological processes and pathways, e.g. apoptosis which is a type of programmed cell death, could provide more information about the cell viability results in this study.[318] Soft-ionization mass spectrometry (MS) techniques could be applied to detect biologics, from small molecules like glutathione to macromolecules such as proteins in the supernatants of cell cultures.[319-320] The methods accessible with modern instrumental methods have the potential to provide new information regarding cellular responses.

In addition, some improvement can be done with the data analysis. For instance, the cytokine expression of insoluble particle types, crystalline silica, CB nanoparticles and the mixtures of them follows a mass-dependent manner. However, besides the mass dosage of the particles, the amount of viable cells is another factor that affects the IL-6 and IL-8 expression. The measured maximum for interleukin secretion corresponded to a trade-off between maximal stimulation of the cells versus minimal cell death. To better assess the effect of particle mass dosage, a normalization factor, i.e. the number of viable cells, can be adopted for ELISA data. As showed in Figure 6.1, after normalization, a better evaluation might be obtained for both IL-6 and IL-8 expression.

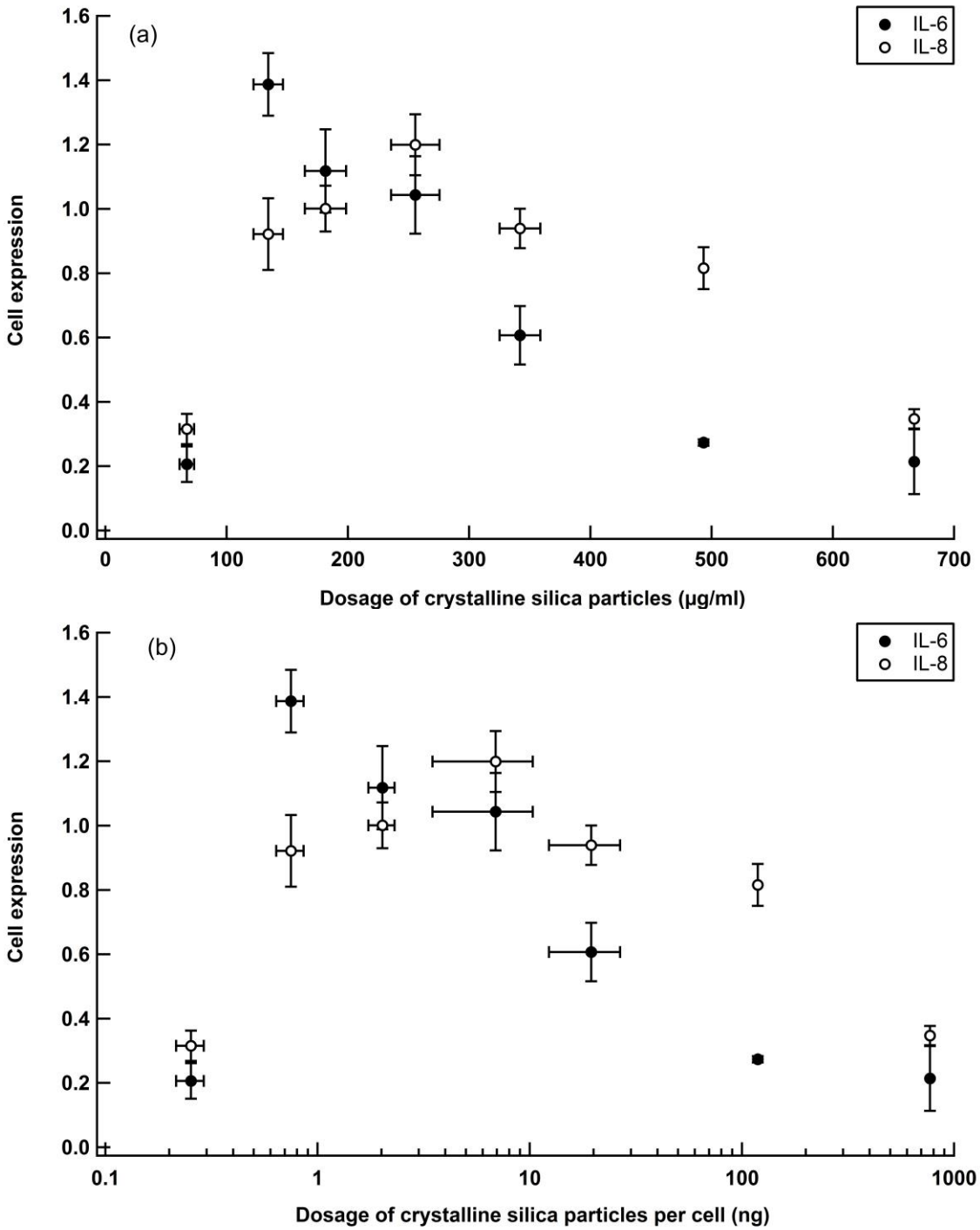

Figure 6.1 **IL-6 and IL-8 expression after 18-hour incubation of A549 cell cultures as a function of dose of crystalline silica: (a) without normalization against the number of viable cells (b) Normalized against the number of viable cells.**

6.2.2. Characterization of liquid-solid interface

The results of the combination of insoluble particles and specific soluble components suggest that the solid-liquid interfacial properties, especially the sorption of the soluble components on the particle surfaces plays an important role. To further investigate that how the solid-liquid interfacial properties would affect the cytotoxicity of the particles, some characterization of particle surfaces and the sorption of specific soluble components on the particle surfaces need to be done in the future. For instance, the X-ray photoelectron spectroscopy (XPS) can be applied to measure the elemental compositions of the particle surfaces. SEM and particle size analyzer can be adopted to obtain the size/size distribution of the particles. And certain experiments need to be designed regarding factors that may modify the interfacial sorption of specific components the particle on surfaces, including particle types, the effect of other solutes, kinetic factors (e.g. temperature, and interaction time), and the speciation of the specific components in the solution.

6.2.3. Selection of particle types/components

Several inorganic representatives of major particle types/components adjacent to roadways were selected in this study, including carbon black nanoparticles, crystalline silica particles, nickel nanoparticles, and water-soluble particle components ammonium nitrate and soluble salts of zinc, lead, and iron. Through a binary particle types/components model of particles (CB nanoparticle or crystalline silica particle) plus water-soluble particle components, chemical composition dependent cellular response was measured, e.g. cytoprotective effect was observed for Zn and Fe, whereas Pb plus crystalline silica lead to a non-linear additive cell expression. To further investigate the interaction between different particle types/components and screen the important particle types/components, the number of component/particle types was increased to a ternary particle types/components model with crystalline silica, iron(II) salt and lead salt. Though lead and iron(II) salt each have an opposite effect on cell response, when combined with crystalline silica, low cytokine expression and high cell viability were measured for the ternary combination. This suggests the important role of reduced redox species that protect the cell from oxidative stress. Studying different particle types/components in an incrementally increasing number of species in the particle types/components model can be expected to generate new information.

Other particle components that should be investigated in the future could include organic compounds such as polycyclic aromatic hydrocarbons and biogenic components such as endotoxin. These organic components are produced in the incomplete combustion of fossil fuels.[4, 12, 14, 26] With respect to the traffic-derived particulate matter, hundreds of organic compounds have been identified in soot. Most of them are PAHs and their derivatives, which have strong carcinogenic and mutagenic potential.[10, 33, 53] They can also generate ROS through biotransformation and lead to inflammation.[5, 26] Biological particle components such as endotoxin can induce oxidative stress and trigger lung inflammatory response through a different mechanism, activation of TLRs pathways.[5, 15, 34] The interaction between organic components, endotoxin, water-soluble components, and particles (e.g. CB nanoparticle or crystalline silica particle) should be studied in the future.

6.2.4. Method development of long-term effect study

Long-term exposure to PM is associated with inflammation, respiratory and cardiovascular diseases, and even deaths.[1-2, 4-5] At the cellular level, several mechanisms are believed to contribute to the chronic effect of ambient particles. For instance, through the generation of ROS, the particles can lead to inflammation. During this process, inflammatory cells such as macrophages may release mitogenic factors to stimulate the proliferation of epithelial cells to replace those that have been damaged. With cell proliferation rate increases, the chance of mutation increases as well.[5, 321] It can lead to fibrosis and structural changes of airways which eventually result in respiratory diseases such as asthma and interstitial pulmonary fibrosis.[5, 136-137]

Investigations on the long-term health effects of ambient particles are mostly epidemiological, whereas *in vitro* methodology, which takes considerably shorter time and less cost, is useful for studying acute effects of ambient particles, and rapid screening of toxic particle types and components due to its limitation of complexity. [79, 140-141] For adherent cells such as A549, the exposure period is usually up to 72 hours.[322] New *in vitro* methods continue to be introduced. General methods describe repeated doses for weeks to assess chronic cellular effects of PM, including traditional sub-cultured cell models and developed models using special bioreactors and microcarriers.[322-324] The question ‘how will a repeated low-doses of particles at each stage of passaging, affect lung cell response?’ is a possible starting point for developing

an *in vitro* model to study the long-term effect of ambient particles on the cellular level in future. CB nanoparticle can be used as the first particle type to be evaluated, as the nanoparticle tends to not be cleared quickly from the respiratory system. A co-culture cell model including A549 cells and macrophages is suggested to be adopted and exposed to a constant low concentration of CB nanoparticles each time after cell passaging. Multiple assays, such as viability assay, enzyme-linked immunosorbent assay for measuring pro-inflammatory cytokines, and genetic assay, can all be adopted in a single study to evaluate the chronic cellular effect of the particles.

6.3. Concluding remarks

An *in vitro* methodology was adopted to investigate the human lung cellular response induced by traffic-derived particles. It was applied for both ambient particle samples and laboratory mimics of multiple particle types/components to investigate two research questions: i. Do interactions between water-insoluble particle types affect toxicity? ii. Do interactions between water-insoluble particle types and water-soluble components, and between water-soluble components affect toxicity?

Several conclusions can be drawn based on our results. The interaction between different particle components/types affects the cellular response in different ways, certain particle components/types including crystalline silica, lead and iron may dominate the toxicity of the whole mixture. One probable mechanism of the compositional interaction is that the water-insoluble particle components play a role as carriers, via endocytosis, for the water/lipid-soluble components. In this study, due to the limitation of the methodology, we don't have sufficient evidence to confirm the internalization of the particles, via endocytosis. All the statements in the results and discussion sections of this thesis about endocytosis are proposed assumptions. Instead of suggesting the importance of endocytosis, based on our results, it would be safer to conclude that the water-insoluble particles are critical, especially when they combined with soluble species that are presented to intact viable cells but have no receptor expressed in the cell membrane. On the cellular level, mass dosage plays an important role in the toxicity of water-insoluble particles. The particle size and surface area do not pre-determine the cytotoxicity of the particles. However, other factors, including chemical compositions and surface chemistry of the particles, should be taken into consideration. For the water-soluble particle components, their toxicity is mainly determined by the chemical

composition. For a given sample of ambient particles, the overall toxicity is affected by several factors and cannot simply be predicted by the sum of the toxicity of the individual components in the particle.

A complexed multi-component model for acute response investigation and toxin screening, and a method development for long-term health effect study are suggested as future work. The goal of such future research is to further improve the understanding of particle toxicity, and screen certain particle types/components which we hope would help to reduce the adverse effect on human health caused by ambient particles.

References

1. Cohen, A. J.; Brauer, M.; Burnett, R.; Anderson, H. R.; Frostad, J.; Estep, K.; Balakrishnan, K.; Brunekreef, B.; Dandona, L.; Dandona, R., Estimates and 25-year trends of the global burden of disease attributable to ambient air pollution: an analysis of data from the Global Burden of Diseases Study 2015. *The Lancet* **2017,** *389* (10082), 1907-1918.

2. Gakidou, E.; Afshin, A.; Abajobir, A. A.; Abate, K. H.; Abbafati, C.; Abbas, K. M.; Abd-Allah, F.; Abdulle, A. M.; Abera, S. F.; Aboyans, V., Global, regional, and national comparative risk assessment of 84 behavioural, environmental and occupational, and metabolic risks or clusters of risks, 1990–2016: a systematic analysis for the Global Burden of Disease Study 2016. *The Lancet* **2017,** *390* (10100), 1345-1422.

3. Global Burden of Disease Collaborative Network, Global Burden of Disease Study 2016 (GBD 2016) GBD Compare | IHME Viz Hub - Data Visualizations. . Institute for Health Metrics and Evaluation (IHME): Seattle, United States, 2017.

4. Brook, R. D.; Rajagopalan, S.; Pope, C. A.; Brook, J. R.; Bhatnagar, A.; Diez-Roux, A. V.; Holguin, F.; Hong, Y.; Luepker, R. V.; Mittleman, M. A., Particulate matter air pollution and cardiovascular disease: an update to the scientific statement from the American Heart Association. *Circulation* **2010,** *121* (21), 2331-2378.

5. Donaldson, K.; Borm, P., *Particle toxicology*. CRC Press: 2006.

6. Lin, C.-C.; Chen, S.-J.; Huang, K.-L.; Lee, W.-J.; Lin, W.-Y.; Liao, C.-J.; Chaung, H.-C.; Chiu, C.-H., Water-soluble ions in nano/ultrafine/fine/coarse particles collected near a busy road and at a rural site. *Environmental Pollution* **2007,** *145* (2), 562-570.

7. Janssen, N. A.; Van Mansom, D. F.; Van Der Jagt, K.; Harssema, H.; Hoek, G., Mass concentration and elemental composition of airborne particulate matter at street and background locations. *Atmospheric Environment* **1997,** *31* (8), 1185-1193.

8. HEI panel on the health effects of traffic-related air pollution, *Traffic-related air pollution: a critical review of the literature on emissions, exposure, and health effects*. Health Effects Institute: Boston, MA, 2010; Vol. HEI special report 17.

9. Tsang, A. M.; Klepeis, N. E. *Descriptive statistics tables from a detailed analysis of the National Human Activity Pattern Survey (NHAPS) data*; Lockheed Martin Environmental Systems and Technologies, Las Vegas, NV (United States); Environmental Protection Agency, National Exposure Research Lab., Las Vegas, NV (United States): 1996.

10. De Kok, T. M.; Driece, H. A.; Hogervorst, J. G.; Briedé, J. J., Toxicological assessment of ambient and traffic-related particulate matter: a review of recent studies. *Mutation Research/Reviews in Mutation Research* **2006,** *613* (2), 103-122.

11. Grahame, T. J.; Schlesinger, R. B., Cardiovascular health and particulate vehicular emissions: a critical evaluation of the evidence. *Air Quality, Atmosphere & Health* **2010,** *3* (1), 3-27.

12. Seinfeld, J. H.; Pandis, S. N., *Atmospheric chemistry and physics: from air pollution to climate change*. John Wiley & Sons: 2016.

13. Kim, K.-H.; Kabir, E.; Kabir, S., A review on the human health impact of airborne particulate matter. *Environment international* **2015,** *74*, 136-143.

14. Kelly, F. J.; Fussell, J. C., Size, source and chemical composition as determinants of toxicity attributable to ambient particulate matter. *Atmospheric Environment* **2012,** *60*, 504-526.

15. Brook, R. D.; Franklin, B.; Cascio, W.; Hong, Y.; Howard, G.; Lipsett, M.; Luepker, R.; Mittleman, M.; Samet, J.; Smith, S. C., Jr.; Tager, I.; Expert Panel on, P.; Prevention Science of the American Heart, A., Air pollution and cardiovascular disease: a statement for healthcare professionals from the Expert Panel on Population and Prevention Science of the American Heart Association. *Circulation* **2004,** *109* (21), 2655-71.

16. DeCarlo, P. F.; Slowik, J. G.; Worsnop, D. R.; Davidovits, P.; Jimenez, J. L., Particle morphology and density characterization by combined mobility and aerodynamic diameter measurements. Part 1: Theory. *Aerosol Science and Technology* **2004,** *38* (12), 1185-1205.

17. U.S. EPA, Air Quality Criteria for Particulate Matter (Final Report, 2004). U.S. Department of Environmental Protection Agency, Ed. EPA 600/P-99/002aF-bF: Washington, DC, 2004.

18. Mansfield, E.; Kaiser, D. L.; Fujita, D.; Van de Voorde, M., *Metrology and Standardization for Nanotechnology: Protocols and Industrial Innovations*. John Wiley & Sons: 2017.

19. Peters, T. M., Use of the aerodynamic particle sizer to measure ambient PM10–2.5: The coarse fraction of PM10. *Journal of the Air & Waste Management Association* **2006,** *56* (4), 411-416.

20. Daigle, C. C.; Chalupa, D. C.; Gibb, F. R.; Morrow, P. E.; Oberdörster, G.; Utell, M. J.; Frampton, M. W., Ultrafine particle deposition in humans during rest and exercise. *Inhalation toxicology* **2003,** *15* (6), 539-552.

21. Amatullah, H.; North, M. L.; Akhtar, U. S.; Rastogi, N.; Urch, B.; Silverman, F. S.; Chow, C.-W.; Evans, G. J.; Scott, J. A., Comparative cardiopulmonary effects of size-fractionated airborne particulate matter. *Inhalation toxicology* **2012,** *24* (3), 161-171.

22. Cho, S.-H.; Tong, H.; McGee, J. K.; Baldauf, R. W.; Krantz, Q. T.; Gilmour, M. I., Comparative toxicity of size-fractionated airborne particulate matter collected at different distances from an urban highway. *Environmental health perspectives* **2009,** *117* (11), 1682.

23. Happo, M.; Salonen, R.; Hälinen, A.; Jalava, P.; Pennanen, A.; Dormans, J.; Gerlofs-Nijland, M.; Cassee, F.; Kosma, V.-M.; Sillanpää, M., Inflammation and tissue damage in mouse lung by single and repeated dosing of urban air coarse and fine particles collected from six European cities. *Inhalation toxicology* **2010,** *22* (5), 402-416.

24. World Health Organization, *Health effects of particulate matter. Policy implications for countries in eastern Europe, Caucasus and central Asia* World Health Organization: Copenhagen, Denmark, 2013.

25. Harrison, R. M.; Yin, J., Particulate matter in the atmosphere: which particle properties are important for its effects on health? *Science of the total environment* **2000,** *249* (1-3), 85-101.

26. Valavanidis, A.; Fiotakis, K.; Vlachogianni, T., Airborne particulate matter and human health: toxicological assessment and importance of size and composition of particles for oxidative damage and carcinogenic mechanisms. *Journal of Environmental Science and Health, Part C* **2008,** *26* (4), 339-362.

27. Li, C.; Martin, R. V.; van Donkelaar, A.; Boys, B. L.; Hammer, M. S.; Xu, J.-W.; Marais, E. A.; Reff, A.; Strum, M.; Ridley, D. A., Trends in chemical composition of global and regional population-weighted fine particulate matter estimated for 25 years. *Environmental Science & Technology* **2017,** *51* (19), 11185-11195.

28. Agranovski, I., *Aerosols: science and technology*. John Wiley & Sons: 2011.

29. Riley, M. R.; Boesewetter, D. E.; Kim, A. M.; Sirvent, F. P., Effects of metals Cu, Fe, Ni, V, and Zn on rat lung epithelial cells. *Toxicology* **2003,** *190* (3), 171-184.

30. Duffin, R.; Gilmour, P. S.; Schins, R. P.; Clouter, A.; Guy, K.; Brown, D. M.; MacNee, W.; Borm, P. J.; Donaldson, K.; Stone, V., Aluminium lactate treatment of DQ12 quartz inhibits its ability to cause inflammation, chemokine expression, and nuclear factor-κB activation. *Toxicology and applied pharmacology* **2001,** *176* (1), 10-17.

31. Flora, G.; Gupta, D.; Tiwari, A., Toxicity of lead: a review with recent updates. *Interdisciplinary toxicology* **2012,** *5* (2), 47-58.

32. Plum, L. M.; Rink, L.; Haase, H., The essential toxin: impact of zinc on human health. *International journal of environmental research and public health* **2010,** *7* (4), 1342-1365.

33. Shiraiwa, M.; Selzle, K.; Pöschl, U., Hazardous components and health effects of atmospheric aerosol particles: reactive oxygen species, soot, polycyclic aromatic compounds and allergenic proteins. *Free radical research* **2012,** *46* (8), 927-939.

34. Degobbi, C.; Saldiva, P. H. N.; Rogers, C., Endotoxin as modifier of particulate matter toxicity: a review of the literature. *Aerobiologia* **2011,** *27* (2), 97-105.

35. Oberdörster, G.; Oberdörster, E.; Oberdörster, J., Nanotoxicology: an emerging discipline evolving from studies of ultrafine particles. *Environmental health perspectives* **2005,** *113* (7), 823.

36. Bakand, S.; Hayes, A.; Dechsakulthorn, F., Nanoparticles: a review of particle toxicology following inhalation exposure. *Inhalation toxicology* **2012,** *24* (2), 125-135.

37. Gwinn, M. R.; Vallyathan, V., Nanoparticles: health effects—pros and cons. *Environmental health perspectives* **2006,** *114* (12), 1818.

38. Warheit, D. B., Nanoparticles: health impacts? *Materials today* **2004,** *7* (2), 32-35.

39. Wallace, W. E.; Keane, M. J.; Murray, D. K.; Chisholm, W. P.; Maynard, A. D.; Ong, T.-m., Phospholipid lung surfactant and nanoparticle surface toxicity: Lessons from diesel soots and silicate dusts. In *Nanotechnology and Occupational Health*, Springer: 2006; pp 23-38.

40. Brown, D.; Kinloch, I.; Bangert, U.; Windle, A.; Walter, D.; Walker, G.; Scotchford, C.; Donaldson, K.; Stone, V., An in vitro study of the potential of carbon nanotubes and nanofibres to induce inflammatory mediators and frustrated phagocytosis. *Carbon* **2007,** *45* (9), 1743-1756.

41. Monteiller, C.; Tran, L.; MacNee, W.; Faux, S.; Jones, A.; Miller, B.; Donaldson, K., The pro-inflammatory effects of low-toxicity low-solubility particles, nanoparticles and fine particles, on epithelial cells in vitro: the role of surface area. *Occupational and environmental medicine* **2007,** *64* (9), 609-615.

42. Braakhuis, H. M.; Park, M. V.; Gosens, I.; De Jong, W. H.; Cassee, F. R., Physicochemical characteristics of nanomaterials that affect pulmonary inflammation. *Particle and fibre toxicology* **2014,** *11* (1), 18.

43. Oberdörster, G.; Stone, V.; Donaldson, K., Toxicology of nanoparticles: a historical perspective. *Nanotoxicology* **2007,** *1* (1), 2-25.

44. Schmid, O.; Möller, W.; Semmler-Behnke, M.; A. Ferron, G.; Karg, E.; Lipka, J.; Schulz, H.; Kreyling, W.; Stoeger, T., Dosimetry and toxicology of inhaled ultrafine particles. *Biomarkers* **2009,** *14* (sup1), 67-73.

45. Sayes, C. M.; Warheit, D. B., Characterization of nanomaterials for toxicity assessment. *Wiley Interdisciplinary Reviews: Nanomedicine and Nanobiotechnology* **2009,** *1* (6), 660-670.

46. Park, S.-J.; Seo, M.-K., *Interface science and composites*. Academic Press: 2011; Vol. 18.

47. Brown, M. A.; Abbas, Z.; Kleibert, A.; Green, R. G.; Goel, A.; May, S.; Squires, T. M., Determination of surface potential and electrical double-layer structure at the aqueous electrolyte-nanoparticle interface. *Physical Review X* **2016,** *6* (1), 011007.

48. Kettler, K.; Veltman, K.; van de Meent, D.; van Wezel, A.; Hendriks, A. J., Cellular uptake of nanoparticles as determined by particle properties, experimental conditions, and cell type. *Environmental toxicology and chemistry* **2014,** *33* (3), 481-492.

49. Shin, S. W.; Song, I. H.; Um, S. H., Role of physicochemical properties in nanoparticle toxicity. *Nanomaterials* **2015,** *5* (3), 1351-1365.

50. Madl, A. K.; Pinkerton, K. E., Health effects of inhaled engineered and incidental nanoparticles. *Critical reviews in toxicology* **2009,** *39* (8), 629-658.

51. Fubini, B., Surface reactivity in the pathogenic response to particulates. *Environmental health perspectives* **1997,** *105* (Suppl 5), 1013.

52. Duffin, R.; Tran, C.; Clouter, A.; Brown, D.; MacNee, W.; Stone, V.; Donaldson, K., The importance of surface area and specific reactivity in the acute pulmonary inflammatory response to particles. *Annals of Occupational Hygiene* **2002,** *46* (suppl_1), 242-245.

53. Amato, F.; Schaap, M.; Reche, C.; Querol, X., Road traffic: a major source of particulate matter in Europe. In *Urban Air Quality in Europe*, Springer: 2013; pp 165-193.

54. Thorpe, A.; Harrison, R. M., Sources and properties of non-exhaust particulate matter from road traffic: a review. *Science of the total environment* **2008,** *400* (1-3), 270-282.

55. International Agency for Research on Cancer (IARC), *IARC Monographs on the evaluation of the carcinogenic risk of chemicals to humans.* . World Health Organization: Lyon, France, 1985; Vol. 35.

56. Watson, A. Y.; Valberg, P. A., Carbon black and soot: two different substances. *AIHAJ-American Industrial Hygiene Association* **2001,** *62* (2), 218-228.

57. International Agency for Research on Cancer (IARC), *IARC monographs on the evaluation of carcinogenic risks to humans.* World Health Organization: Lyon, France, 2012; Vol. 100F.

58. Wilson, S. J.; Miller, M. R.; Newby, D. E., Effects of diesel exhaust on cardiovascular function and oxidative stress. *Antioxidants & redox signaling* **2018,** *28* (9), 819-836.

59. Grigoratos, T.; Martini, G., Brake wear particle emissions: a review. *Environmental Science and Pollution Research* **2015,** *22* (4), 2491-2504.

60. Garg, B. D.; Cadle, S. H.; Mulawa, P. A.; Groblicki, P. J.; Laroo, C.; Parr, G. A., Brake wear particulate matter emissions. *Environmental Science & Technology* **2000,** *34* (21), 4463-4469.

61. Chow, J. C.; Watson, J. G.; Houck, J. E.; Pritchett, L. C.; Rogers, C. F.; Frazier, C. A.; Egami, R. T.; Ball, B. M., A laboratory resuspension chamber to measure fugitive dust size distributions and chemical compositions. *Atmospheric Environment* **1994,** *28* (21), 3463-3481.

62. Han, S.; Youn, J.-S.; Jung, Y.-W., Characterization of PM10 and PM2. 5 source profiles for resuspended road dust collected using mobile sampling methodology. *Atmospheric environment* **2011,** *45* (20), 3343-3351.

63. U.S. EPA, National Emissions Inventory (NEI) Air Pollutant Emissions Trends Data. https://www.epa.gov/air-emissions-inventories/air-pollutant-emissions-trends-data, 2017.

64. Environment and Climate Change Canada, 1990-2016 Air Pollutant Emission Inventory Report. Minsiter of Environment and Climate, C., Ed. Minsiter of Environment and Climate, Canada: Gatineau, QC, 2018.

65. Zhu, Y.; Hinds, W. C.; Kim, S.; Shen, S.; Sioutas, C., Study of ultrafine particles near a major highway with heavy-duty diesel traffic. *Atmospheric environment* **2002,** *36* (27), 4323-4335.

66. Roorda-Knape, M. C.; Janssen, N. A.; De Hartog, J. J.; Van Vliet, P. H.; Harssema, H.; Brunekreef, B., Air pollution from traffic in city districts near major motorways. *Atmospheric Environment* **1998,** *32* (11), 1921-1930.

67. Schwartz, J.; Laden, F.; Zanobetti, A., The concentration-response relation between PM (2.5) and daily deaths. *Environmental health perspectives* **2002,** *110* (10), 1025.

68. Lipfert, F.; Wyzga, R.; Baty, J.; Miller, J., Traffic density as a surrogate measure of environmental exposures in studies of air pollution health effects: long-term mortality in a cohort of US veterans. *Atmospheric Environment* **2006,** *40* (1), 154-169.

69. Heinrich, J.; Schwarze, P. E.; Stilianakis, N.; Momas, I.; Medina, S.; Totlandsdal, A. I.; Von Bree, L.; Kuna-Dibbert, B.; Krzyzanowski, M., Studies on health effects of transport-related air pollution. *Health effects of transport-related air pollution* **2005**, 125.

70. Hoffmann, B.; Moebus, S.; Möhlenkamp, S.; Stang, A.; Lehmann, N.; Dragano, N.; Schmermund, A.; Memmesheimer, M.; Mann, K.; Erbel, R., Residential exposure to traffic is associated with coronary atherosclerosis. *Circulation* **2007,** *116* (5), 489-496.

71. Finkelstein, M. M.; Jerrett, M.; Sears, M. R., Environmental inequality and circulatory disease mortality gradients. *Journal of Epidemiology & Community Health* **2005,** *59* (6), 481-487.

72. Gehring, U.; Heinrich, J.; Krämer, U.; Grote, V.; Hochadel, M.; Sugiri, D.; Kraft, M.; Rauchfuss, K.; Eberwein, H. G.; Wichmann, H.-E., Long-term exposure to ambient air pollution and cardiopulmonary mortality in women. *Epidemiology* **2006,** *17* (5), 545-551.

73. Hofmann, W., Modelling inhaled particle deposition in the human lung—a review. *Journal of Aerosol Science* **2011,** *42* (10), 693-724.

74. Kleinstreuer, C.; Zhang, Z., Airflow and particle transport in the human respiratory system. *Annual Review of Fluid Mechanics* **2010,** *42*, 301-334.

75. Kleinstreuer, C.; Zhang, Z.; Donohue, J., Targeted drug-aerosol delivery in the human respiratory system. *Annu. Rev. Biomed. Eng.* **2008,** *10*, 195-220.

76. Ionescu, C. M., The human respiratory system. In *The Human Respiratory System*, Springer: 2013; pp 13-22.

77. Bair, W., The ICRP human respiratory tract model for radiological protection. *Radiation Protection Dosimetry* **1995,** *60* (4), 307-310.

78. Smith, H., Human respiratory tract model for radiological protection. *ICRP publication 66* **1994,** *24(1-3)*, 1-482.

79. BéruBé, K.; Aufderheide, M.; Breheny, D.; Clothier, R.; Combes, R.; Duffin, R.; Forbes, B.; Gaça, M.; Gray, A.; Hall, I., In vitro models of inhalation toxicity and disease. *Alternatives to Laboratory Animals* **2009,** *37* (1), 89-141.

80. Widdicombe, J.; Bastacky, S.; Wu, D.; Lee, C., Regulation of depth and composition of airway surface liquid. *European Respiratory Journal* **1997,** *10* (12), 2892-2897.

81. Franciosi, L.; Govorukhina, N.; ten Hacken, N.; Postma, D.; Bischoff, R., Proteomics of epithelial lining fluid obtained by bronchoscopic microprobe sampling. In *Nanoproteomics*, Springer: 2011; pp 17-28.

82. Cantin, A.; North, S.; Hubbard, R.; Crystal, R., Normal alveolar epithelial lining fluid contains high levels of glutathione. *Journal of applied physiology* **1987,** *63* (1), 152-157.

83. Stanke, F., The contribution of the airway epithelial cell to host defense. *Mediators of inflammation* **2015,** *2015*.

84. Boers, J. E.; Ambergen, A. W.; Thunnissen, F. B., Number and proliferation of basal and parabasal cells in normal human airway epithelium. *American journal of respiratory and critical care medicine* **1998,** *157* (6), 2000-2006.

85. Wallaert, B.; Fahy, O.; Tsicopoulos, A.; Gosset, P.; Tonnel, A., Experimental systems for mechanistic studies of toxicant induced lung inflammation. *Toxicology letters* **2000,** *112*, 157-163.

86. Foster, K. A.; Oster, C. G.; Mayer, M. M.; Avery, M. L.; Audus, K. L., Characterization of the A549 cell line as a type II pulmonary epithelial cell model for drug metabolism. *Experimental cell research* **1998,** *243* (2), 359-366.

87. Mühlfeld, C.; Blank, F.; Rothen-Rutishauser, B.; Gehr, P., *Particle-lung interactions*. CRC Press: 2009.

88. Ryan, R. M.; Mineo-Kuhn, M. M.; Kramer, C. M.; Finkelstein, J. N., Growth factors alter neonatal type II alveolar epithelial cell proliferation. *American Journal of Physiology-Lung Cellular and Molecular Physiology* **1994,** *266* (1), L17-L22.

89. Riley, M. R.; Boesewetter, D. E.; Turner, R. A.; Kim, A. M.; Collier, J. M.; Hamilton, A., Comparison of the sensitivity of three lung derived cell lines to metals from combustion derived particulate matter. *Toxicology in Vitro* **2005,** *19* (3), 411-419.

90. Ward, H.; Nicholas, T., Alveolar type I and type II cells. *Australian and New Zealand journal of medicine* **1984,** *14*, 731-734.

91. Ito, T.; Kitamura, H.; Inayama, Y.; Nozawa, A.; Kanisawa, M., Uptake and intracellular transport of cationic ferritin in the bronchiolar and alveolar epithelia of the rat. *Cell and tissue research* **1992,** *268* (2), 335-340.

92. Stearns, R. C.; Paulauskis, J. D.; Godleski, J. J., Endocytosis of ultrafine particles by A549 cells. *American journal of respiratory cell and molecular biology* **2001,** *24* (2), 108-115.

93. Bai, Y.; Suzuki, A. K.; Sagai, M., The cytotoxic effects of diesel exhaust particles on human pulmonary artery endothelial cells in vitro: role of active oxygen species. *Free Radical Biology and Medicine* **2001,** *30* (5), 555-562.

94. Wang, T.; Shimizu, Y.; Wu, X.; Kelly, G. T.; Xu, X.; Wang, L.; Qian, Z.; Chen, Y.; Garcia, J. G., Particulate matter disrupts human lung endothelial cell barrier integrity via Rho-dependent pathways. *Pulmonary circulation* **2017,** *7* (3), 617-623.

95. Lenasi, H., *Endothelial Dysfunction*. IntechOpen: 2018.

96. World Health Organization, *WHO Air quality guidelines for particulate matter, ozone, nitrogen dioxide and sulfur dioxide: global update 2005: summary of risk assessment*. World Health Organization: Geneva, Switzerland, 2006.

97. Pope, C. A.; Thun, M. J.; Namboodiri, M. M.; Dockery, D. W.; Evans, J. S.; Speizer, F. E.; Heath, C. W., Particulate air pollution as a predictor of mortality in a prospective study of US adults. *American journal of respiratory and critical care medicine* **1995,** *151* (3), 669-674.

98. U.S. EPA, National Ambient Air Quality Standards. U.S. Environmental Protection Agency, Ed. Washington, DC 2015.

99. U.S. EPA, Clean Air Act. U.S. Environmental Protection Agency, Ed. Washington, DC 1990.

100. Agency for Toxic Substances and Disease Registry (ATSDR), Toxicological profile for lead. U.S. Department of Health and Human Services, Public Health Service: Atlanta, Georgia, 2007.

101. U.S. EPA, Menu Of Control Measures. U.S. Environmental Protection Agency, Ed. Washington, DC 2012.

102. Canadian Council of Ministers of the Environment Air Quality Management System (AQMS). (accessed Jun 26).

103. Canadian Council of Ministers of the Environment, Canadian Ambient Air Quality Standards. Canadian Council of Ministers of the Environment, Ed. http://www.ec.gc.ca/default.asp?lang=En&n=56D4043B-1&news=A4B2C28A-2DFB-4BF4-8777-ADF29B4360BD (Accessed Jun 26, 2018), 2012.

104. Environment Directorate General of the European Commission, Air Quality Standards. Environment Directorate General of the European Commission, Ed. http://ec.europa.eu/environment/basics/home_en.htm (Accessed Jun 26, 2018), 2017.

105. Directorate General for Internal Market Industry Entrepreneurship and SMEs of European Commission Emissions in the automotive sector. (accessed June 26).

106. Heyder, J., Deposition of inhaled particles in the human respiratory tract and consequences for regional targeting in respiratory drug delivery. *Proceedings of the American Thoracic Society* **2004,** *1* (4), 315-320.

107. Smith, H., Human respiratory tract model for radiological protection. *ICRP publication 66. Ann. ICRP* **1994,** *24* (1-3), 1-482.

108. Hussain, M.; Madl, P.; Khan, A., Lung deposition predictions of airborne particles and the emergence of contemporary diseases, Part-I. *Health* **2011,** *2* (2), 51-59.

109. Miyata, R.; van Eeden, S. F., The innate and adaptive immune response induced by alveolar macrophages exposed to ambient particulate matter. *Toxicology and applied pharmacology* **2011,** *257* (2), 209-226.

110. Lippmann, M.; Yeates, D.; Albert, R., Deposition, retention, and clearance of inhaled particles. *Occupational and Environmental Medicine* **1980,** *37* (4), 337-362.

111. Kumar, S.; Verma, M. K.; Srivastava, A. K., Ultrafine particles in urban ambient air and their health perspectives. *Reviews on environmental health* **2013,** *28* (2-3), 117-128.

112. Smith, J.; Bailey, M.; Etherington, G.; Shutt, A.; Youngman, M., Effect of particle size on slow particle clearance from the bronchial tree. *Experimental lung research* **2008,** *34* (6), 287-312.

113. Warheit, D.; Hansen, J.; Yuen, I.; Kelly, D.; Snajdr, S.; Hartsky, M., Inhalation of high concentrations of low toxicity dusts in rats results in impaired pulmonary clearance mechanisms and persistent inflammation. *Toxicology and applied pharmacology* **1997,** *145* (1), 10-22.

114. Morrow, P., Possible mechanisms to explain dust overloading of the lungs. *Toxicological Sciences* **1988,** *10* (3), 369-384.

115. Mukherjee, S.; Ghosh, R. N.; Maxfield, F. R., Endocytosis. *Physiological reviews* **1997,** *77* (3), 759-803.

116. Gehr, P.; Clift, M.; Brandenberger, C.; Lehmann, A.; Herzog, F.; Rothen-Rutishauser, B., Endocytosis of environmental and engineered micro-and nanosized particles. *Compr. Physiol* **2011,** *1*, 1159-1174.

117. Greenberg, S.; Grinstein, S., Phagocytosis and innate immunity. *Current opinion in immunology* **2002,** *14* (1), 136-145.

118. Aderem, A.; Underhill, D. M., Mechanisms of phagocytosis in macrophages. *Annual review of immunology* **1999,** *17* (1), 593-623.

119. Silverstein, S. C.; Steinman, R. M.; Cohn, Z. A., Endocytosis. *Annual review of biochemistry* **1977,** *46* (1), 669-722.

120. Lim, J. P.; Gleeson, P. A., Macropinocytosis: an endocytic pathway for internalising large gulps. *Immunology and cell biology* **2011,** *89* (8), 836.

121. Kerr, M. C.; Teasdale, R. D., Defining macropinocytosis. *Traffic* **2009,** *10* (4), 364-371.

122. Muhlfeld, C.; Gehr, P.; Rothen-Rutishauser, B., Translocation and cellular entering mechanisms of nanoparticles in the respiratory tract. *Swiss medical weekly* **2008,** *138* (27/28), 387.

123. Boland, S.; Hussain, S.; Baeza-Squiban, A., Carbon black and titanium dioxide nanoparticles induce distinct molecular mechanisms of toxicity. *Wiley interdisciplinary reviews. Nanomedicine and nanobiotechnology* **2014,** *6* (6), 641-52.

124. Hussain, S.; Thomassen, L. C.; Ferecatu, I.; Borot, M.-C.; Andreau, K.; Martens, J. A.; Fleury, J.; Baeza-Squiban, A.; Marano, F.; Boland, S., Carbon black and titanium dioxide nanoparticles elicit distinct apoptotic pathways in bronchial epithelial cells. *Particle and fibre toxicology* **2010,** *7* (1), 10.

125. Bayr, H., Reactive oxygen species. *Critical care medicine* **2005,** *33* (12), S498-S501.

126. Finkel, T.; Holbrook, N. J., Oxidants, oxidative stress and the biology of ageing. *Nature* **2000,** *408* (6809), 239.

127. Britton, R. S.; Leicester, K. L.; Bacon, B. R., Iron toxicity and chelation therapy. *International journal of hematology* **2002,** *76* (3), 219-228.

128. Dixon, S. J.; Stockwell, B. R., The role of iron and reactive oxygen species in cell death. *Nature chemical biology* **2014,** *10* (1), 9-17.

129. Fubini, B.; Hubbard, A., Serial review: role of reactive oxygen and nitrogen species (ROS/RNS) in lung injury and diseases. *Free Radical Biology & Medicine* **2003,** *34* (12), 1507-1516.

130. Shi, X.; Castranova, V.; Halliwell, B.; Vallyathan, V., Reactive oxygen species and silica-induced carcinogenesis. *Journal of Toxicology and Environmental Health, Part B Critical Reviews* **1998,** *1* (3), 181-197.

131. Dutta, D.; Moudgil, B. M., Crystalline silica particles mediated lung injury. *KONA Powder and Particle Journal* **2007,** *25*, 76-87.

132. Coussens, L. M.; Werb, Z., Inflammation and cancer. *Nature* **2002,** *420* (6917), 860.

133. Gabay, C., Interleukin-6 and chronic inflammation. *Arthritis research & therapy* **2006,** *8* (2), S3.

134. Astrakianakis, G.; Murray, E., Conflicting Effects of Occupational Endotoxin Exposure on Lung Health-A Hypothesis-Generating Review of Cancer and COPD Risk. *J Environ Immunol Toxicol* **2014,** *1* (3), 128-139.

135. Khansari, N.; Shakiba, Y.; Mahmoudi, M., Chronic inflammation and oxidative stress as a major cause of age-related diseases and cancer. *Recent patents on inflammation & allergy drug discovery* **2009,** *3* (1), 73-80.

136. Snider, G. L., Interstitial pulmonary fibrosis. *Chest* **1986,** *89* (3), 115S-121S.

137. Bateman, E. D.; Hurd, S.; Barnes, P.; Bousquet, J.; Drazen, J.; FitzGerald, M.; Gibson, P.; Ohta, K.; O'byrne, P.; Pedersen, S., Global strategy for asthma management and prevention: GINA executive summary. *European Respiratory Journal* **2008,** *31* (1), 143-178.

138. Bokulic, R. E., The lung: Scientific foundations. By Ronald G. Crystal and John D. West. New York: Raven Press, Ltd., 1991, 2 volumes, 2,224 pp. Wiley Online Library: 1992.

139. Pasanen, K.; Pukkala, E.; Turunen, A. W.; Patama, T.; Jussila, I.; Makkonen, S.; Salonen, R. O.; Verkasalo, P. K., Mortality among population with exposure to industrial air pollution containing nickel and other toxic metals. *Journal of occupational and environmental medicine* **2012,** *54* (5), 583-591.

140. Devlin, R. B.; Frampton, M. L.; Ghio, A. J., In vitro studies: What is their role in toxicology? *Experimental and Toxicologic Pathology* **2005,** *57*, 183-188.

141. Nemmar, A.; Holme, J. A.; Rosas, I.; Schwarze, P. E.; Alfaro-Moreno, E., Recent advances in particulate matter and nanoparticle toxicology: a review of the in vivo and in vitro studies. *BioMed research international* **2013,** *2013*.

142. Zou, Y.; Jin, C.; Su, Y.; Li, J.; Zhu, B., Water soluble and insoluble components of urban PM2. 5 and their cytotoxic effects on epithelial cells (A549) in vitro. *Environmental pollution* **2016,** *212*, 627-635.

143. Valberg, P. A., Is PM more toxic than the sum of its parts? Risk-assessment toxicity factors vs. PM-mortality "effect functions". *Inhalation toxicology* **2004,** *16 Suppl 1*, 19-29.

144. Bakand, S.; Winder, C.; Khalil, C.; Hayes, A., Toxicity assessment of industrial chemicals and airborne contaminants: transition from in vivo to in vitro test methods: a review. *Inhalation toxicology* **2005,** *17* (13), 775-787.

145. Paur, H.-R.; Cassee, F. R.; Teeguarden, J.; Fissan, H.; Diabate, S.; Aufderheide, M.; Kreyling, W. G.; Hänninen, O.; Kasper, G.; Riediker, M., In-vitro cell exposure studies for the assessment of nanoparticle toxicity in the lung—A dialog between aerosol science and biology. *Journal of Aerosol Science* **2011,** *42* (10), 668-692.

146. International Agency for Research on Cancer (IARC), *IARC Monographs on the evaluation of the carcinogenic risk of chemicals to humans*. World Health Organization: Lyon, France, 1997; Vol. 68.

147. Antognelli, C.; Gambelunghe, A.; Del Buono, C.; Murgia, N.; Talesa, V. N.; Muzi, G., Crystalline silica Min-U-Sil 5 induces oxidative stress in human bronchial epithelial cells BEAS-2B by reducing the efficiency of antiglycation and antioxidant enzymatic defenses. *Chemico-biological interactions* **2009,** *182* (1), 13-21.

148. Øvrevik, J.; Refsnes, M.; Namork, E.; Becher, R.; Sandnes, D.; Schwarze, P. E.; Låg, M., Mechanisms of silica-induced IL-8 release from A549 cells: initial kinase-activation does not require EGFR activation or particle uptake. *Toxicology* **2006,** *227* (1-2), 105-116.

149. Donaldson, K.; Borm, P. J., The quartz hazard: a variable entity. *The Annals of occupational hygiene* **1998,** *42* (5), 287-294.

150. Bégin, R.; Massé, S.; Sébastien, P.; Martel, M.; Bossé, J.; Dubois, F.; Geoffroy, M.; Labbe, J., Sustained efficacy of aluminum to reduce quartz toxicity in the lung. *Experimental lung research* **1987,** *13* (2), 205-222.

151. Castranova, V.; Vallyathan, V.; Ramsey, D. M.; McLaurin, J. L.; Pack, D.; Leonard, S.; Barger, M. W.; Ma, J.; Dalal, N. S.; Teass, A., Augmentation of pulmonary reactions to quartz inhalation by trace amounts of iron-containing particles. *Environmental Health Perspectives* **1997,** *105* (Suppl 5), 1319.

152. Cullen, R.; Vallyathan, V.; Hagen, S.; Donaldson, K., Protection by iron against the toxic effects of quartz. *The Annals of Occupational Hygiene* **1997,** *41*, 420-425.

153. Giard, D. J.; Aaronson, S. A.; Todaro, G. J.; Arnstein, P.; Kersey, J. H.; Dosik, H.; Parks, W. P., In vitro cultivation of human tumors: establishment of cell lines derived from a series of solid tumors. *Journal of the National Cancer Institute* **1973,** *51* (5), 1417-1423.

154. Lieber, M.; Todaro, G.; Smith, B.; Szakal, A.; Nelson-Rees, W., A continuous tumor-cell line from a human lung carcinoma with properties of type II alveolar epithelial cells. *International journal of cancer* **1976,** *17* (1), 62-70.

155. Chung, K. F.; Barnes, P. J., Cytokines in asthma. *Thorax* **1999,** *54* (9), 825-857.

156. Strieter, R. M.; Kunkel, S. L.; Bone, R. C., Role of tumor necrosis factor-alpha in disease states and inflammation. *Critical care medicine* **1993,** *21* (10 Suppl), S447-63.

157. Standiford, T. J.; Kunkel, S.; Phan, S.; Rollins, B.; Strieter, R., Alveolar macrophage-derived cytokines induce monocyte chemoattractant protein-1 expression from human pulmonary type II-like epithelial cells. *Journal of Biological Chemistry* **1991,** *266* (15), 9912-9918.

158. Hunter, C. A.; Jones, S. A., IL-6 as a keystone cytokine in health and disease. *Nature immunology* **2015,** *16* (5), 448.

159. Scheller, J.; Chalaris, A.; Schmidt-Arras, D.; Rose-John, S., The pro-and anti-inflammatory properties of the cytokine interleukin-6. *Biochimica et Biophysica Acta (BBA)-Molecular Cell Research* **2011,** *1813* (5), 878-888.

160. Harada, A.; Sekido, N.; Akahoshi, T.; Wada, T.; Mukaida, N.; Matsushima, K., Essential involvement of interleukin-8 (IL-8) in acute inflammation. *Journal of leukocyte biology* **1994,** *56* (5), 559-564.

161. Hetland, R. B.; Refsnes, M.; Myran, T.; Johansen, B. V.; Uthus, N.; Schwarze, P. E., Mineral and/or metal content as critical determinants of particle-induced release of IL-6 and IL-8 from A549 cells. *Journal of Toxicology and Environmental Health Part A* **2000,** *60* (1), 47-65.

162. Arnold, R.; Humbert, B.; Werchau, H.; Gallati, H.; König, W., Interleukin-8, interleukin-6, and soluble tumour necrosis factor receptor type I release from a human pulmonary epithelial cell line (A549) exposed to respiratory syncytial virus. *Immunology* **1994,** *82* (1), 126.

163. Gan, S. D.; Patel, K. R., Enzyme immunoassay and enzyme-linked immunosorbent assay. *J Invest Dermatol* **2013,** *133* (9), e12.

164. Strober, W., Trypan blue exclusion test of cell viability. *Current protocols in immunology* **2015,** *111* (1), A3. B. 1-A3. B. 3.

165. Ravishankara, A., Heterogeneous and multiphase chemistry in the troposphere. *Science* **1997,** *276* (5315), 1058-1065.

166. Adamson, I. Y.; Prieditis, H.; Vincent, R., Soluble and insoluble air particle fractions induce differential production of tumor necrosis factor α in rat lung. *Experimental lung research* **2004,** *30* (5), 355-368.

167. Yi, S.; Zhang, F.; Qu, F.; Ding, W., Water-insoluble fraction of airborne particulate matter (PM10) induces oxidative stress in human lung epithelial A549 cells. *Environmental toxicology* **2014,** *29* (2), 226-233.

168. Palleschi, S.; Rossi, B.; Armiento, G.; Montereali, M. R.; Nardi, E.; Tagliani, S. M.; Inglessis, M.; Gianfagna, A.; Silvestroni, L., Toxicity of the readily leachable fraction of urban PM 2.5 to human lung epithelial cells: Role of soluble metals. *Chemosphere* **2017**.

169. Adamson, I. Y.; Prieditis, H.; Vincent, R., Pulmonary toxicity of an atmospheric particulate sample is due to the soluble fraction. *Toxicology and applied pharmacology* **1999,** *157* (1), 43-50.

170. Imrich, C.-A. W. G. A.; Ning, H. D. Y., Analysis of air pollution particulate-mediated oxidant stress in alveolar macrophages. *Journal of Toxicology and Environmental Health Part A* **1998,** *54* (7), 529-545.

171. Kodavanti, U. P.; Hauser, R.; Christiani, D. C.; Meng, Z. H.; McGee, J.; Ledbetter, A.; Richards, J.; Costa, D. L., Pulmonary responses to oil fly ash particles in the rat differ by virtue of their specific soluble metals. *Toxicological Sciences* **1998,** *43* (2), 204-212.

172. Okeson, C. D.; Riley, M. R.; Fernandez, A.; Wendt, J. O., Impact of the composition of combustion generated fine particles on epithelial cell toxicity: influences of metals on metabolism. *Chemosphere* **2003,** *51* (10), 1121-1128.

173. Prieditis, H.; Adamson, I., Comparative pulmonary toxicity of various soluble metals found in urban particulate dusts. *Experimental lung research* **2002,** *28* (7), 563-576.

174. Huang, M.; Kang, Y.; Wang, W.; Chan, C. Y.; Wang, X.; Wong, M. H., Potential cytotoxicity of water-soluble fraction of dust and particulate matters and relation to metal (loid) s based on three human cell lines. *Chemosphere* **2015,** *135*, 61-66.

175. Imrich, A.; Ning, Y.; Kobzik, L., Insoluble components of concentrated air particles mediate alveolar macrophage responses in vitro. *Toxicology and applied pharmacology* **2000,** *167* (2), 140-150.

176. Ghio, A. J., Metals associated with both the water-soluble and insoluble fractions of an ambient air pollution particle catalyze an oxidative stress. *Inhalation toxicology* **1999,** *11* (1), 37-49.

177. Jalava, P. I.; Salonen, R. O.; Pennanen, A. S.; Happo, M. S.; Penttinen, P.; Hälinen, A. I.; Sillanpää, M.; Hillamo, R.; Hirvonen, M.-R., Effects of solubility of urban air fine and coarse particles on cytotoxic and inflammatory responses in RAW 264.7 macrophage cell line. *Toxicology and Applied Pharmacology* **2008,** *229* (2), 146-160.

178. Soukup, J. M.; Becker, S., Human alveolar macrophage responses to air pollution particulates are associated with insoluble components of coarse material, including particulate endotoxin. *Toxicology and applied pharmacology* **2001,** *171* (1), 20-26.

179. Ayres, J. G.; Borm, P.; Cassee, F. R.; Castranova, V.; Donaldson, K.; Ghio, A.; Harrison, R. M.; Hider, R.; Kelly, F.; Kooter, I. M., Evaluating the toxicity of airborne particulate matter and nanoparticles by measuring oxidative stress potential—a workshop report and consensus statement. *Inhalation toxicology* **2008,** *20* (1), 75-99.

180. Beck-Speier, I.; Kreyling, W. G.; Maier, K. L.; Dayal, N.; Schladweiler, M. C.; Mayer, P.; Semmler-Behnke, M.; Kodavanti, U. P., Soluble iron modulates iron oxide particle-induced inflammatory responses via prostaglandin E 2 synthesis: In vitro and in vivo studies. *Particle and fibre toxicology* **2009,** *6* (1), 34.

181. Fujii, T.; Hayashi, S.; Hogg, J. C.; Vincent, R.; Van Eeden, S. F., Particulate matter induces cytokine expression in human bronchial epithelial cells. *American Journal of Respiratory Cell and Molecular Biology* **2001,** *25* (3), 265-271.

182. Kunzli, N.; Kaiser, R.; Medina, S.; Studnicka, M., Public-health impact of outdoor and traffic-related air pollution: a European assessment. *The Lancet* **2000,** *356* (9232), 795.

183. Hoek, G.; Brunekreef, B.; Goldbohm, S.; Fischer, P.; van den Brandt, P. A., Association between mortality and indicators of traffic-related air pollution in the Netherlands: a cohort study. *The lancet* **2002,** *360* (9341), 1203-1209.

184. Künzli, N.; Kaiser, R.; Medina, S.; Studnicka, M.; Chanel, O.; Filliger, P.; Herry, M.; Horak, F.; Puybonnieux-Texier, V.; Quénel, P., Public-health impact of outdoor and traffic-related air pollution: a European assessment. *The Lancet* **2000,** *356* (9232), 795-801.

185. Lippmann, M., Toxicological and epidemiological studies of cardiovascular effects of ambient air fine particulate matter (PM2. 5) and its chemical components: coherence and public health implications. *Critical reviews in toxicology* **2014,** *44* (4), 299-347.

186. Riedl, M.; Diaz-Sanchez, D., Biology of diesel exhaust effects on respiratory function. *Journal of Allergy and Clinical Immunology* **2005,** *115* (2), 221-228.

187. Shah, S. D.; Cocker, D. R.; Miller, J. W.; Norbeck, J. M., Emission rates of particulate matter and elemental and organic carbon from in-use diesel engines. *Environmental Science & Technology* **2004,** *38* (9), 2544-2550.

188. Vohler, O.; GmbH, S.; Collin, G.; V., D. E.; Wege, E.; Gmbh, S.; Meitingen; Forhs, W., *Ullmann's Encyclopedia of chemical technology*. 6 ed.; Wiley-VCH: New York, 2003; Vol. 6.

189. Rivin, D.; Hutzinger, O.; Beek, B.; Metzler, M., *The handbook of environmental chemistry*. Springer: Berlin, 1986; Vol. 3.

190. Hussain, S.; Boland, S.; Baeza-Squiban, A.; Hamel, R.; Thomassen, L. C.; Martens, J. A.; Billon-Galland, M. A.; Fleury-Feith, J.; Moisan, F.; Pairon, J. C.; Marano, F., Oxidative stress and proinflammatory effects of carbon black and titanium dioxide nanoparticles: role of particle surface area and internalized amount. *Toxicology* **2009,** *260* (1-3), 142-9.

191. Donaldson, K.; Tran, L.; Jimenez, L. A.; Duffin, R.; Newby, D. E.; Mills, N.; MacNee, W.; Stone, V., Combustion-derived nanoparticles: a review of their toxicology following inhalation exposure. *Particle and fibre toxicology* **2005,** *2* (1), 10.

192. Aam, B. B.; Fonnum, F., Carbon black particles increase reactive oxygen species formation in rat alveolar macrophages in vitro. *Archives of toxicology* **2007,** *81* (6), 441-6.

193. Foucaud, L.; Goulaouic, S.; Bennasroune, A.; Laval-Gilly, P.; Brown, D.; Stone, V.; Falla, J., Oxidative stress induction by nanoparticles in THP-1 cells with 4-HNE production: stress biomarker or oxidative stress signalling molecule? *Toxicology in vitro : an international journal published in association with BIBRA* **2010,** *24* (6), 1512-20.

194. Garza, K. M.; Soto, K. F.; Murr, L. E., Cytotoxicity and reactive oxygen species generation from aggregated carbon and carbonaceous nanoparticulate materials. *International journal of nanomedicine* **2008,** *3* (1), 83.

195. Mroz, R.; Schins, R.; Li, H.; Drost, E.; Macnee, W.; Donaldson, K., NANOPARTICLE CARBON BLACK DRIVEN DNA DAMAGE INDUCES GROWTH ARREST AND AP-1 AND NFκB DNA BINDING IN LUNG EPITHELIAL A549 CELL LINE. *Journal of physiology and pharmacology* **2007,** *58* (5), 461-470.

196. Chuang, H.-C.; Chen, L.-C.; Lei, Y.-C.; Wu, K.-Y.; Feng, P.-H.; Cheng, T.-J., Surface area as a dose metric for carbon black nanoparticles: A study of oxidative stress, DNA single-strand breakage and inflammation in rats. *Atmospheric Environment* **2015,** *106*, 329-334.

197. Sager, T. M.; Castranova, V., Surface area of particle administered versus mass in determining the pulmonary toxicity of ultrafine and fine carbon black: comparison to ultrafine titanium dioxide. *Part Fibre Toxicol* **2009,** *6*, 15.

198. Val, S.; Hussain, S.; Boland, S.; Hamel, R.; Baeza-Squiban, A.; Marano, F., Carbon black and titanium dioxide nanoparticles induce pro-inflammatory responses in bronchial epithelial cells: need for multiparametric evaluation due to adsorption artifacts. *Inhalation toxicology* **2009,** *21* (sup1), 115-122.

199. Nel, A.; Xia, T.; Mädler, L.; Li, N., Toxic potential of materials at the nanolevel. *science* **2006,** *311* (5761), 622-627.

200. Kolling, A.; Ernst, H.; Rittinghausen, S.; Heinrich, U., Relationship of pulmonary toxicity and carcinogenicity of fine and ultrafine granular dusts in a rat bioassay. *Inhalation toxicology* **2011,** *23* (9), 544-554.

201. Bonn, P. J.; Driscoll, K., Particles, inflammation and respiratory tract carcinogenesis. *Toxicology letters* **1996,** *88* (1), 109-113.

202. Nikula, K.; Snipes, M.; Barr, E.; Griffith, W.; Henderson, R.; Mauderly, J., Comparative pulmonary toxicities and carcinogenicities of chronically inhaled diesel exhaust and carbon black in F344 rats. *Fundamental and Applied Toxicology* **1995,** *25* (1), 80-94.

203. McCunney, R. J., *Particle overload in the rat lung and lung cancer: implications for human risk assessment*. CRC Press: 1996.

204. International Agency for Research on Cancer (IARC), *IARC monographs on the evaluation of carcinogenic risks to humans.* World Health Organization: Lyon, France, 2010; Vol. 93.

205. Vander Wal, R. L.; Bryg, V. M.; Hays, M. D., Fingerprinting soot (towards source identification): Physical structure and chemical composition. *Journal of Aerosol Science* **2010,** *41* (1), 108-117.

206. International Agency for Research on Cancer (IARC), *Overall evaluations of carcinogenicity: an updating of IARC monographs volumes 1 to 42*. World Health Organization: Lyon, France, 1987; Vol. 7.

207. Medalia, A. I.; Rivin, D., Particulate carbon and other components of soot and carbon black. *Carbon* **1982,** *20* (6), 481-492.

208. Medalia, A. I.; Rivin, D.; Sanders, D. R., A comparison of carbon black with soot. *Science of the total environment* **1983,** *31* (1), 1-22.

209. Gilman, P., Health assessment document for diesel engine exhaust. *US Environmental Protection Agency* **2002**.

210. Elvers, B.; Hawkins, S.; Russey, W., *Ullmann's encyclopedia of industrial chemistry*. Wiley Online Library: Weinheim, Germany, 2003; Vol. 32.

211. Uhrlandt, S., *Encyclopedia of chemical technology*. Wiley-Interscience: Hoboken, New Jersey, 2006; Vol. 22.

212. EPA., U. S., Health Effects of Inhaled Crystalline and Amorphous Silica. Development, U. S. E. P. A. O. o. R. a., Ed. National Center For Environmental Assessment, Research Triangle Park Office: Research Triangle Park, NC, 1996.

213. Rice, F., *Crystalline silica, Quartz*. World Health Organization: Geneva, 2000.

214. Chu, Z.; Huang, Y.; Li, L.; Tao, Q.; Li, Q., Physiological pathway of human cell damage induced by genotoxic crystalline silica nanoparticles. *Biomaterials* **2012,** *33* (30), 7540-7546.

215. Hamilton, R. F.; Thakur, S. A.; Holian, A., Silica binding and toxicity in alveolar macrophages. *Free Radical Biology and Medicine* **2008,** *44* (7), 1246-1258.

216. Rimal, B.; Greenberg, A. K.; Rom, W. N., Basic pathogenetic mechanisms in silicosis: current understanding. *Current opinion in pulmonary medicine* **2005,** *11* (2), 169-173.

217. Fanizza, C.; Ursini, C. L.; Paba, E.; Ciervo, A.; Di Francesco, A.; Maiello, R.; De Simone, P.; Cavallo, D., Cytotoxicity and DNA-damage in human lung epithelial cells exposed to respirable α-quartz. *Toxicology in vitro* **2007,** *21* (4), 586-594.

218. Kawasaki, H., A mechanistic review of silica-induced inhalation toxicity. *Inhalation toxicology* **2015,** *27* (8), 363-377.

219. Davis, B. L.; Johnson, L. R.; Stevens, R. K.; Courtney, W. J.; Safriet, D. W., The quartz content and elemental composition of aerosols from selected sites of the EPA inhalable particulate network. *Atmospheric Environment (1967)* **1984,** *18* (4), 771-782.

220. Howson, T. E.; Tien, J. K.; Tundermann, J. H., *Encyclopedia of chemical technology*. Wiley-Interscience: Hoboken, New Jersey, 2006; Vol. 17.

221. Elvers, B.; Hawkins, S.; Russey, W., *Ullmann's encyclopedia of industrial chemistry*. Wiley Online Library: Weinheim, Germany, 2003; Vol. 22.

222. International Agency for Research on Cancer (IARC), *IARC monographs on the evaluation of carcinogenic risk of chemicals to man*. World Health Organization: Lyon, France, 2017; Vol. 100C-10.

223. Agency for Toxic Substances and Disease Registry (ATSDR), Toxicological profile for nickel. U.S. Department of Health and Human Services, Public Health Service: Atlanta, Georgia, 2005.

224. Cempel, M.; Nikel, G., Nickel: A Review of Its Sources and Environmental Toxicology. *Polish Journal of Environmental Studies* **2006,** *15* (3).

225. Schaumlöffel, D., Nickel species: analysis and toxic effects. *Journal of Trace Elements in Medicine and Biology* **2012,** *26* (1), 1-6.

226. Environment Canada; Health Canada, Canadian Environmental Protection Act. Nickel and Its Compounds Canada, E.; Canada, H., Eds. Ottawa, CA, 1994.

227. Newhook, R.; Hirtle, H.; Byrne, K.; Meek, M., Releases from copper smelters and refineries and zinc plants in Canada: human health exposure and risk characterization. *Science of the Total Environment* **2003,** *301* (1), 23-41.

228. Grimsrud, T. K.; Berge, S. R.; Resmann, F.; Norseth, T.; Andersen, A., Assessment of historical exposures in a nickel refinery in Norway. *Scandinavian journal of work, environment & health* **2000**, 338-345.

229. Muñoz, A.; Costa, M., Elucidating the mechanisms of nickel compound uptake: a review of particulate and nano-nickel endocytosis and toxicity. *Toxicology and applied pharmacology* **2012,** *260* (1), 1-16.

230. Das, K.; Das, S.; Dhundasi, S., Nickel, its adverse health effects & oxidative stress. *Indian Journal of Medical Research* **2008,** *128* (4), 412.

231. Ahamed, M., Toxic response of nickel nanoparticles in human lung epithelial A549 cells. *Toxicology in Vitro* **2011,** *25* (4), 930-936.

232. Barchowsky, A.; Soucy, N. V.; O'Hara, K. A.; Hwa, J.; Noreault, T. L.; Andrew, A. S., A novel pathway for nickel-induced interleukin-8 expression. *Journal of Biological Chemistry* **2002,** *277* (27), 24225-24231.

233. Salnikow, K.; Su, W.; Blagosklonny, M. V.; Costa, M., Carcinogenic metals induce hypoxia-inducible factor-stimulated transcription by reactive oxygen species-independent mechanism. *Cancer research* **2000,** *60* (13), 3375-3378.

234. Hartwig, A.; Krüger, I.; Beyersmann, D., Mechanisms in nickel genotoxicity: the significance of interactions with DNA repair. *Toxicology letters* **1994,** *72* (1-3), 353-358.

235. Fenwick, S. L. Development of an In Vitro Method to Study Heterogeneous Particle Mimic Exposures. (Thesis) Ph.D., Simon Fraser University, BC, Canada, 2016.

236. Herseth, J.; Refsnes, M.; Låg, M.; Hetland, G.; Schwarze, P., IL-1β as a determinant in silica-induced cytokine responses in monocyte-endothelial cell co-cultures. *Human & experimental toxicology* **2008,** *27* (5), 387-399.

237. Konecny, R.; Leonard, S.; Shi, X.; Robinson, V. A.; Castranova, V., Reactivity of free radicals on hydroxylated quartz surface and its implications for pathogenicity of silicas: experimental and quantum mechanical study. *Journal of environmental pathology, toxicology and oncology* **2001,** *20* (Suppl. 1).

238. Borm, P. J., Toxicity and occupational health hazards of coal fly ash (CFA). A review of data and comparison to coal mine dust. *The Annals of occupational hygiene* **1997,** *41* (6), 659-676.

239. Magaye, R.; Zhou, Q.; Bowman, L.; Zou, B.; Mao, G.; Xu, J.; Castranova, V.; Zhao, J.; Ding, M., Metallic nickel nanoparticles may exhibit higher carcinogenic potential than fine particles in JB6 cells. *PloS one* **2014,** *9* (4), e92418.

240. Capasso, L.; Camatini, M.; Gualtieri, M., Nickel oxide nanoparticles induce inflammation and genotoxic effect in lung epithelial cells. *Toxicology letters* **2014,** *226* (1), 28-34.

241. Magaye, R.; Zhao, J., Recent progress in studies of metallic nickel and nickel-based nanoparticles' genotoxicity and carcinogenicity. *Environmental toxicology and pharmacology* **2012,** *34* (3), 644-650.

242. Pongpiachan, S.; Iijima, A., Assessment of selected metals in the ambient air PM10 in urban sites of Bangkok (Thailand). *Environmental Science and Pollution Research* **2016,** *23* (3), 2948-2961.

243. Lu, C.-F.; Yuan, X.-Y.; Li, L.-Z.; Zhou, W.; Zhao, J.; Wang, Y.-M.; Peng, S.-Q., Combined exposure to nano-silica and lead induced potentiation of oxidative stress and DNA damage in human lung epithelial cells. *Ecotoxicology and environmental safety* **2015,** *122*, 537-544.

244. Agency for Toxic Substances and Disease Registry (ATSDR), Toxicological profile for zinc. U.S. Department of Health and Human Services, Public Health Service: Atlanta, Georgia, 2005.

245. Walsh, C. T.; Sandstead, H. H.; Prasad, A. S.; Newberne, P. M.; Fraker, P. J., Zinc: health effects and research priorities for the 1990s. *Environmental health perspectives* **1994,** *102* (Suppl 2), 5.

246. Friedlander, S.; Yeh, E., The submicron atmospheric aerosol as a carrier of reactive chemical species: case of peroxides. *Applied occupational and environmental hygiene* **1998,** *13* (6), 416-420.

247. Jang, M.; Czoschke, N. M.; Lee, S.; Kamens, R. M., Heterogeneous atmospheric aerosol production by acid-catalyzed particle-phase reactions. *Science* **2002,** *298* (5594), 814-817.

248. Rohr, A. C.; Wyzga, R. E., Attributing health effects to individual particulate matter constituents. *Atmospheric Environment* **2012,** *62*, 130-152.

249. Schwarze, P.; Øvrevik, J.; Låg, M.; Refsnes, M.; Nafstad, P.; Hetland, R.; Dybing, E., Particulate matter properties and health effects: consistency of epidemiological and toxicological studies. *Human & experimental toxicology* **2006,** *25* (10), 559-579.

250. Reiss, R.; Anderson, E. L.; Cross, C. E.; Hidy, G.; Hoel, D.; McClellan, R.; Moolgavkar, S., Evidence of health impacts of sulfate-and nitrate-containing particles in ambient air. *Inhalation toxicology* **2007,** *19* (5), 419-449.

251. Schlesinger, R. B.; Cassee, F., Atmospheric secondary inorganic particulate matter: the toxicological perspective as a basis for health effects risk assessment. *Inhalation toxicology* **2003,** *15* (3), 197-235.

252. Committee on the Environment and Natural Resources; Air Quality Research Subcommittee, Atmospheric Ammonia: Sources and Fate. Laboratory, N. A., Ed. NOAA Aeronomy Laboratory: Boulder Colorado, USA, 2000.

253. United States Environmental Protection Agency, Air Quality Criteria for Particulate Matter. EPA., U. S., Ed. Office of Research and Development: Research Triangle Park, NC, 2004; Vol. I.

254. Wexler, A. S.; Seinfeld, J. H., The distribution of ammonium salts among a size and composition dispersed aerosol. *Atmospheric Environment. Part A. General Topics* **1990,** *24* (5), 1231-1246.

255. Harrison, R. M.; Jones, A. M.; Lawrence, R. G., Major component composition of PM 10 and PM 2.5 from roadside and urban background sites. *Atmospheric Environment* **2004,** *38* (27), 4531-4538.

256. Lipfert, F.; Baty, J.; Miller, J.; Wyzga, R., PM2. 5 constituents and related air quality variables as predictors of survival in a cohort of US military veterans. *Inhalation toxicology* **2006,** *18* (9), 645-657.

257. Last, J. A.; Hyde, D. M.; Chang, D. P., A mechanism of synergistic lung damage by ozone and a respirable aerosol. *Experimental lung research* **1984,** *7* (3-4), 223-235.

258. Hattis, D.; Wasson, J. M.; Page, G. S.; Stern, B.; Franklin, C. A., Acid particles and the tracheobronchial region of the respiratory system—an “irritation-signaling” model for possible health effects. *JAPCA* **1987,** *37* (9), 1060-1066.

259. Dreher, K. L., Particulate matter physicochemistry and toxicology: In search of causality—A critical perspective. *Inhalation toxicology* **2000,** *12* (sup3), 45-57.

260. Frank E.Goodwin, *Encyclopedia of chemical technology*. Wiley-Interscience: Hoboken, New Jersey, 2007; Vol. 26.

261. Gunter G. Graf, *Ullmann's encyclopedia of industrial chemistry*. Wiley Online Library: Weinheim, Germany, 2003; Vol. 39.

262. Zumdahl, S.; DeCoste, D. J., *Chemical principles*. Nelson Education: 2012.

263. WHO, Zinc. Envrionmental Health Criteria 221 Organization, W. H., Ed. Geneva, Switzerland, 2001.

264. Lioy, P. J.; Wolff, G. T.; Kneip, T. J., Toxic airborne elements in the New York metropolitan area. *Journal of the Air Pollution Control Association* **1978,** *28* (5), 510-512.

265. Stands Development Branch Ontario Ministry of the Environment, Ontario's Ambient Air Quality Criteria. Environment, O. M. o. t., Ed. Ontario, Canada, 2012; Vol. PIBS # 6570e01.

266. Stefanidou, M.; Maravelias, C.; Dona, A.; Spiliopoulou, C., Zinc: a multipurpose trace element. *Archives of toxicology* **2006,** *80* (1), 1.

267. Jomova, K.; Valko, M., Advances in metal-induced oxidative stress and human disease. *Toxicology* **2011,** *283* (2), 65-87.

268. Dreosti, I. E., *Trace elements, micronutrients, and free radicals*. Springer Science & Business Media: 1991.

269. Cooper, R. G., Zinc toxicology following particulate inhalation. *Indian journal of occupational and environmental medicine* **2008,** *12* (1), 10.

270. Homma, S.; Jones, R.; Qvist, J.; Zapol, W. M.; Reid, L., Pulmonary vascular lesions in the adult respiratory distress syndrome caused by inhalation of zinc chloride smoke: a morphometric study. *Human pathology* **1992,** *23* (1), 45-50.

271. Freitag, A.; Caduff, B., ARDS caused by military zinc fumes exposure. *Schweizerische medizinische Wochenschrift* **1996,** *126* (23), 1006-1010.

272. Hjortso, E.; Ovist, J.; Bud, M.; Thomsen, J.; Andersen, J.; Wiberg-Jørgensen, F.; Jensen, N.; Jones, R.; Reid, L.; Zapol, W., ARDS after accidental inhalation of zinc chloride smoke. *Intensive care medicine* **1988,** *14* (1), 17-24.

273. Schenker, M. B.; Speizer, F. E.; Taylor, J. O., Acute upper respiratory symptoms resulting from exposure to zinc chloride aerosol. *Environmental research* **1981,** *25* (2), 317-324.

274. Ishiyama, H.; Ogino, K.; Sato, M.; Ogura, M.; Dan, S.; Hobara, T., Histopathological changes induced by zinc hydroxide in rat lungs. *Experimental and Toxicologic Pathology* **1997,** *49* (3-4), 261-266.

275. Hirshon, J. M.; Shardell, M.; Alles, S.; Powell, J. L.; Squibb, K.; Ondov, J.; Blaisdell, C. J., Elevated ambient air zinc increases pediatric asthma morbidity. *Environmental health perspectives* **2008,** *116* (6), 826.

276. Charles A. Sutherland; Edward F. Milner; Robert C. Kerby; Herbert Teindl; Albert Melin, *Ullmann's encyclopedia of industrial chemistry*. Wiley Online Library: Weinheim, Germany, 2003; Vol. 19.

277. Joseph Breen; Stephen C. DeVito; Michael King; R. David Prengaman; venkoba Ramachandran, *Encyclopedia of chemical technology*. Wiley-Interscience: Hoboken, New Jersey, 2005; Vol. 14.

278. International Agency for Research on Cancer (IARC), *IARC monographs on the evaluation of carcinogenic risk of chemicals to man*. World Health Organization: Lyon, France, 2006; Vol. 87.

279. WHO, Expoure to Lead: a Major Public Health Concern. Organization, W. H., Ed. WHO: Geneva, Switzerland, 2010.

280. WHO, Air quality guidelines for Europe. second edition ed.; Organization, W. H., Ed. Geneva, Switzerland, 2000; pp 149-153.

281. Health Canada, Final Human Health State of the Science Report on Lead. Canada, H., Ed. Health Canada: Ottawa, Ontario, 2013.

282. Brochin, R.; Leone, S.; Phillips, D.; Shepard, N.; Zisa, D.; Angerio, A., The Cellular Effect of Lead Poisioning and Its Clinical Picture. *Issues* **2008,** *5* (2).

283. Patrick, L., Lead toxicity, a review of the literature. Part I: exposure, evaluation, and treatment. *Alternative medicine review* **2006,** *11* (1), 2-23.

284. Gillis, B. S.; Arbieva, Z.; Gavin, I. M., Analysis of lead toxicity in human cells. *BMC genomics* **2012,** *13* (1), 344.

285. Patrick, L., Lead toxicity part II: the role of free radical damage and the use of antioxidants in the pathology and treatment of lead toxicity. *Alternative Medicine Review* **2006,** *11* (2), 114.

286. Yedjou, C.; Haynes, L.; Dorsey, W.; McMurray, R.; Tchounwou, P. B., Lead-Induced Cytotoxicity and Oxidative Stress in Human Leukemia (HL-60) Cells. *Archives of environmental contamination and toxicology* **2003,** *44* (3), 417.

287. Gordon H. Geiger; J. A. Lepinski; Jeffrey C. Myers; Alan M. Stolzenberg, *Encyclopedia of chemical technology*. Wiley-Interscience: Hoboken, New Jersey, 2005; Vol. 14.

288. Charles A. Sutherland; Edward F. Milner; Robert C. Kerby; Herbert Teindl; Albert Melin, *Ullmann's encyclopedia of industrial chemistry*. Wiley Online Library: Weinheim, Germany, 2003; Vol. 18.

289. WHO, *Iron in drinking-water*. World Health Organization: 2003.

290. Paxton, H. W., *Encyclopedia of chemical technology*. Wiley-Interscience: Hoboken, New Jersey, 2007; Vol. 23.

291. Mahowald, N. M.; Engelstaedter, S.; Luo, C.; Sealy, A.; Artaxo, P.; Benitez-Nelson, C.; Bonnet, S.; Chen, Y.; Chuang, P. Y.; Cohen, D. D., Atmospheric iron deposition: global distribution, variability, and human perturbations. **2008**.

292. Wang, R.; Balkanski, Y.; Boucher, O.; Bopp, L.; Chappell, A.; Ciais, P.; Hauglustaine, D.; Peñuelas, J.; Tao, S., Sources, transport and deposition of iron in the global atmosphere. *Atmospheric Chemistry and Physics* **2015,** *15* (11), 6247-6270.

293. Oakes, M.; Weber, R.; Lai, B.; Russell, A.; Ingall, E., Characterization of iron speciation in urban and rural single particles using XANES spectroscopy and micro X-ray fluorescence measurements: investigating the relationship between speciation and fractional iron solubility. *Atmospheric Chemistry and Physics* **2012,** *12* (2), 745-756.

294. Majestic, B.; Schauer, J.; Shafer, M., Application of synchrotron radiation for measurement of iron red-ox speciation in atmospherically processed aerosols. *Atmospheric Chemistry and Physics* **2007,** *7* (10), 2475-2487.

295. Wang, J.; Pantopoulos, K., Regulation of cellular iron metabolism. *Biochemical Journal* **2011,** *434* (3), 365-381.

296. Fraga, C. G.; Oteiza, P. I., Iron toxicity and antioxidant nutrients. *Toxicology* **2002,** *180* (1), 23-32.

297. Eaton, J. W.; Qian, M., Molecular bases of cellular iron toxicity. *Free Radical Biology and Medicine* **2002,** *32* (9), 833-840.

298. Nettesheim, P.; Creasia, D.; Mitchell, T., Carcinogenic and cocarcinogenic effects of inhaled synthetic smog and ferric oxide particles. *Journal of the National Cancer Institute* **1975,** *55* (1), 159-169.

299. EPA., U. S., Health effects assessment for iron (and compounds). U.S. Environmental Protection Agency; Office of Reasearch and Development; Office of Health and Environmental Assessment; Environmental Criteria and Assessment Office; Office of Emergency and Remedial Response; Response, O. o. S. W. a. E., Eds. Cincinnati, OH, U.S., 1984.

300. International Agency for Research on Cancer (IARC), *Occupational exposures during iron and steel founding*. World Health Organization: Lyon, France, 2012; Vol. 100F-34.

301. Bray, T. M.; Bettger, W. J., The physiological role of zinc as an antioxidant. *Free Radical Biology and Medicine* **1990,** *8* (3), 281-291.

302. Chai, F.; Truong-Tran, A. Q.; Ho, L. H.; Zalewski, P. D., Regulation of caspase activation and apoptosis by cellular zinc fluxes and zinc deprivation: A review. *Immunology & Cell Biology* **1999,** *77* (3).

303. Stumm, W.; Morgan, J. J., *Aquatic chemistry: chemical equilibria and rates in natural waters*. John Wiley & Sons: 2012; Vol. 126.

304. Gurer, H.; Ercal, N., Can antioxidants be beneficial in the treatment of lead poisoning? *Free Radical Biology and Medicine* **2000,** *29* (10), 927-945.

305. Kamimura, D.; Ishihara, K.; Hirano, T., IL-6 signal transduction and its physiological roles: the signal orchestration model. *Reviews of physiology, biochemistry and pharmacology* **2003,** *149*, 1-38.

306. Kunkel, S. L.; Standiford, T.; Kasahara, K.; Strieter, R. M., Interleukin-8 (IL-8): the major neutrophil chemotactic factor in the lung. *Experimental lung research* **1991,** *17* (1), 17-23.

307. Suwa, T.; Hogg, J. C.; Klut, M. E.; Hards, J.; van EEDEN, S. F., Interleukin-6 changes deformability of neutrophils and induces their sequestration in the lung. *American journal of respiratory and critical care medicine* **2001,** *163* (4), 970-976.

308. Guo, B.; Zebda, R.; Drake, S. J.; Sayes, C. M., Synergistic effect of co-exposure to carbon black and Fe 2 O 3 nanoparticles on oxidative stress in cultured lung epithelial cells. *Particle and fibre toxicology* **2009,** *6* (1), 4.

309. Zhou, Y.-M.; Zhong, C.-Y.; Kennedy, I. M.; Leppert, V. J.; Pinkerton, K. E., Oxidative stress and NFκB activation in the lungs of rats: a synergistic interaction between soot and iron particles. *Toxicology and applied pharmacology* **2003,** *190* (2), 157-169.

310. Vidrio, E.; Jung, H.; Anastasio, C., Generation of hydroxyl radicals from dissolved transition metals in surrogate lung fluid solutions. *Atmospheric Environment* **2008,** *42* (18), 4369-4379.

311. Wilson, M. R.; Lightbody, J. H.; Donaldson, K.; Sales, J.; Stone, V., Interactions between ultrafine particles and transition metals in vivo and in vitro. *Toxicology and applied pharmacology* **2002,** *184* (3), 172-179.

312. Lander, H. M., An essential role for free radicals and derived species in signal transduction. *The FASEB journal* **1997,** *11* (2), 118-124.

313. Naik, E.; Dixit, V. M., Mitochondrial reactive oxygen species drive proinflammatory cytokine production. *Journal of Experimental Medicine* **2011,** *208* (3), 417-420.

314. Ovrevik, J.; Hetland, R. B.; Schins, R. P.; Myran, T.; Schwarze, P. E., Iron release and ROS generation from mineral particles are not related to cytokine release or apoptosis in exposed A549 cells. *Toxicology letters* **2006,** *165* (1), 31-8.

315. Stefánsson, A., Iron (III) hydrolysis and solubility at 25 C. *Environmental Science & Technology* **2007,** *41* (17), 6117-6123.

316. Ghio, A. J.; Stoneheurner, J.; McGee, J. K.; Kinsey, J. S., Sulfate content correlates with iron concentrations in ambient air pollution particles. *Inhalation toxicology* **1999,** *11* (4), 293-307.

317. Rahman, I.; MacNee, W., Oxidative stress and regulation of glutathione in lung inflammation. *European Respiratory Journal* **2000,** *16* (3), 534-554.

318. Ward, T. H.; Cummings, J.; Dean, E.; Greystoke, A.; Hou, J.-M.; Backen, A.; Ranson, M.; Dive, C., Biomarkers of apoptosis. *British journal of cancer* **2008,** *99* (6), 841.

319. Aebersold, R.; Mann, M., Mass spectrometry-based proteomics. *Nature* **2003,** *422* (6928), 198.

320. Domon, B.; Aebersold, R., Mass spectrometry and protein analysis. *science* **2006,** *312* (5771), 212-217.

321. BéruBé, K. A.; Quinlan, T. R.; Moulton, G.; Hemenway, D.; O'Shaughnessy, P.; Vacek, P.; Mossman, B. T., Comparative proliferative and histopathologic changes in rat lungs after inhalation of chrysotile or crocidolite asbestos. *Toxicology and applied pharmacology* **1996,** *137* (1), 67-74.

322. Mrakovcic, M.; Meindl, C.; Roblegg, E.; Fröhlich, E., Reaction of monocytes to polystyrene and silica nanoparticles in short-term and long-term exposures. *Toxicology research* **2014,** *3* (2), 86-97.

323. Mrakovcic, M.; Absenger, M.; Riedl, R.; Smole, C.; Roblegg, E.; Fröhlich, L. F.; Fröhlich, E., Assessment of long-term effects of nanoparticles in a microcarrier cell culture system. *PLoS One* **2013,** *8* (2), e56791.

324. Thurnherr, T.; Brandenberger, C.; Fischer, K.; Diener, L.; Manser, P.; Maeder-Althaus, X.; Kaiser, J.-P.; Krug, H. F.; Rothen-Rutishauser, B.; Wick, P., A comparison of acute and long-term effects of industrial multiwalled carbon nanotubes on human lung and immune cells in vitro. *Toxicology letters* **2011,** *200* (3), 176-186.